



universität
wien

DISSERTATION

Titel der Dissertation

“Anatomical and functional dissection of
fruitless positive courtship circuit
in *Drosophila melanogaster*”

Verfasser

Tianxiao Liu (Bachelor of Science)

angestrebter akademischer Grad

Doctor of Philosophy (PhD)

Wien, Oktober, 2012

Studienkennzahl lt. Studienblatt:	A 091 490
Dissertationsgebiet lt. Studienblatt:	Molekulare Biologie
Betreuerin / Betreuer:	Dr. Barry J. Dickson

Acknowledgments:

This work would not have been possible without the help and support of the following people.

Barry J. Dickson has provided constant support and supervision throughout my Ph.D.

Anne von Philipsborn initiated the thermal activation screen and kindly shared the result with me. She has performed all the behavioral analysis regarding with the courtship song project.

David Mahringer performed part of the thermal activation screen.

Martin Kinberg and Vera Belyaeva provided help with the X-gal screen.

Christopher Masser, Salil Bidaye, Alex Stark, Michaella Fellner ,Katarina Bartalska, VDRC, and Barry J. Dickson contributed to the generation of VT lines.

Jai Yu introduced me into basic fly genetics and established staining protocol and image registration protocol.

Wolfgang Lugmayr provided technical support on image registration.

Attila Gyorgy and Hirofumi Toda provided support on fly husbandry.

Pawel Pasierbek provided technical support on confocal microscopy.

Kristin Scott generously shared fly stocks.

Simon Rumpel and Jürgen Knoblich monitored my progress through the PhD and provided helpful suggestions as my PhD committee members.

Anne von Philipsborn, Salil Bidaye, Hirofumi Toda, Ines Ribeiro, Joshua Lillvis, and Barry Dickson provided helpful feedback on my thesis.

All service departments of IMP/IMBA provided indispensable support throughout the project.

All past and current members of Dickson lab provided a great working atmosphere especially at the coffee break after lunch and invaluable scientific discussions and support throughout my PhD. Thanks for great time in Vienna.

Table of Contents

Synopsis.....	4
Zusammenfassung	6
1.Introduction	8
1.1.Overview	8
1.2. Courtship ritual.....	8
1.3. <i>fruitless</i>	9
1.4. <i>fruitless</i> is expressed in the adult nervous system.....	10
1.5. Anatomy of individual <i>fru+</i> neurons	11
1.6. Function of individual <i>fru+</i> neurons	12
Aim of thesis.....	13
References.....	15
2. Anatomical dissection of fruitless neurons.....	19
2.1. Motivation.....	19
2.2. Genetic tools to characterize <i>fru+</i> neurons	19
2.3 Genetic dissection of <i>fru+</i> neurons with VT lines	20
2.4. Anatomical overlap of <i>fru+</i> neurons	21
Olfaction.....	22
Vision.....	22
Audition.....	22
Gustation.....	23
Sensory integration.....	23
Other integration sites	23
Motor control.....	24
3. Functional dissection of <i>fru+</i> neurons.....	40
3.1. Strategies for functional dissection.....	40
3.2. Song neurons.....	41
3.3. Bending neurons	41
3.3.1. Motivation.....	41
3.3.2. Thermal activation Screen for neurons involved in copulation attempt and copulation	41
3.3.3. Identification and characterization of neurons involved in copulation attempt and copulation	41
dAB4, dAB5 and dAB8; potential motor neurons	42
dMT3	42
dAB7 and vAB2: two ascending neurons	42

dAB4 and dAB8 is specifically required for copulation, but not for other courtship steps	43
3.4. Courtship-driving neurons	50
3.4.1 Motivation	50
3.4.2 Thermal activation screen for neurons that drive courtship	50
3.4.3 Identification and characterization of neurons that drive courtship	51
LAN1	51
P1, pMP4 and pMP4_1	51
aSP2	52
Activation of VT61081+ fru+ neurons elicit following without wing extension	52
pIP6	52
aSP4	53
aSP21	53
vAB3	53
Neuronal epistasis between P1 and aSP2	54
References	65
3. Discussion	67
3.1 Anatomical analysis of <i>fru+</i> neurons	67
Specific targeting of Fruitless neurons by enhancer tiles	67
Functional relevance estimated from anatomical overlap	68
Lateral protocerebral complex is an integration center	68
3.2. Manipulation of a single neuronal class	69
3.3. <i>fru+</i> neurons involved in copulation attempt and copulation	69
Motor control by dAB4, dAB5 and dAB8	69
Signals from or to the brain through dAB7 and vAB2	70
3.4 <i>fru+</i> neurons that drive courtship	71
Sensory representations that drive courtship	71
Integration center for driving courtship	72
How is the “command” to court delivered to VNC?	49
Conclusion	75
References	76
Materials and methods	81
Supplementary figures	84
Appendix	110
Curriculum vitae	125

Synopsis

Drosophila melanogaster male display a complex innate behaviors, the courtship ritual. Male flies initiates the following based on the sensory cues from females. During the courtship, males extend their wing unilaterally and vibrate it to create the courtship song. In the end, males attempt the copulation by bending his abdomen and succeed in copulation. What is the neuronal basis for courtship?

Neurons that express the gene *fruitless* (*fru+* neurons) are essential for courtship and have been proposed to form courtship circuit. The aim of this study was to identify the components of the courtship circuit anatomically and functionally. We used FLP-in system and a new GAL4 library (Vienna Tile lines; VT lines) generated in the lab to target specific subsets of *fru+* neurons. We performed an anatomical screen with VT lines. We found that VT lines label smaller subsets of *fru+* neurons compared to enhancer trap GAL4 lines. The sparse labeling with VT lines enabled us to indentify and characterize previously uninvestigated *fru+* neurons and extend the courtship circuit diagram.

In order to elucidate how the *fru+* neurons are functionally involved in courtship, we performed neuronal activation screens with isolated males. We identified four types of *fru+* neurons (P1, pIP10, dPR1 and vPR6) that triggered courtship song and one type of *fru+* neurons (vMS11) that triggered unilateral wing extension upon thermal activation. Neuronal silencing of these neurons reduces the courtship song during courtship. Additionally, we identified six types of *fru+* neuron (dAB4, dAB5, dAB8, dMT3, vAB2, and dAB7) that trigger edabdominal bending on activation. Neuronal silencing of dAB4 or dAB5 did not affect the vigorousness of courtship but abolished copulation, suggesting their specific necessity for copulation. We thus identified two groups of neurons involved in different steps of courtship ritual, song production and copulation.

To identify the *fru+* neurons that drive the courtship behavior, we performed a thermal activation screen in the presence of a target male. We found P1 and LAN1 from this screen which are known to trigger courtship toward target males on activation. In addition, we found two subtypes of P1 (pMP4 and pMP4_1) and four other types of *fru+* neurons (aSP2, pIP6, aSP21, aSP4) that trigger courtship towards target males on activation. Silencing of P1 or aSP2 reduced courtship dramatically, while the silencing of other identified neurons had either minor impact or no impact on courtship. This suggests that P1 and aSP2 are necessary for courtship and may play a role in integrating multiple sensory signals which are required for

courtship. The extensive overlap of these neurons in the brain suggests potential connections and involvement in mediating and integrating sensory inputs.

Thus, in this study, we developed new tools providing restricted genetic access to individual *fru+* neurons and obtained a more detailed anatomical map of *fru+* neurons. Moreover, we identified *fru+* neurons involved in specific courtship steps such as courtship song and copulation. Another different approach allowed isolation of different types of *fru+* neurons that promote the courtship behavior.

Zusammenfassung

Angeborene Verhaltensweisen beruhen auf genetisch determinierten Verschaltungen im Nervensystem. Das bemerkenswerteste angeborene Verhaltensmuster von *Drosophila melanogaster* ist das Balzverhalten. Während der Balz verarbeiten männliche Fliegen vielfache sensorische Reize von weiblichen Fliegen. Wie kann das stereotyp verschaltete Nervensystem diese Reize wahrnehmen und prozessieren um darauf beruhend Entscheidungen über das Balzverhalten zu treffen?

Laut einem gängigen Modell bilden Neurone, die *fruitless* exprimieren (*fru+* Neurone) einen spezifischen Schaltkreis für das Balzverhalten, das für dieses unabhömmlich ist. Das Ziel der vorliegenden Arbeit ist es, die Bestandteile dieses neuronalen Schaltkreises anatomisch und funktional zu charakterisieren. Um ausgewählte *fru+* Neurone zu manipulieren, wurde ein FLP-in System und eine neuartige Bibliothek von GAL4 Linien (VT Linien) verwendet und ein anatomischer Screen durchgeführt. Im Vergleich zu Enhancer Trap GAL4 Linien exprimieren VT Linien in kleineren Teilmengen der *fru+* Neurone, was es möglich machte, verschiedene Klassen von *fru+* Neuronen zu beschreiben und sie in den Schaltplan für das Balzverhalten einzufügen.

Für eine funktionelle Charakterisierung der *fru+* Neurone wurden neuronale Aktivierungsscreens durchgeführt. Auf diese Weise wurden vier verschiedene Klassen von *fru+* Neuronen identifiziert, die bei Aktivierung Balzgesang evozieren (P1, pIP10, dPR1 und vPR6) sowie die neuronale Klasse vMS11, die bei thermischer Aktivierung einseitige Flügelbewegung hervorruft. Die Inaktivierung dieser Neurone vermindert die Produktion von Balzgesang. Des Weiteren wurden sechs neuronale Klassen gefunden, die bei Aktivierung eine Krümmung des Abdomen induzieren (dAB4, dAB5, dAB8, dMT3, vAB2 und dAB7). Die Inaktivierung von dAB4 oder dAB5 hat keinen Einfluss auf die Intensität des Balzverhaltens, verhindert aber die Kopulation. Das weist darauf hin, dass dAB4 und dAB5 spezifisch für das Kopulationsverhalten benötigt werden.

Um *fru+* Neurone ausfindig zu machen, die die Balzmotivation steuern, wurde ein thermischer Aktivierungsscreen in der Anwesenheit einer zweiten, als Balzobjekt dienenden männlichen Fliege durchgeführt. In diesem Screen wurden die neuronalen Klassen P1 und LAN1 gefunden, von denen bereits zuvor bekannt war, dass ihre Aktivierung an ein Männchen gerichtetes Balzverhalten hervorrufen kann. Zusätzlich wurden zwei Unterklassen von P1 (pMP4 und pMP4_1) und 4 andere Klassen von *fru+* Neuronen (aSP2, pIP6, aSP21, aSP4)

identifiziert, die an ein Männchen gerichtetes Balzverhalten auslösen, wenn sie aktiviert werden. Die Inaktivierung von P1 und aSP2 vermindern das Balzverhalten dramatisch, wohingegen die Inaktivierung der anderen neuronalen Klassen nur einen geringen oder keinen messbaren Einfluss auf das Balzverhalten hat. P1 und aSP2 sind Kandidaten für Sensorische Integration, die für das Balzverhalten benötigt werden. Die großen Überlappungsbereiche der Arborisierungen dieser Neurone im Hirn legt es nahe, dass sie miteinander verbunden sind und deutet darauf hin, dass sie möglicherweise sensorische Reize verarbeiten und integrieren.

In der vorliegenden Arbeit wurde ein verfeinerter und detaillierter anatomischer Schaltplan der *fru+* Neuronen erstellt und Neurone identifiziert, die eine funktionelle Rolle für den Balzgesang, das Kopulationsverhalten und die Balzmotivation spielen.

1.Introduction

1.1.Overview

The nervous system senses external environment, processes it in order to make sense, and executes behaviors through motor control. One of the major goals of neuroscience is to understand how the nervous system achieves these tasks. The nervous system is composed of various circuits which in turn are composed of individual neurons. The simplest components of the circuit would be, first, sensory neurons which are involved in sensing external environment and generate sensory representations, second, integration neurons which receive those various sensory inputs to create commands, third command neurons which conveys command to central pattern generator, fourth interneurons that produce the patterns of neural activity underlying behaviors and lastly the motor neurons to control the muscles. In order to understand how an individual circuit collects the stimuli and process them to generate behaviors, neuronal building blocks need to be identified and manipulated to test their role in behavior. *Drosophila melanogaster* is a great model organism for this purpose, with a relatively small and stereotyped nervous system compared to vertebrates while presenting rich behaviors. What makes it most attractive as a model organism for neuroscience is its well established genetic toolbox which enables individual neurons to be targeted for investigation.

1.2. Courtship ritual

One of the most conspicuous behaviors of *D. melanogaster* is its courtship ritual. When a *D. melanogaster* male encounters a virgin female, he may initiate courtship ritual. The courtship ritual consists of orientating towards the female, following her, tapping her abdomen, unilateral wing extension, wing vibration, licking of her genitalia and ultimately copulation attempt and copulation (Hall, 1994; Sokolowski, 2001).

During the courtship ritual, males and females perceive their chemical profiles of the opposite sex which include both volatile and nonvolatile pheromones. Female-enriched nonvolatile cuticular hydrocarbons, 7,11-heptacosadiene (7,11-HD) and 7,11-nonacosadiene (7,11-ND) can stimulate males to court (Ferveur, 2005; Jallon, 1984). Chemical profile is not only used to attract males to females but also for males to discriminate sex and species, and to assess the quality of female. A *D. melanogaster* female which lack the cuticle hydrocarbon is vigorously courted by other *Drosophila* species (Billeter et al., 2009). The cuticle of *D.*

melanogaster males are enriched in 7-tricosene (7T) which serves as repulsive signal and allows male to discriminate females from males (Ferveur, 2005; Jallon, 1984; Thistle et al., 2012). A volatile hydrocarbon, 11-cis-vaccenyl acetate (cVA), that is enriched in males also serves as repulsive cue for male and stimulates female receptivity (Kurtovic et al., 2007). cVA is transferred from males to females during copulation which then allows experienced males to discriminate virgins and mated females (Keleman et al., 2012)

Unilateral wing extension and its vibration by male flies during the courtship ritual generate the courtship song (Shorey, 1962). Courtship song is crucial for successful copulation since the wingless males show very low levels of copulation success (Bennet-Clark et. al., 1967). Playback of recorded courtship song can rescue the low level of copulation success to the wild type level (Bennet-Clark et. al., 1967). This indicates that the low level of courtship success of wingless male is due to low female receptivity. The courtship song consists of sine songs and pulse songs. Sine songs are humming sound which are proposed to have priming effect on female receptivity (Schilcher, 1976). However, the key component of the courtship song appears to be the pulse song. Playback of the pulse song is sufficient to rescue the low level of copulation of wingless males (Bennet-Clark et. al., 1967). The interval between each pulse (IPI, interpulse interval) is species-specific (Watson et. al., 2007). Playback of the pulse song with the *D. melanogaster* IPI (~34ms) stimulates female receptivity the most compared to playback of other species songs, suggesting that IPI is used for species recognition (Ritchie et al., 1999; Schilcher, 1976).

1.3. fruitless

Investigation of the genetic basis of this behavior was initiated almost 50 years ago by the discovery of a mutant *fru*¹ generated by an X-radiation mutagenesis screen (Gill, 1963). This mutation is a recessive mutation, located on the third chromosome and causes male sterility (Gailey and Hall, 1989). Various *fru* mutants were identified through deletion or P-element insertion (Castrillon et al., 1993; Ito et al., 1996). The linkage between the gene *fruitless* and this courtship defect was made in 1996 (Ito et al., 1996; Ryner et al., 1996). The *fru* gene has eight exons that are spliced in various ways and controlled by four different promoters (P1-P4). The critical promoter for courtship behavior is the P1 promoter and its product is different between male and females (Goodwin et al., 2000). The transcript from the P1 promoter contains S-exon which is spliced differentially in males and females. In females

binding of *transformer* (*tra*) and *transformer-2* (*tra-2*) to the S-exon splice the S-exon out, while in male S-exon remain due to the absence of *tra*. This generates an early stop codon in female and gives rise to no protein. In males, P1 promoter gives rise to Fru^M proteins which contain 101 amino acids translated from S-exon. Transcripts from other promoters (P2-P4) are called Fru^{COM} which are crucial during development in both sexes (Anand et al., 2001; Ryner et al., 1996). The loss of Fru^M proteins demasculinizes neuronal arborizations and their expression in female masculinizes them (Datta et al., 2008; Mellert et al., 2009).

What is the molecular function of Fru protein? Fru proteins contain two known motifs; BTB domain and Zn-finger motif. BTB domains are commonly found in *Drosophila* transcription factors which mediate hetero- or homodimerisation (Zollman et al., 1994). Exons of the C-terminus of *fru* isoforms contain a Zn-finger motif, which is a DNA binding domain. The presence of these two motifs implies that Fru is a transcription factor. Recently, Fru^M protein has been shown to bind to two chromatin regulators through a cofactor Bonus (*bon*) (Ito et al., 2012). Fru^M protein can recruit either Histone deacetylase 1, which masculinizes sexually dimorphic neurons or Heterochromatin protein 1 (HP1), which demasculinizes them.

Fru^M proteins are not only necessary but also sufficient for courtship behavior (Demir and Dickson, 2005; Manoli et al., 2005). Females which have their *fru* transcripts spliced in the male manner follow and sing to another female, which is never observed in normal females. (Demir and Dickson, 2005). Similarly, Fru^M overexpression with its endogenous promoter in female generates certain aspects of courtship behavior in wild-type females (Manoli et al., 2005).

1.4. *fruitless* is expressed in the adult nervous system

fruitless is found to be expressed in ~1700 neurons (*fru+* neurons) in the adult *D. melanogaster* central nervous system (CNS) (Lee et al., 2000). This was later confirmed by the expression of GAL4 under the control of endogenous *fruitless* promoter (Manoli et al., 2005; Stockinger et al., 2005). Furthermore, *fru+* neurons are present not only in the CNS but also in the peripheral nervous system such as eye, antenna, proboscis, leg, wing, accessory organ and external genitalia (Billeter and Goodwin, 2004; Manoli et al., 2005; Stockinger et al., 2005). This implies that the *fru+* neurons may play roles in sensory input, sensory integration, command generation and motor control.

Are the *fru+* neurons required for courtship behavior? The synaptic silencing of *fru+* neurons dramatically reduces courtship behavior toward target females without interrupting other general behaviors (Manoli et al., 2005; Stockinger et al., 2005). Specific silencing of *fru+* olfactory and visual neurons impairs courtship behavior (Stockinger et al., 2005). Do only the *fru+* olfactory and visual neurons play roles in courtship behavior? This does not seem to be the case. When the rest of *fru+* neurons are silenced, males perform courtship poorly (Stockinger et al., 2005). These experiments indicate the functional necessity of both the peripheral and central *fru+* neurons for courtship behavior. Additionally, artificial activation of all *fru+* neurons through photoactivatable or thermosensitive cation channels can elicit courtship song and abdominal bending, suggesting that *fru+* neurons are sufficient to produce the courtship behavior (Clyne and Miesenbock, 2008; Pan et al., 2011). Collectively, these anatomical and functional investigations suggest that *fru+* neurons form the basis of the neuronal circuit which regulates the courtship behavior. The further investigation is crucial to understand how this courtship circuit functions at the level of individual neuronal types.

1.5. Anatomy of individual *fru+* neurons

In order to address how the *fru+* courtship circuit functions, we need to characterize individual *fru+* neurons and determine their functional role. The anatomical map of individual *fru+* neurons was made by labeling of subsets of *fru+* neurons by MARCM or a FLP-in method (Cachero et al., 2010; Yu et al., 2010). These studies provided several insights into the anatomical organization of *fru+* neurons. *fru+* neurons are classified into 100 types of anatomically distinct neurons. One type of neuron can consist of one to ~30 neurons that share several anatomical features such as cell body location, axonal tract and regions where they innervate. *fru+* neurons consist of second order or higher order neurons that convey and integrate various sensory inputs as well as sensory neurons itself. There are also *fru+* descending or ascending neurons that enable the communication between integration neurons in the brain and motor control neurons in the ventral nerve cord (VNC). There are various types of *fru+* neurons in the VNC as well which may function as part of central pattern generator (CPG) or directly control muscles regulating the wings or the abdomen. A region of dense innervation of many types of *fru+* neurons is found in the brain which is called as lateral protocerebral complex (LPC) or male enlarged region (MER) (Figure S1A and B) (Cachero et al.,

2010; Yu et al., 2010). This region is hypothesized to be the integration center. Individual types of *fru+* neurons are largely sexually dimorphic both in the cell number and the arborization.

1.6. Function of individual *fru+* neurons

What is the function of individual *fru+* neurons? There are only a small number of *fru+* neurons whose function has been reported. There are three glomeruli in the antenna lobe which are larger in male than females. These glomeruli are innervated by *fru+* positive olfactory receptor neurons (ORNs). One of them, DA1 innervated by Or67d+ ORNs (Kurtovic et al., 2007). Or67d responds to male specific volatile pheromone cVA (Kurtovic et al., 2007). cVA can inhibit male's courting males and promote female receptivity through Or67d (Billeter et al., 2009; Kurtovic et al., 2007). The projection neurons (PNs) which innervate DA1 are *fru* positive as well. PNs are second order neurons which convey the olfactory signal to the mushroom body (MB) and lateral horn (LH). Two types of *fru+* neurons, aSP5 and aSP8, have been shown to be functionally connected with DA1 PNs in the LH (Datta et al., 2008). Their functional relevance to the cVA-mediated behaviors in males and females is not yet clear. Another sexually dimorphic glomerulus is VA1v, where Or47b+ ORNs innervate. Or47b responds to both male and female extracts (van der Goes van Naters and Carlson, 2007). The genetic perturbation of Or47b+ ORN increases latency of courtship initiation (Root et al., 2008). The other sexually dimorphic glomerulus is VL2a, where Ir84a+ ORNs innervate. Ir84a responds to phenylacetic acid and phenylacetaldehyde, which are widely present in fruit (Grosjean et al., 2012). *Ir84a* mutant males court target females less vigorously than wild-type males (Grosjean et al., 2012). The downstream neurons of the PNs innervating VA1v and VL2a are unknown.

Two nonvolatile pheromones 7,11-HD and 7,11-ND are enriched in females and enhances male courtship behavior (Ferveur, 2005; Jallon, 1984). *ppk23+ fru+* double positive foreleg afferent neurons, LAN1, are necessary for this response and their activation is sufficient to enhance courtship behavior (Thistle et al., 2012; Toda et al., 2012). Sensilla recording and Ca²⁺ imaging of LAN1 revealed that they physiologically respond to 7,11-HD and 7,11-ND (Thistle et al., 2012; Toda et al., 2012). The second order neuron of LAN1 is not identified yet.

Gr32a positive foreleg afferent neurons are required for appropriate unilateral wing extension toward the target female (Koganezawa et al., 2010). *Gr32a* positive neurons innervate subesophageal ganglion (SOG) and overlap with the dendrites of mAL, which is also

known as aDT2 (Kimura et al., 2005; Koganezawa et al., 2010). The neuronal silencing of mAL increases frequency of bilateral wing extension during courtship (Koganezawa et al., 2010).

The function of few *fru+* neurons has been disclosed in the central nervous system. Males in which RNAi against Fru^M is expressed in the *fru+* neurons mcAL, which is also known as aDT6, display a shortened courtship ritual, simultaneously vibrate their wings and prematurely attempt copulation, suggesting that mcAL is required to maintain the proper sequence of the courtship ritual (Manoli and Baker, 2004). *Drosophila* males, after the experience of rejection by mated females, court mated females less vigorously than the males without such rejection experience. A type of *fru+* dopaminergic neurons, aSP13, has been identified to be necessary for this courtship learning (Keleman et al., 2012).

P1 is the most well studied *fru+* neurons. It has first been identified as a male-specific neuronal class whose masculinization in the female brain potentiates females to follow and extend the unilateral wing toward target females. (Kimura et al., 2005). Such behavior is otherwise never observed in wild-type females. Thermal activation of P1 with trpA1 can elicit courtship song (Kohatsu et al., 2011; von Philipsborn et al., 2011). P1 is a male-specific neuronal class and innervates the LPC, thus it is proposed to be an integration neuron. Activation of a descending *fru+* neuron pIP10 which is contained in P2b can trigger courtship song as well (Kohatsu et al., 2011; von Philipsborn et al., 2011). In the VNC, 3 types of *fru+* neurons, dPR1, vPR6 and vMS11, are found to be able to trigger courtship song or unilateral wing extension upon heat-induced activation (von Philipsborn et al., 2011). pIP10, dPR1, vPR6 and vMS11 innervate the mesothoracic triangle and overlap with each other, which suggests that they form synaptic connections with each other (Figure S1G) (von Philipsborn et al., 2011).

Aim of thesis

D. melanogaster males display courtship ritual as an innate behavior. This behavior is regulated by *fruitless* which is sex specifically spliced and translated only in male. *fruitless* is expressed in ~1700 neurons in the adult nervous system. Those *fru+* neurons can be anatomically classified into 100 types of neurons which are proposed to form courtship circuit. *fru+* neurons are functionally necessary and to some extent sufficient for courtship behavior, providing a good entry point to understand how the courtship circuit executes the innate reproductive behavior. The functions of *fru+* neurons have been investigated but the functional organization and regulation of the courtship circuit is still unknown. The first aim of

this study is to extend the anatomical mapping of fru+ neurons by a new collection of sparse GAL4 lines. While this anatomical study yielded good insight into the organization of fru+ neurons and their potential functions, additional experiments were necessary to further support functional connections proposed by anatomical data. Thus, we performed functional screens by artificially activating different types of fru+ neurons in order to elucidate the functional components of courtship circuit in singing, copulation and courtship promotion. In the long run, we expect that the anatomical mapping and functional mapping of fru+ neurons compensate each other and enable us to elucidate the neuronal basis underlying the courtship behavior.

References

- Anand, A., Vilella, A., Ryner, L.C., Carlo, T., Goodwin, S.F., Song, H.J., Gailey, D.A., Morales, A., Hall, J.C., Baker, B.S., *et al.* (2001). Molecular genetic dissection of the sex-specific and vital functions of the *Drosophila melanogaster* sex determination gene *fruitless*. *Genetics* *158*, 1569-1595.
- Bennet-Clark, H.C., and Ewing, A.W. (1967). Stimuli provided by Courtship of Male *Drosophila melanogaster*. *Nature* *215*, 669-671.
- Billeter, J.C., Atallah, J., Krupp, J.J., Millar, J.G., and Levine, J.D. (2009). Specialized cells tag sexual and species identity in *Drosophila melanogaster*. *Nature* *461*, 987-991.
- Billeter, J.C., and Goodwin, S.F. (2004). Characterization of *Drosophila fruitless-gal4* transgenes reveals expression in male-specific *fruitless* neurons and innervation of male reproductive structures. *J Comp Neurol* *475*, 270-287.
- Cachero, S., Ostrovsky, A.D., Yu, J.Y., Dickson, B.J., and Jefferis, G.S. (2010). Sexual dimorphism in the fly brain. *Curr Biol* *20*, 1589-1601.
- Castrillon, D.H., Gonczy, P., Alexander, S., Rawson, R., Eberhart, C.G., Viswanathan, S., DiNardo, S., and Wasserman, S.A. (1993). Toward a molecular genetic analysis of spermatogenesis in *Drosophila melanogaster*: characterization of male-sterile mutants generated by single P element mutagenesis. *Genetics* *135*, 489-505.
- Clyne, J.D., and Miesenbock, G. (2008). Sex-specific control and tuning of the pattern generator for courtship song in *Drosophila*. *Cell* *133*, 354-363.
- Datta, S.R., Vasconcelos, M.L., Ruta, V., Luo, S., Wong, A., Demir, E., Flores, J., Balonze, K., Dickson, B.J., and Axel, R. (2008). The *Drosophila* pheromone cVA activates a sexually dimorphic neural circuit. *Nature* *452*, 473-477.
- Demir, E., and Dickson, B.J. (2005). *fruitless* splicing specifies male courtship behavior in *Drosophila*. *Cell* *121*, 785-794.
- Ferveur, J.F. (2005). Cuticular hydrocarbons: their evolution and roles in *Drosophila* pheromonal communication. *Behav Genet* *35*, 279-295.
- Gailey, D.A., and Hall, J.C. (1989). Behavior and cytogenetics of *fruitless* in *Drosophila melanogaster*: different courtship defects caused by separate, closely linked lesions. *Genetics* *121*, 773-785.

- Goodwin, S.F., Taylor, B.J., Vilella, A., Foss, M., Ryner, L.C., Baker, B.S., and Hall, J.C. (2000). Aberrant splicing and altered spatial expression patterns in fruitless mutants of *Drosophila melanogaster*. *Genetics* *154*, 725-745.
- Grosjean, Y., Rytz, R., Farine, J.P., Abuin, L., Cortot, J., Jefferis, G.S., and Benton, R. (2012). An olfactory receptor for food-derived odours promotes male courtship in *Drosophila*. *Nature* *478*, 236-240.
- Hall, J.C. (1994). The mating of a fly. *Science* *264*, 1702-1714.
- Ito, H., Fujitani, K., Usui, K., Shimizu-Nishikawa, K., Tanaka, S., and Yamamoto, D. (1996). Sexual orientation in *Drosophila* is altered by the satori mutation in the sex-determination gene fruitless that encodes a zinc finger protein with a BTB domain. *Proc Natl Acad Sci U S A* *93*, 9687-9692.
- Ito, H., Sato, K., Koganezawa, M., Ote, M., Matsumoto, K., Hama, C., and Yamamoto, D. (2012). Fruitless recruits two antagonistic chromatin factors to establish single-neuron sexual dimorphism. *Cell* *149*, 1327-1338.
- Jallon, J.M. (1984). A few chemical words exchanged by *Drosophila* during courtship and mating. *Behav Genet* *14*, 441-478.
- Keleman, K., Vrontou, E., Kruttner, S., Yu, J.Y., Kurtovic-Kozaric, A., and Dickson, B.J. (2012). Dopamine neurons modulate pheromone responses in *Drosophila* courtship learning. *Nature* *489*, 145-149.
- Kimura, K., Ote, M., Tazawa, T., and Yamamoto, D. (2005). Fruitless specifies sexually dimorphic neural circuitry in the *Drosophila* brain. *Nature* *438*, 229-233.
- Koganezawa, M., Haba, D., Matsuo, T., and Yamamoto, D. (2010). The shaping of male courtship posture by lateralized gustatory inputs to male-specific interneurons. *Curr Biol* *20*, 1-8.
- Kohatsu, S., Koganezawa, M., and Yamamoto, D. (2011). Female contact activates male-specific interneurons that trigger stereotypic courtship behavior in *Drosophila*. *Neuron* *69*, 498-508.
- Kurtovic, A., Widmer, A., and Dickson, B.J. (2007). A single class of olfactory neurons mediates behavioural responses to a *Drosophila* sex pheromone. *Nature* *446*, 542-546.
- Lee, G., Foss, M., Goodwin, S.F., Carlo, T., Taylor, B.J., and Hall, J.C. (2000). Spatial, temporal, and sexually dimorphic expression patterns of the fruitless gene in the *Drosophila* central nervous system. *J Neurobiol* *43*, 404-426.

- Manoli, D.S., and Baker, B.S. (2004). Median bundle neurons coordinate behaviours during *Drosophila* male courtship. *Nature* 430, 564-569.
- Manoli, D.S., Foss, M., Vilella, A., Taylor, B.J., Hall, J.C., and Baker, B.S. (2005). Male-specific fruitless specifies the neural substrates of *Drosophila* courtship behaviour. *Nature* 436, 395-400.
- Mellert, D.J., Knapp, J.M., Manoli, D.S., Meissner, G.W., and Baker, B.S. (2009). Midline crossing by gustatory receptor neuron axons is regulated by fruitless, doublesex and the Roundabout receptors. *Development* 137, 323-332.
- Pan, Y., Robinett, C.C., and Baker, B.S. (2011). Turning males on: activation of male courtship behavior in *Drosophila melanogaster*. *PLoS One* 6, e21144.
- Root, C.M., Masuyama, K., Green, D.S., Enell, L.E., Nassel, D.R., Lee, C.H., and Wang, J.W. (2008). A presynaptic gain control mechanism fine-tunes olfactory behavior. *Neuron* 59, 311-321.
- Ryner, L.C., Goodwin, S.F., Castrillon, D.H., Anand, A., Vilella, A., Baker, B.S., Hall, J.C., Taylor, B.J., and Wasserman, S.A. (1996). Control of male sexual behavior and sexual orientation in *Drosophila* by the fruitless gene. *Cell* 87, 1079-1089.
- Shorey, H.H. (1962). Nature of the Sound Produced by *Drosophila melanogaster* during Courtship. *Science* 137, 677-678.
- Sokolowski, M.B. (2001). *Drosophila*: genetics meets behaviour. *Nat Rev Genet* 2, 879-890.
- Stockinger, P., Kvitsiani, D., Rotkopf, S., Tirian, L., and Dickson, B.J. (2005). Neural circuitry that governs *Drosophila* male courtship behavior. *Cell* 121, 795-807.
- Thistle, R., Cameron, P., Ghorayshi, A., Dennison, L., and Scott, K. (2012). Contact chemoreceptors mediate male-male repulsion and male-female attraction during *Drosophila* courtship. *Cell* 149, 1140-1151.
- Toda, H., Zhao, X., and Dickson, B.J. (2012). The *Drosophila* Female Aphrodisiac Pheromone Activates ppk23(+) Sensory Neurons to Elicit Male Courtship Behavior. *Cell Rep* 1, 599-607.
- van der Goes van Naters, W., and Carlson, J.R. (2007). Receptors and neurons for fly odors in *Drosophila*. *Curr Biol* 17, 606-612.
- von Philipsborn, A.C., Liu, T., Yu, J.Y., Masser, C., Bidaye, S.S., and Dickson, B.J. (2011). Neuronal control of *Drosophila* courtship song. *Neuron* 69, 509-522.

- WATSON, E., RODEWALD, E., and COYNE, J.A., (2007). The courtship song of *Drosophila santomea* and a comparison to its sister species *D. yakuba* (Diptera: Drosophilidae) *Eur. J. Entomol.* 104: 145–148,
- Yu, J.Y., Kanai, M.I., Demir, E., Jefferis, G.S., and Dickson, B.J. (2010). Cellular organization of the neural circuit that drives *Drosophila* courtship behavior. *Curr Biol* 20, 1602-1614.
- Zollman, S., Godt, D., Prive, G.G., Couderc, J.L., and Laski, F.A. (1994). The BTB domain, found primarily in zinc finger proteins, defines an evolutionarily conserved family that includes several developmentally regulated genes in *Drosophila*. *Proc Natl Acad Sci U S A* 91, 10717-10721.

2. Anatomical dissection of fruitless neurons

2.1. Motivation

Two studies were dedicated to characterize individual types of *fruitless* neurons (*fru+* neurons) (Cachero et al., 2010; Yu et al., 2010). One used a method to achieve stochastic clonal labeling of *fru+* neurons, which is called mosaic analysis with a repressible cell marker (MARCM) (Cachero et al., 2010; Lee and Luo, 1999). MARCM enabled sparse labeling of *fru+* neurons revealing their anatomical dimorphism, but has its limitation in the fact that we cannot target the same cell repeatedly in an efficient manner. The latter study, taking the advantage of FLP recombinase expressed under the *fru* promoter, used a FLP-in system (Yu et al., 2010). By using a reporter construct which harbors a stop cassette flanked by two FRT sites between UAS (upstream activating sequence) and the reporter (UAS>stop>reporter), the expression of reporter driven by Gal4 can be restricted to the neurons expressing FLP recombinase, namely *fru+* neurons (Figure 1A). By using different sets of Gal4 driver, different sets of *fru+* neurons become easily and repeatedly accessible. The FLP-in system poses the following challenges firstly to get enough large collection of Gal4 drivers to cover the entire *fru+* neurons and secondly to find a sparse enough collection of Gal4 drivers to target individual *fru+* neurons. Indeed, MARCM analysis of *fru+* neurons reveals larger number of types of *fru+* neurons than that of FLP-in system with *fru*^{FLP} (Cachero et al., 2010; Yu et al., 2010). The Gal4 collection used in Yu et al., 2010 was conventional enhancer trap lines, which were generated by random insertion of the Gal4-containing P element. Each driver of this collection labeled approximately two dozens of types of *fru+* neurons with FLP-in system (Figure 1D) which prevent the assessment of the functionality of the *fru+* neurons. To further understand the *fru+* neurons anatomically and functionally, we performed a screen with new set of Gal4 driver.

2.2. Genetic tools to characterize *fru+* neurons

In order to genetically dissect *fru+* neurons we used FLP- in system as described before (Yu et al., 2010). For the Gal4 drivers, we used an enhancer tile library (Vienna tiles, VT lines) which was made in the lab based on the strategy described in (Pfeiffer et al., 2008), expecting that we can get sparser labeling of *fru+* neurons. Shortly, a 2-3 kb of DNA fragment was cloned

to drive the expression of Gal4 and then transgenic flies were generated with *phiC31* site-specific integration (Groth et al., 2004)(Masser 2011; Bidaye 2012).

In order to collect VT lines that label a subset of *fru*⁺ neurons, we have screened 3233 VT lines by crossing them with *UAS>stop>tauLacZ; fru^{FLP}* (Figure 1B). We dissected brains and VNCs and subjected them to X-gal staining. When there are overlap neurons between *fru*⁺ neurons and Gal4-expressing neurons, we could observe some blue staining in such neurons (Figure 1B). In total, we found 1283 VT lines labeling *fru*⁺ neurons with this screen.

2.3 Genetic dissection of *fru*⁺ neurons with VT lines

We selected 473 lines for further anatomical analysis of *fru*⁺ neurons based on sparse X-gal staining. We crossed these 473 VT lines with *UAS>stop>mCD8GFP; fru^{FLP}*, carried out antibody staining and image acquisition with confocal microscope to identify which types of *fru*⁺ neurons are labeled by individual VT lines. We used neuropil staining, nc82 staining, as a reference to guide nonrigid image registration (Jefferis et al., 2007; Rohlfing and Maurer, 2003). This allowed us to compare *fru*⁺ neurons between different samples. We analyzed male brains and ventral nerve cords (VNCs) for all those 473 lines and female brains and VNCs for 289 VT lines.

473 VT lines show 96% coverage of previously described neurons by conventional Gal4 enhancer trap lines in Yu et al., 2010 (96 types out of 100 types, Figure 1C). This indicates that VT lines do not have biased labeling of *fru*⁺ neurons compared to conventional Gal4 enhancer trap lines. As expected the average number of the types of *fru*⁺ neurons labeled by a single VT line is much less than that by conventional Gal4 enhancer trap lines (4.6 ± 0.16 by a VT line, 25.4 ± 1.4 by a enhancer trap line, Figure 1D). The tendency of sparse labeling by VT lines is both true in brain and VNC (Figure 1D). We also generated a catalogue of VT lines and *fru*⁺ neurons (data not shown). This catalogue enables us to find the types of neuron labeled by a certain VT line or the VT lines which label a certain *fru*⁺ neuron. Thanks to the sparseness, we could also elucidate the uncharacterized arborizations of 19 types of *fru*⁺ neurons and subdivided aSP8 and pMP4 into 2 types of neurons respectively (Figure S2). In addition to the 100 previously described types of *fru*⁺ neurons, we could identify additional 54 types of *fru*⁺ neurons which are morphologically distinctive from what has been described before with same FLP-in system (Figure 2A-D and S3) (Yu et al., 2010).

In this study, a “type” of neurons can be composed of 1-30 neurons which are morphologically distinctive from other types of neurons. Neurons in the *D. melanogaster* nervous system are typically generated from neuronal progenitors, called as neuroblasts (NB), which undergo asymmetric divisions to generate a neuroblast and intermediate progenitors, called as ganglion mother cells (GMCs). GMCs can further undergo a symmetric division to create two sibling post-mitotic cells. Neuroblasts can be identified by their position and sibling neurons derived from the same NBs share the same axon tract (Doe, 1992; Lee, 2009; Lin and Lee, 2012; Yu et al., 2009). Thus we first used the position of cell body and the axon tracts as landmarks to distinguish between different types of neurons. The position of the cell bodies can be variable to some extent, but the axon tracts have little variability between samples (Figure S4A). The regions where neurons innervate, arborizations, are also used to discriminate different types of neurons. For example, although the cell bodies of aSP12 and aSP20 are close and their axon tracts are partially shared (Figure S4B and S4C), their arborizations clearly indicate the difference between them (Figure S4B). One type of neurons that we describe in this study, of course, can potentially be further subdivided anatomically and functionally, but it is the minimum set of neurons that we can subdivided anatomically with our labeling method.

Each of these new 54 types of *fru+* neurons were labeled by multiple VT lines (9.0 ± 2.0 , average \pm SEM) and observed in different brain or VNC samples. Thus, we believe those 54 types of *fru+* neurons are not morphologically distinctive because of some developmental error.

2.4. Anatomical overlap of *fru+* neurons

There is evidence that *fru+* neurons are involved in sensory processing, multimodal sensory integration and motor control (Cachero et al., 2010; Clyne and Miesenbock, 2008; Stockinger et al., 2005; Thistle et al., 2012; Toda et al., 2012; Yu et al., 2010). We segmented neuronal representation of cell body, projection and arborization from registered images. Based on the study of mammalian cortices, the structural synapses are formed on the overlap of dendrites and axons and the probability of having a certain number of synapses can be estimated from their overlap, which is known as Peter’s rule (Peters et al., 1976). Thus, we examined the overlap of arborizations and predicted potential connections at different regions of brain. Based on this analysis, we extended the courtship circuit diagram (Figure 2E) (Yu et.

al., 2010). Here, we will focus mainly on the detailed description of the 19 newly resolved neurons and 54 newly identified neurons by going through discrete regions of the brain and VNC involved in different functionalities.

Olfaction

Olfactory input is mediated by olfactory sensory neurons and relayed by projection neurons from the antenna lobe to mushroom body (MB) calyx and lateral horn (LH). It has been described that aSP5, aSP8, and aSP9 arborize at the anterior ventral part of LH which was proposed to be the integration site of volatile pheromones (Datta et al., 2008; Jefferis et al., 2007). We found aSP21 and pSP3 also arborize in the same region (Figure 3.1 A and B1). pSP3 arborizes in the dorsal part of LH as well (Figure 3.1 B1 and B2).

Vision

pIP3, pIP8 and LP1 were described as *fru*+ visual projection neurons which connect the lobula and the central brain (Yu et al., 2010). We found that pIP8 overlaps with pIP13 as well as aSP1 in the central brain (Figure 3.2B1). In the central brain, pIP3 arborizes at the ring part of the LPC and overlaps with aIP31, aIP3, aSP4, pIP1 and pIP2 (Yu et al., 2010). In this study, we found that pIP3 also overlaps with aSP21, aSP8_1, pIP13 (Figure 3.2B2). We confirmed the presence of LV with our FLP-in system (Kimura et al., 2005). LV arborizes at lobula and optic tubercle (OT) (Figure 3.2B3). In addition to aSP11, we found that aSP14, aSP16 and pIP2 arborize at OT. These three neurons then arborize at the LPC, providing another possible visual input to LPC (Figure 3.6B1) aIP6 arborizes at dorsal side of lobula and its arborization in the central brain overlaps with aSG4, pSG4, and pMP7 (Figure 3.2B4). We did not find any *fru*+ neuron that overlaps with LP1 in the central brain.

Audition

Auditory input is mediated through Johnston's organ neurons (JON) from antenna to antennal mechanosensory motor complex (AMMC). AMMC is innervated by aIP5 and aSP18 as well as aDT5 (Figure 3.3A, B). aIP5 arborizes at lateral crescent of LPC (Figure 3.7 B1), serving as a potential entry point from AMMC to LPC.

Gustation

Gustatory input is mediated through proboscis and legs. We could not identify any *fru+* sensory neuron coming from proboscis in this study. There are four types of *fru+* chemosensory neurons at legs; LAN1, LAN2, LAN3, LAN4. LAN1 is *ppk23+* *fru+* positive neurons and mediates female aphrodisiac pheromones 7,11-HD and 7,11-ND (Thistle et al., 2012; Toda et al., 2012). In addition to vAB3, we found 5 additional neurons that overlap with LAN1. They are dAB2, dPR2, dMS6, vPR7 and vPR11. dAB2, vAB3 and dMS6 are ascending neurons which can potentially convey gustatory input from LAN1 to brain.

Sensory integration

LPC has been proposed to be a major site for integration of individual sensory input (Figure S1B and E) (Yu et al., 2010). LPC was divided from its anatomical features into four parts; arch, lateral junction, ring and lateral crescent (Figure S1E).

We found additional nine types of *fru+* neurons that arborize at the arch part of LPC. One of them is pMP5, which is a descending neuron. Furthermore, there are three ascending neurons dMS3, vAB2, and dAB7 (Figure 3.5B1). aSP17, pSP5, vAB2, dAB7 and aSP21 arborize at lateral junction of LPC as well. Six of those nine neurons (aSP17, pMP5, pMP9, dMS3, vAB2, and dAB7) arborize at tritocerebral loop, suggesting a functional connection between the arch and tritocerebral loop (Figure 3.5B3 and Figure S1).

We found 11 types of *fru+* neurons that arborize in the ring part of LPC (Figure 3.6A and 3.6B1). Among them, dMS6 and vAB6 are ascending neurons. Most of them also overlap at the lateral junction of LPC (Figure 3.6B2)

Other integration sites

fru+ Kenyon cells of mushroom body innervate predominantly gamma lobe but alpha-beta lobe as well (Figure S2). aSP13 was identified to innervate the tip of the gamma lobe (Yu et al., 2010, Figure 3.9A, B). In this study, we identified aSP19 which innervate medial lobe and spur of gamma lobe (Figure 3.9A, B). Innervations of medial gamma lobe by aSP13 and aSP19 share only a small area of overlap (Figure 3.9B).

Central complex which is localized centrally in the brain was proposed to be involved in higher locomotor control (Strauss, 2002). Two *fru+* neurons, aSP20 and pSP6, innervate one neuropil of central complex, which is called fan-shape body.

Motor control

Activation of pIP10, dPR1, vPR6 and vMS11 through heat-sensitive cation channel elicit courtship song or wing extension (von Philipsborn et al., 2011). These neurons overlap all at mesothoracic triangle, indicating its relevance for the control of courtship song (Figure S1). In addition to dMS2 and pMP2, we found dPR2, vMS12, vPR10, and vPR11 localize at the mesothoracic triangle. dPR2, vPR10, and vPR11 overlap at the roof part of mesothoracic triangle where pMP2, pIP10, and dPR1 innervate (Figure 3.10B1). vMS12 and vPR10 overlap at the floor part of mesothoracic ganglion where vMS11, vPR6, and dMS2 innervate (Figure 3.10B2).

Nsyb-GAL4 UAS>stop>mCD8GFP fru^{FLP} reveals prominent innervations of *fru+* neurons at the dorsal side of metathoracic ganglion (Figure S1F). In addition to dAB3, pIP1, and pMP2, we found dMS7, dMT2, dMT4, dMT5, pSG2, and vAB5 innervate this dorsal part of metathoracic ganglion (Figure 3.11A and B). We do not know what kind of motor control these neurons are responsible for.

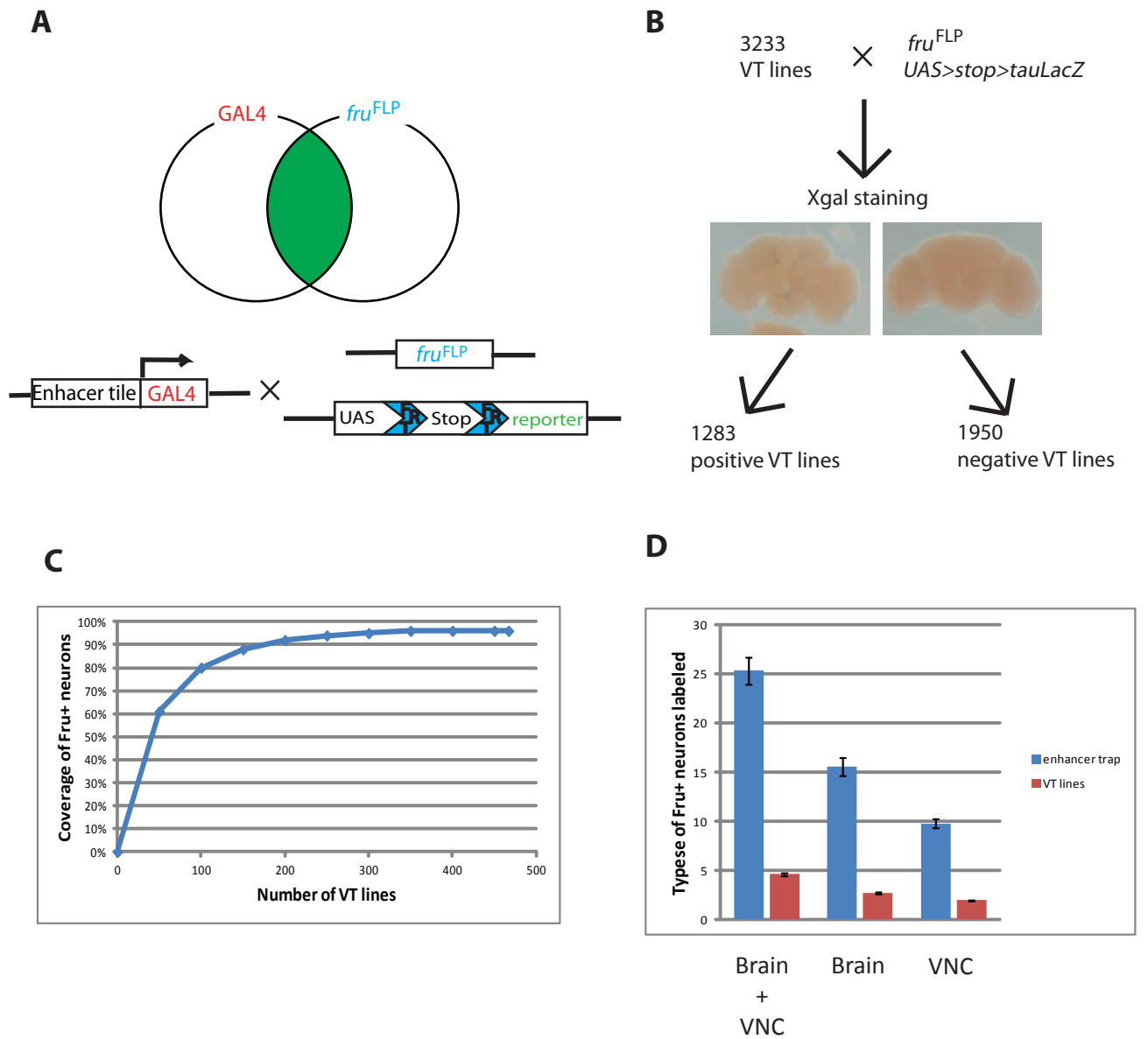


Figure 1

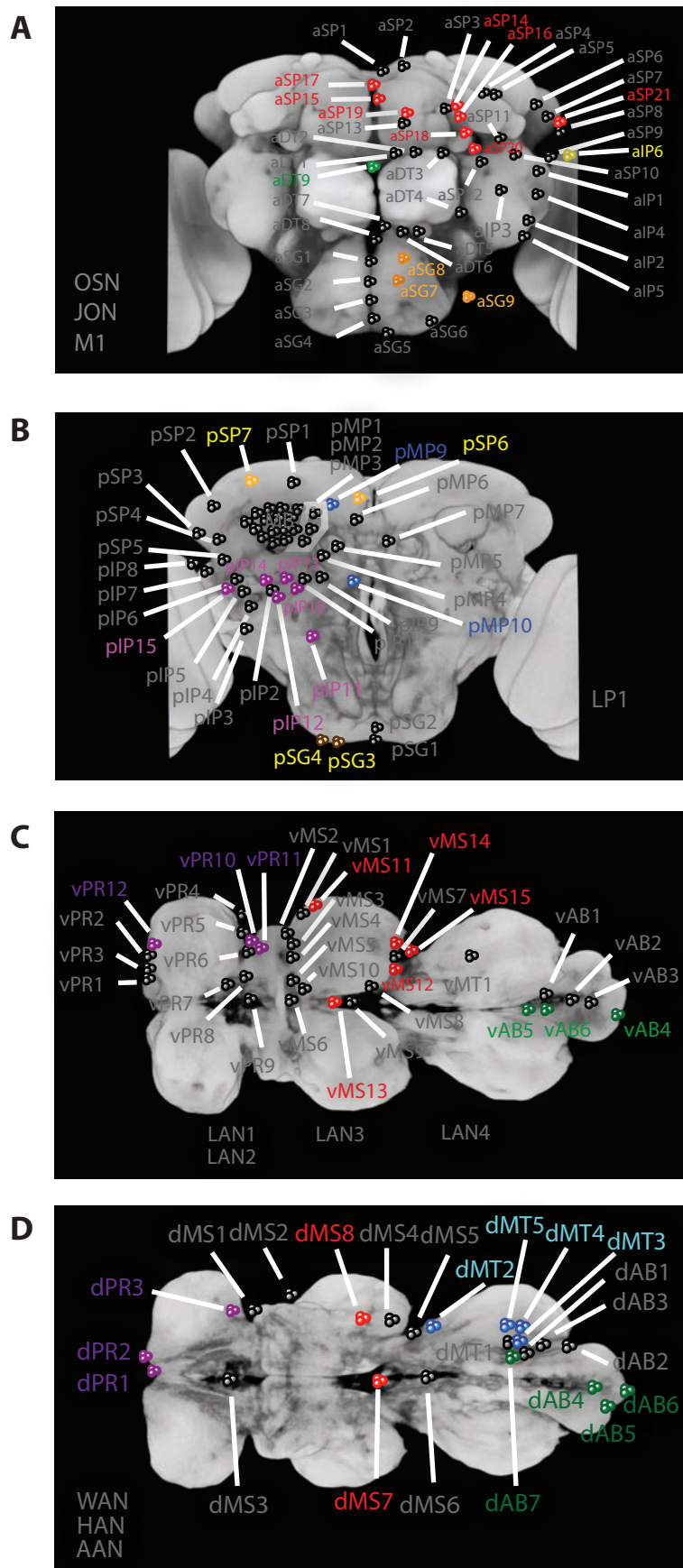
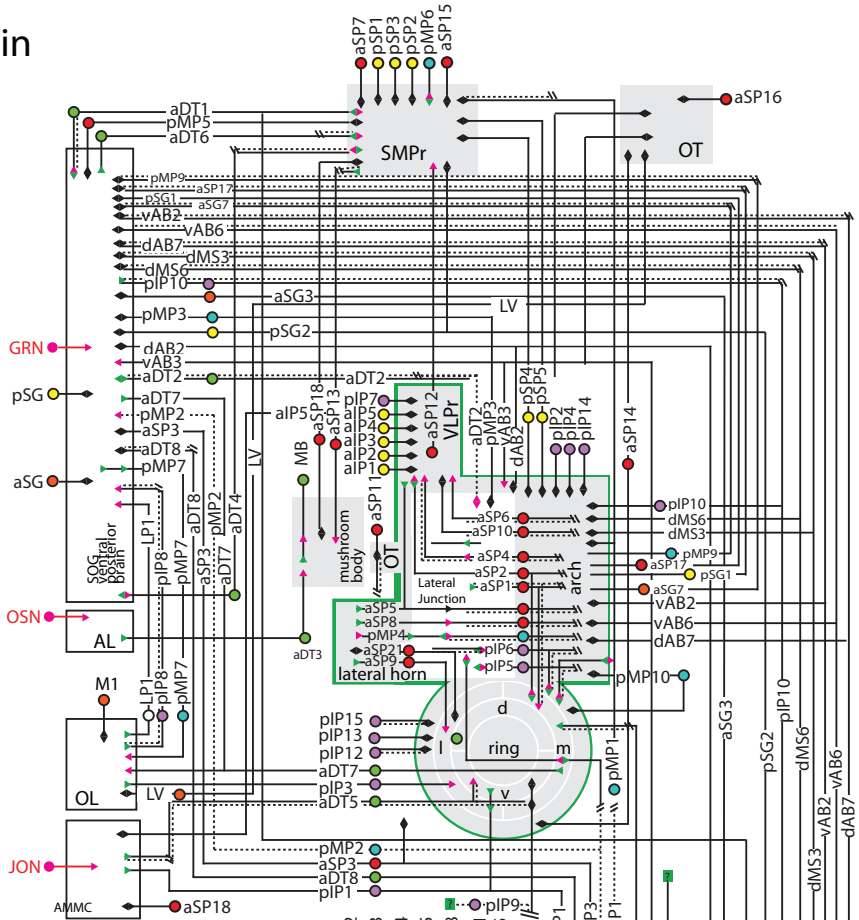
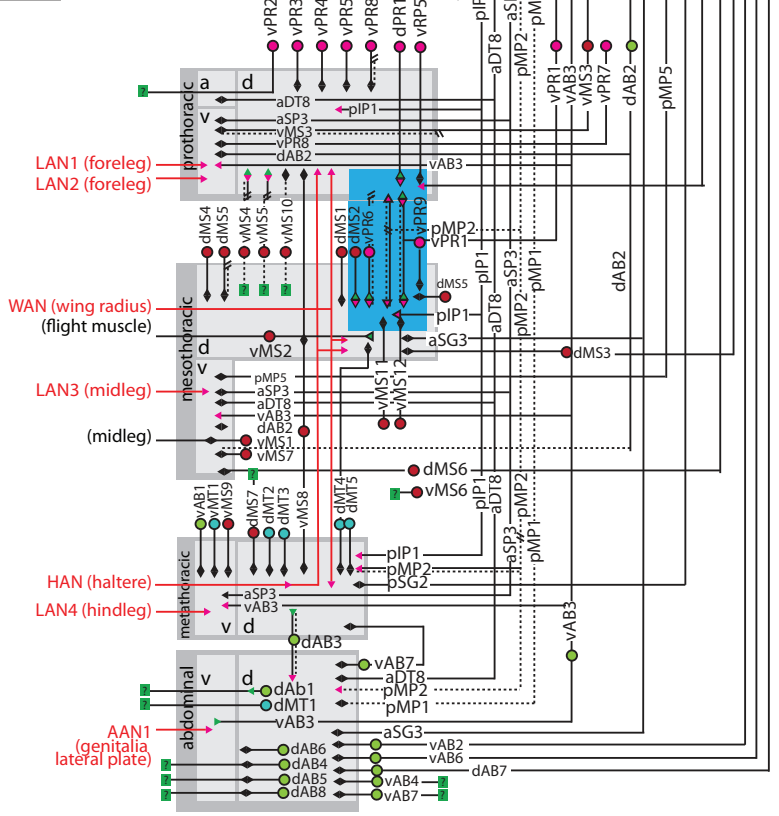


Figure 2

Brain



VNC



Legend

- neuronal type
- neurite
- contralateral neurite
- sensory afferent
- ▶ presynaptic terminal
- ▼ dendritic terminal
- ◆ unresolved terminal
- unresolved
- lateral protocerebral complex
- dorsal triangle

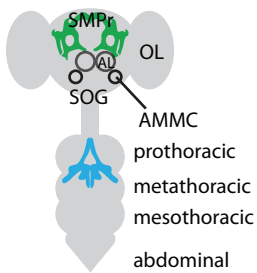
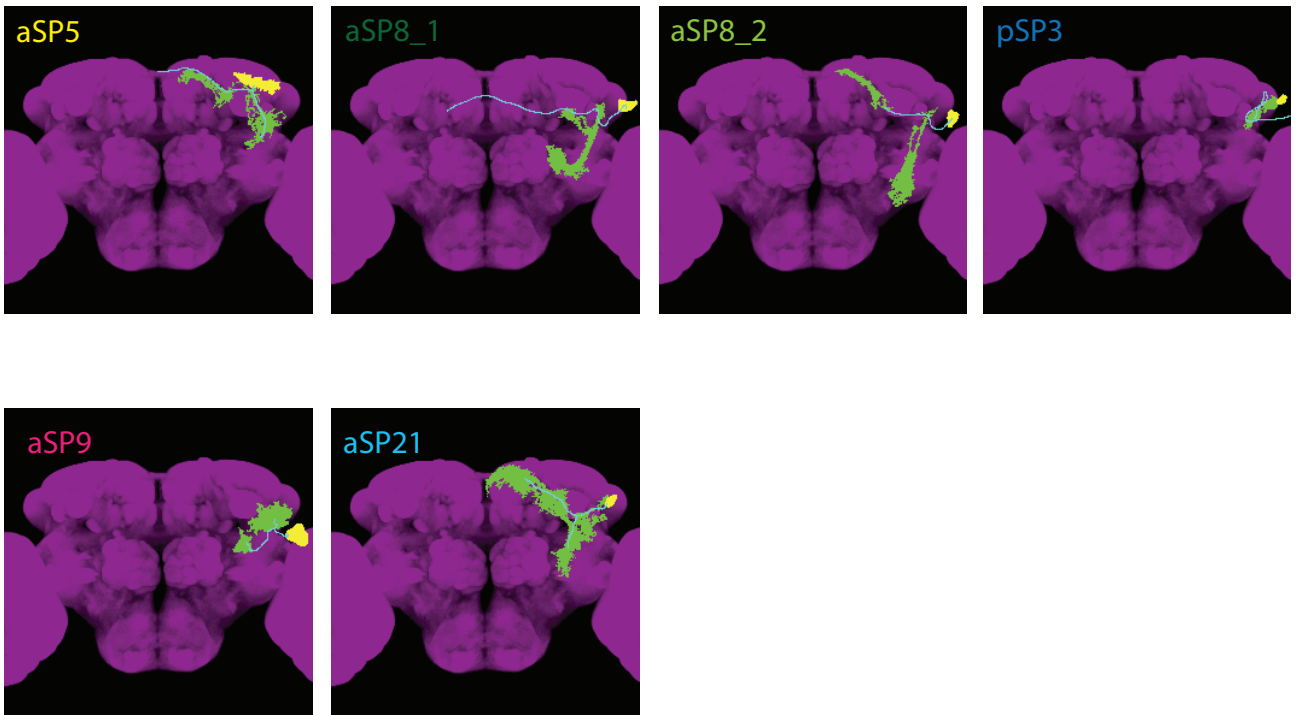
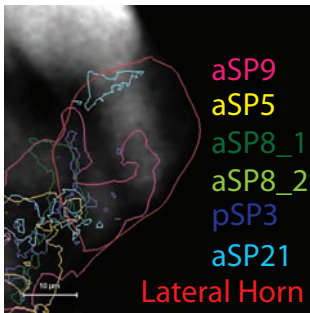


Figure 2E

A



B1



B2

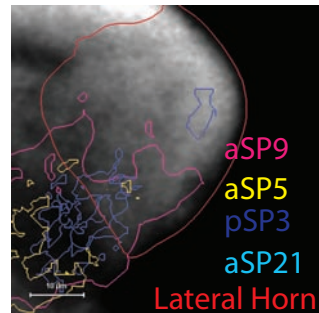
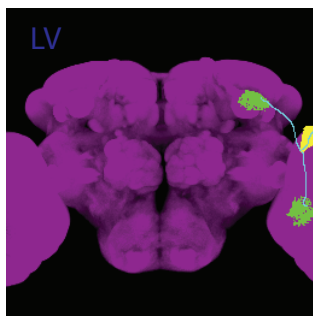
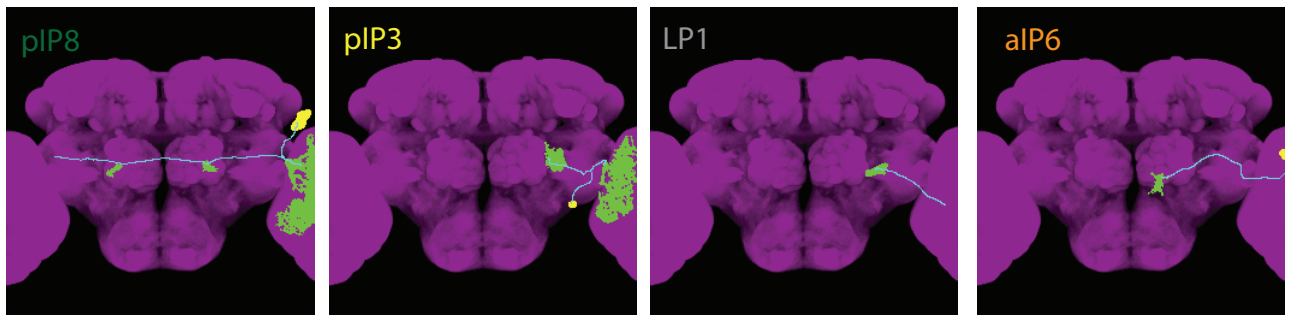
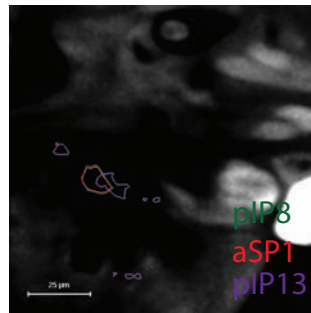


Figure 3.1

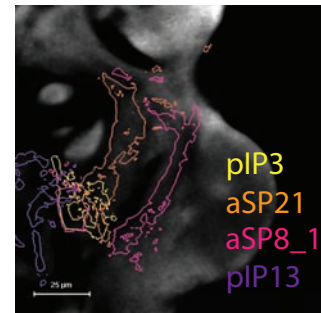
A



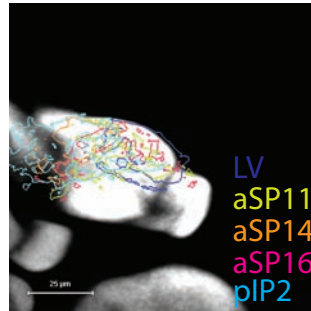
B1



B2



B3



B4

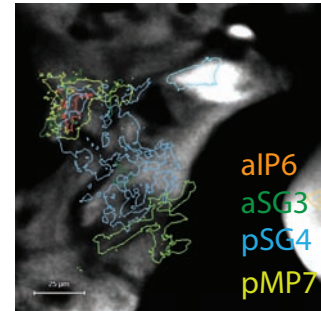
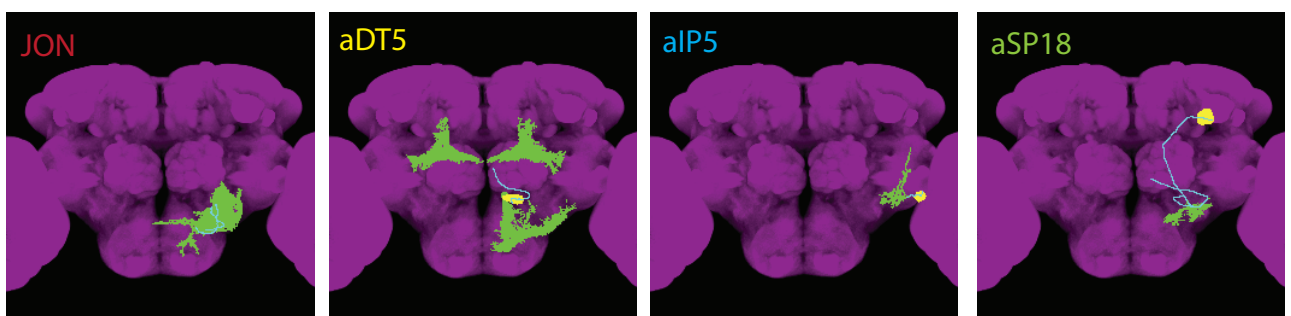


Figure 3.2

A



B

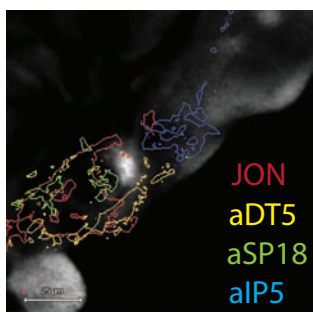
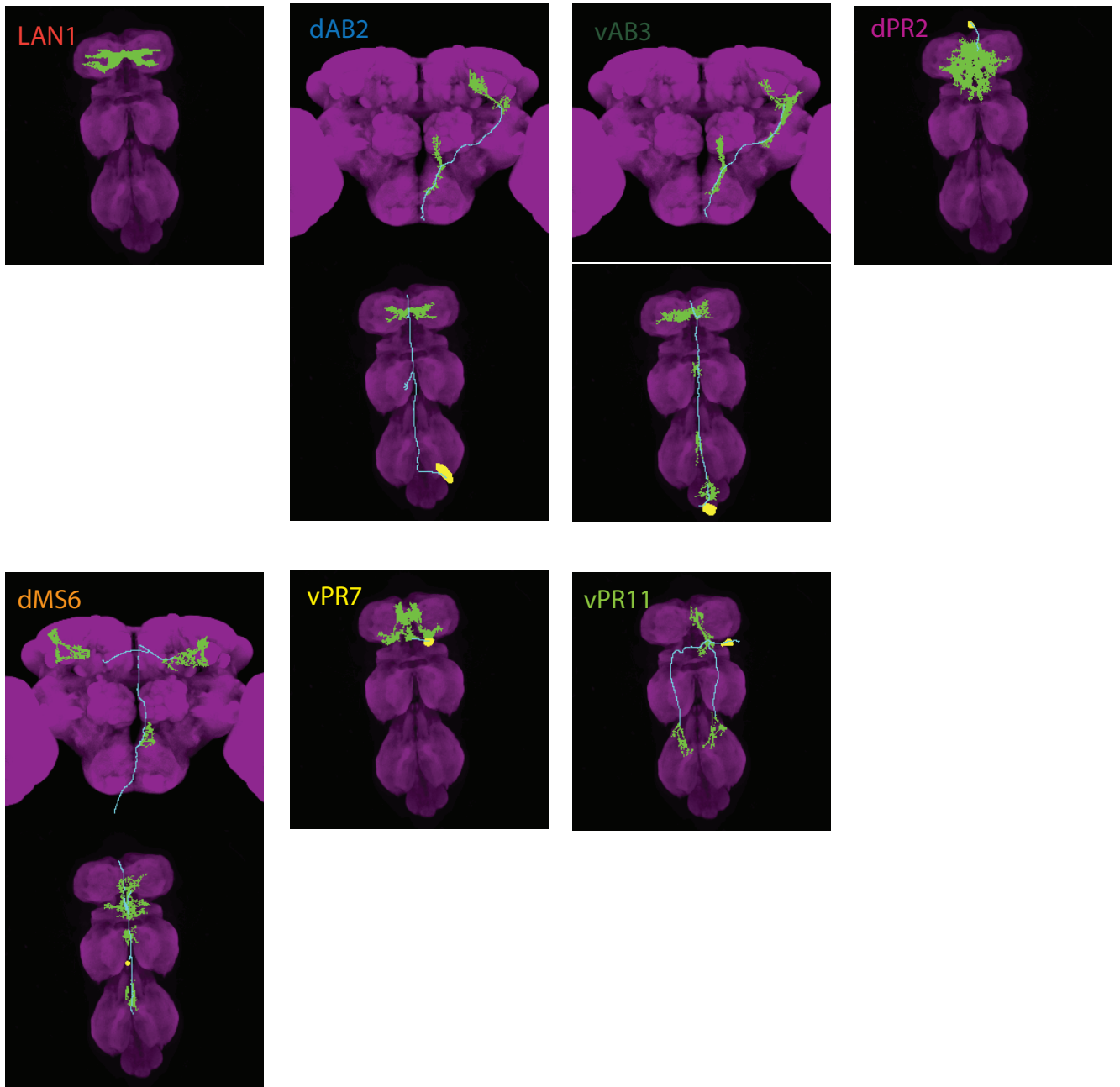
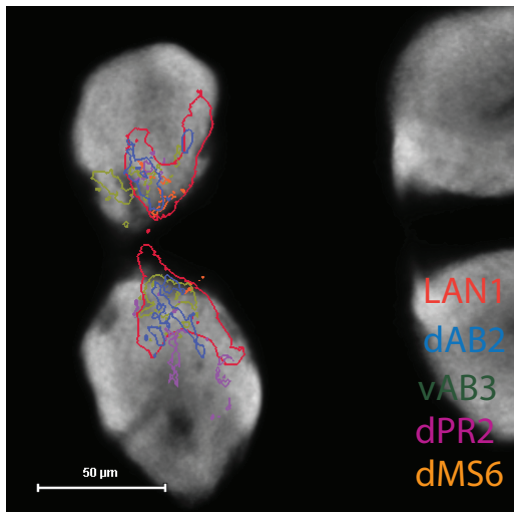


Figure 3.3

A



B1



B2

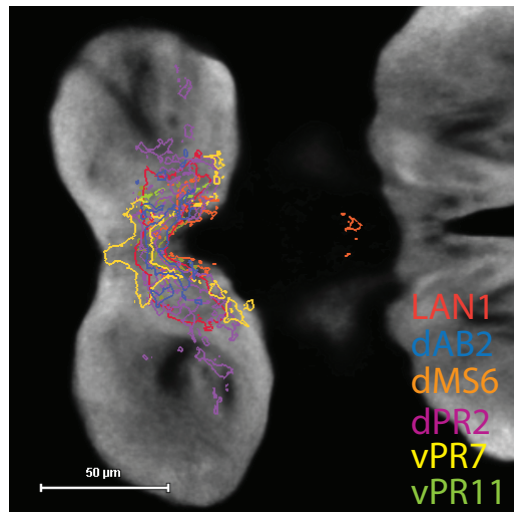
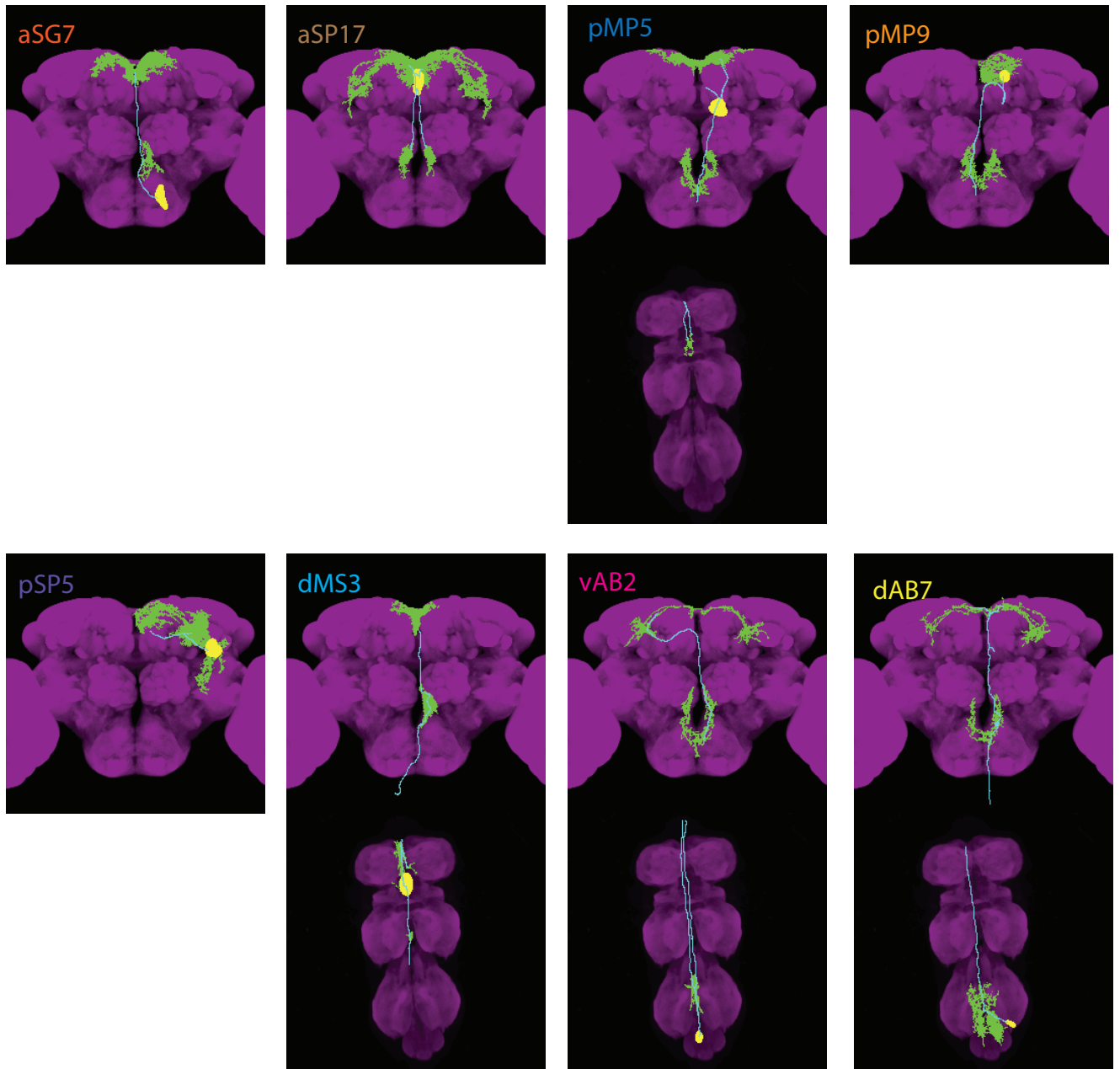
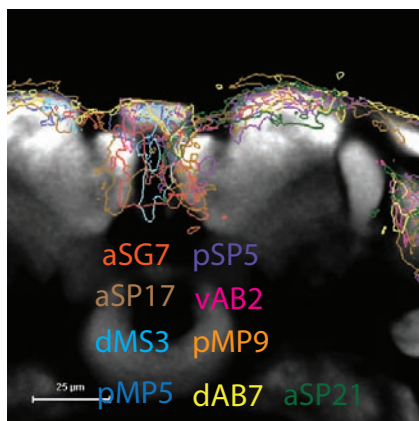


Figure 3.4

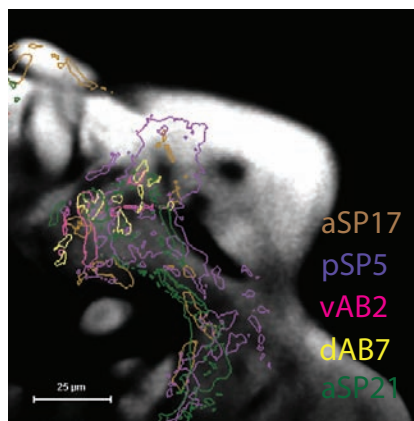
A



B1



B2



B3

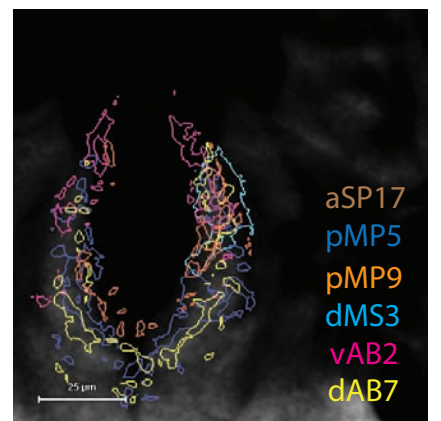
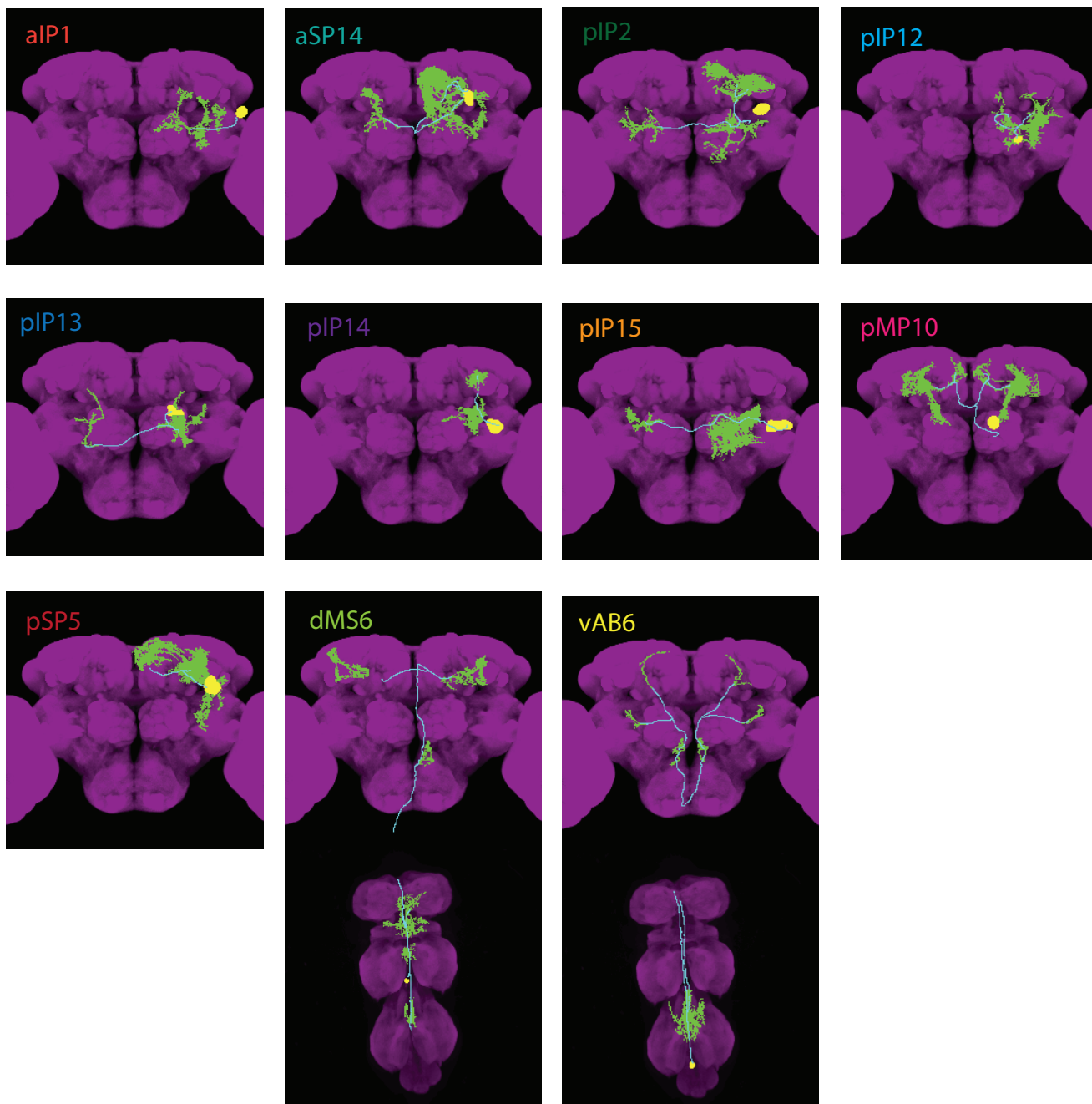
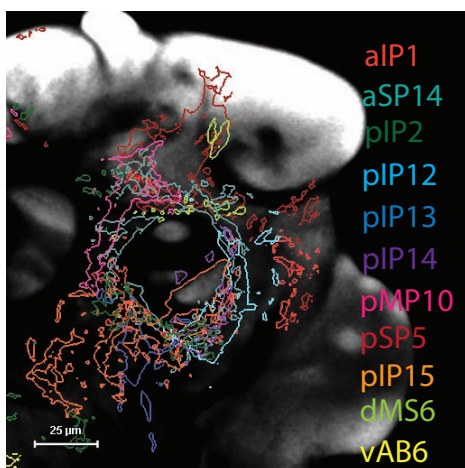


Figure 3.5

A



B1



B2

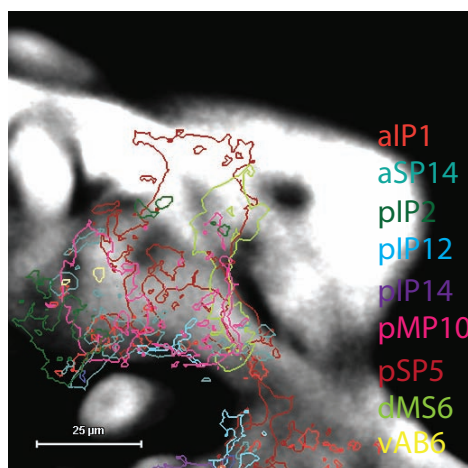


Figure 3.6

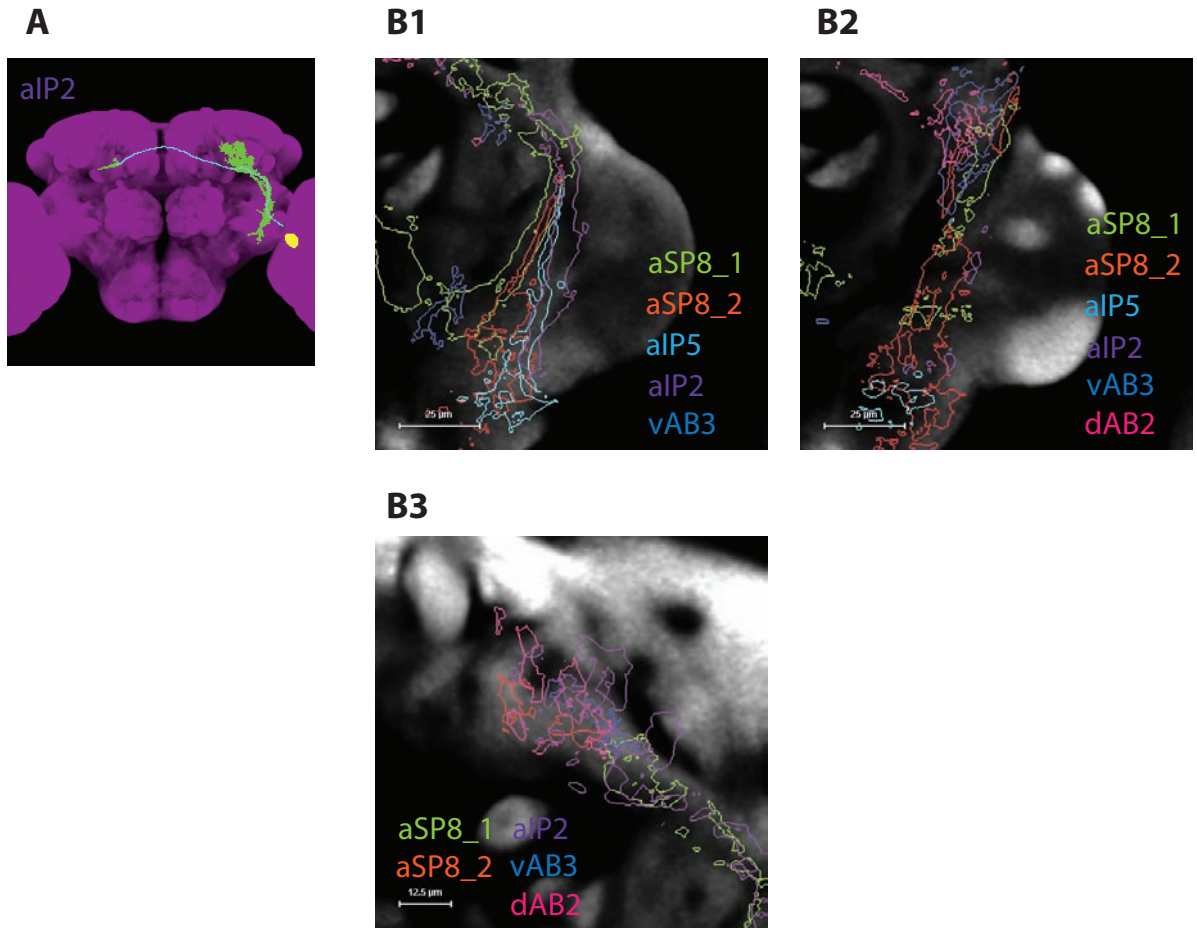
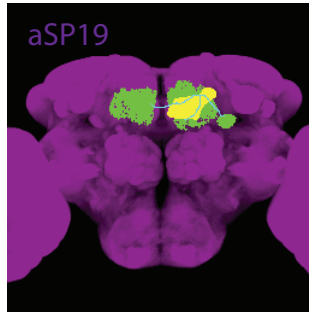
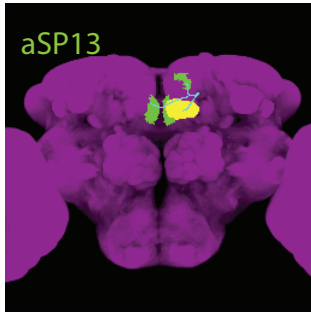


Figure 3.7

A



B

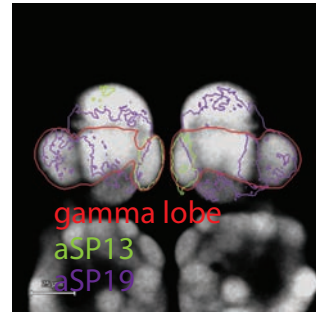
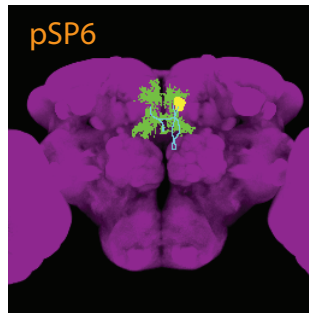
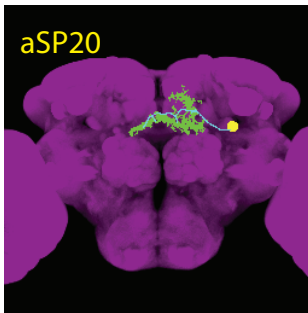


Figure 3.8

A



B

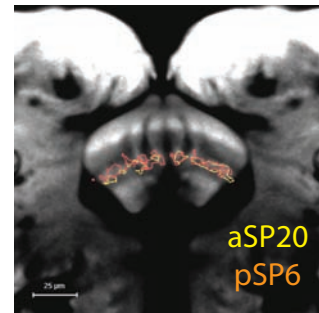
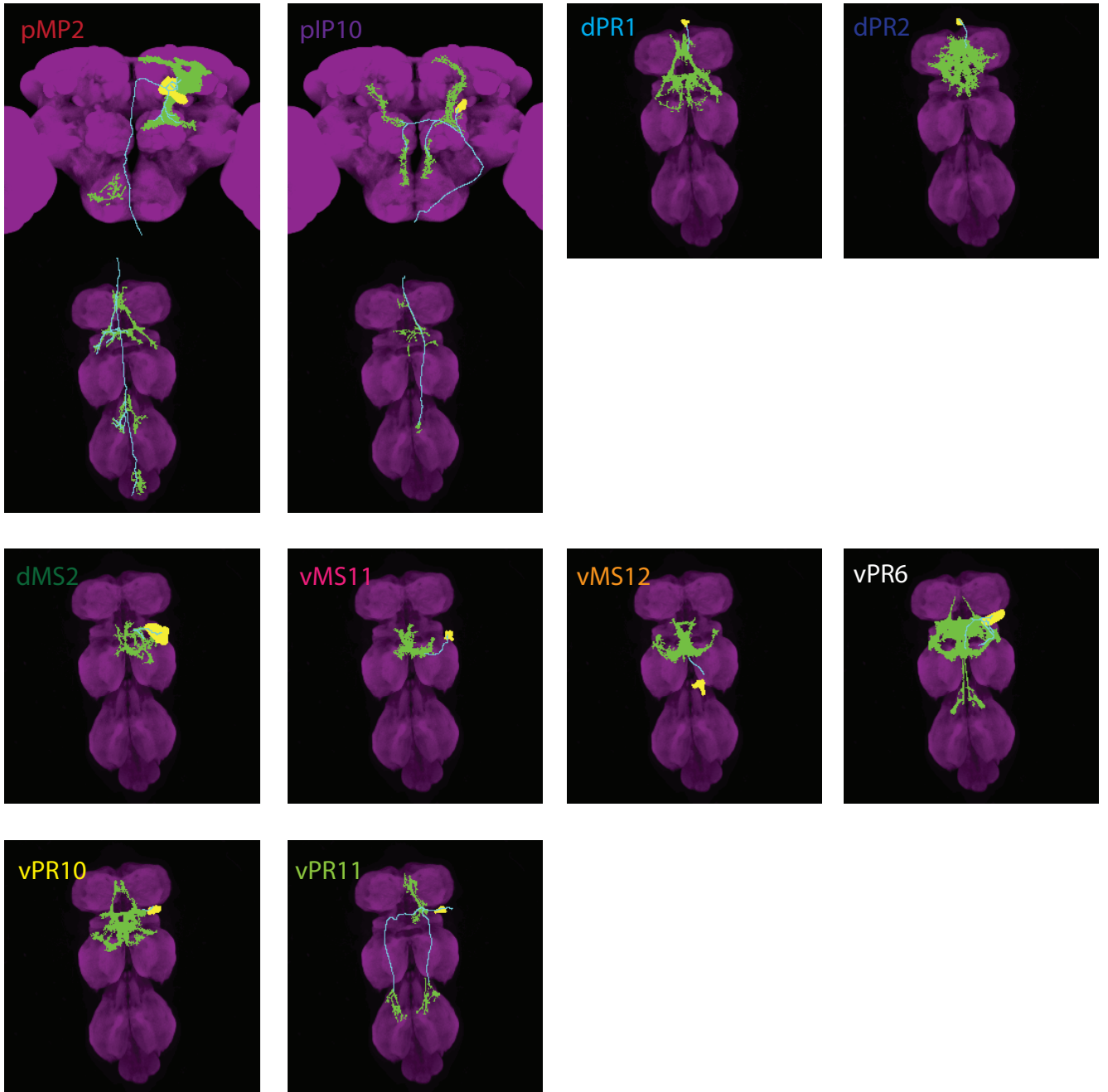
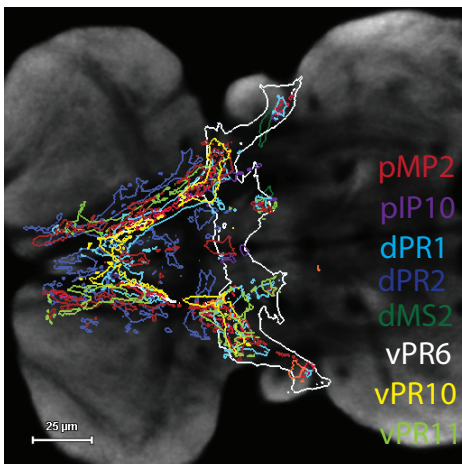


Figure 3.9

A



B1



B2

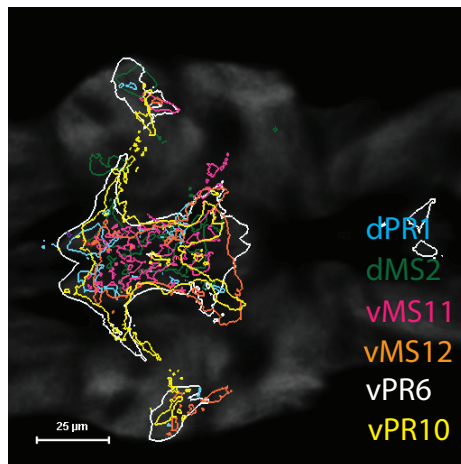


Figure 3.10

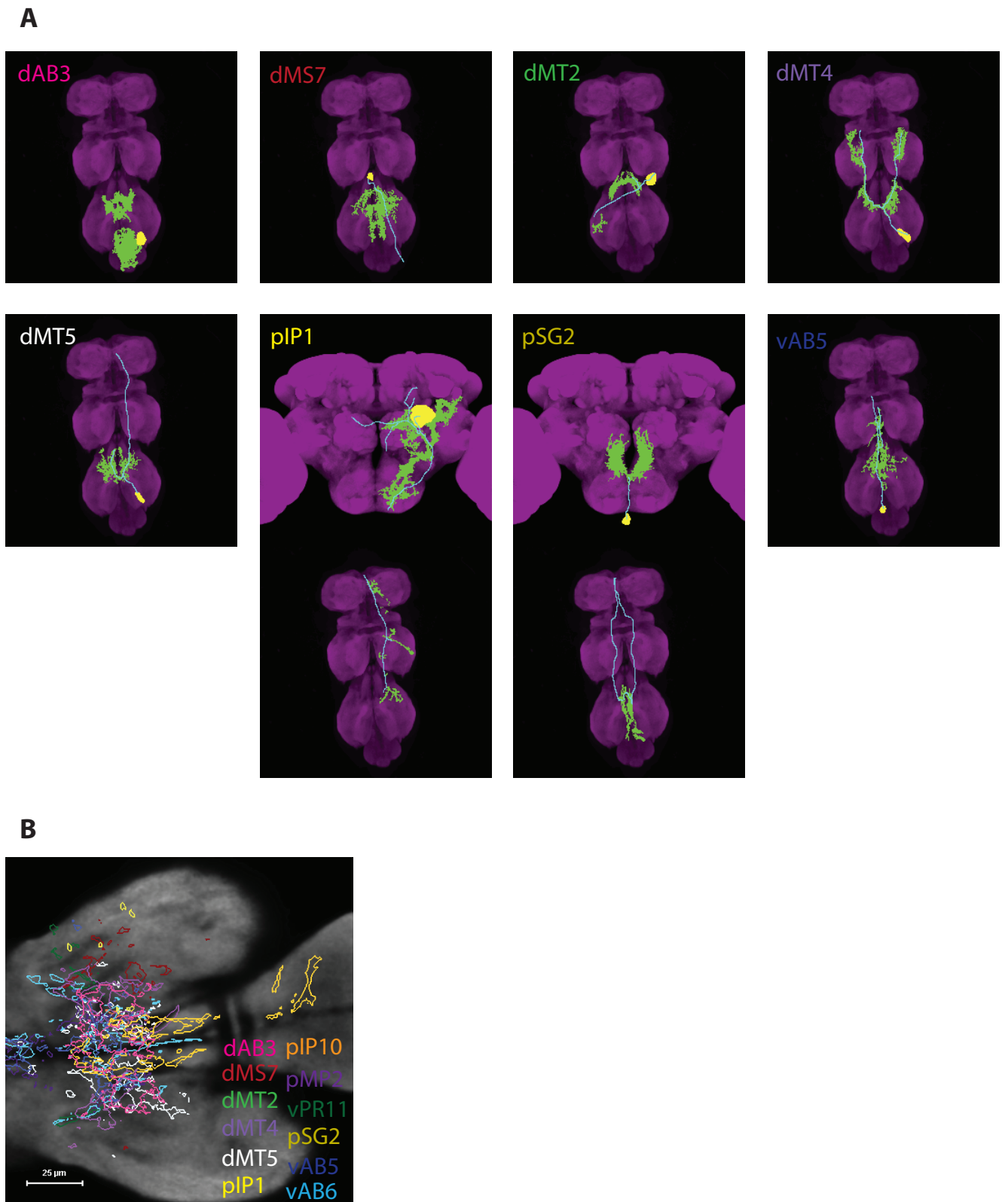


Figure 3.11

Figure 1. Genetic dissection of fru+ neurons

Intersectional genetic strategy for subdividing fru+ neurons.

Scheme for X-gal screening.

Coverage of 100 types of fru+ neurons described in Yu et. al., 2010 by VT lines.

The number of types of fru+ neurons labeled by enhancer trap Gal4 lines (blue) (n=128) and VT lines (red) (n=473) .

Figure 2. Cell body location of fru+ neurons

A-D. Grey colored cell bodies are identified in Yu. et. al., 2010 and colored cell bodies are identified in this study. A and B. Anterior and posterior view of brain. C and D. Ventral and dorsal view of VNC

E. Circuit diagram of the *fru+* neurons which is modified from Yu et. al., 2010. The following abbreviations are used: a, anterior; AL, antennal lobe; AMMC, antennal mechanosensory motor complex; d, dorsal; DV, dorsal ventral brain; l, lateral; LPC, lateral protocerebral complex; m, medial; MB, mushroom body; OL, optic lobe SMPr, superior medial protocerebrum; SOG, subesophageal ganglion; OT, optic tubercle; v, ventral; VLPr, ventrolateral protocerebrum; VNC, ventral nerve cord.

Figure 3.1. *fru+* neurons involved in olfaction

Neuronal representation of neurons. Cell body is in yellow, projection is in Grey and arborizations are in Green. nc82 staining in magenta.

B1 and B2. Ventral and dorsal close-up of lateral horn. nc82 staining in Grey.

Figure 3.2. *fru+* neurons involved in Vision

Neuronal representation of fru + neurons.

B1. Close-up slice view of pIP8 arborization in central brain.

B2. Close-up slice view of pIP3 arborization in central brain.

B3. Close-up slice view of aIP6 arborization in central brain.

B4. Close-up slice view of LV arborization in central brain.

Figure 3.3. *fru*⁺ neurons involved in Audition

Neuronal representation of *fru*⁺ neurons.

Close-up slice view of AMMC

Figure 3.4. *fru*⁺ neurons involved in Gustation

Neuronal representation of *fru*⁺ neurons.

B1 and B2. Ventral and dorsal close-up slice view of Prothoracic ganglion.

Figure 3.5. *fru*⁺ neurons innervating the arch of LPC

Neuronal representation of *fru*⁺ neurons.

B1. Close up slice view of the arch of LPC.

B2. Close-up slice view of the lateral junction of LPC.

B3. Close-up slice view of the tritocerebral loop of LPC.

Figure 3.6. *fru*⁺ neurons innervating the ring of LPC

Neuronal representation of *fru*⁺ neurons.

B1. Close-up slice view of the ring of LPC

B2. Close-up slice view of the lateral junction of LPC

Figure 3.7. *fru*⁺ neurons innervating the lateral crescent of LPC

Neuronal representation of *fru*⁺ neurons.

B1 and B2. Ventral and dorsal slice view of lateral crescent of LPC

B3. Close-up slice view of the tritocerebral loop of LPC

Figure 3.8. *fru*⁺ neurons innervating MB

Neuronal representation of *fru*⁺ neurons.

Close-up slice view of MB gamma lobe.

Figure 3.9. *fru*⁺ neurons innervating fan-shape body

Neuronal representation of *fru*⁺ neurons

Close-up slice view of fan-shape body.

Figure 3.10 *fru+* neurons innervating mesothoracic triangle

Neuronal representation of *fru* + neurons.

B1. Close-up slice view of ventral mesothoracic triangle.

B2. Close-up slice view of dorsal mesothoracic triangle at mesothoracic ganglion.

Figure 3.11. *fru+* neurons innervating dorsal side of metathoracic ganglion

Neuronal representation of *fru* + neurons.

Close-up slice view of dorsal metathoracic ganglion.

3. Functional dissection of *fru*+ neurons

3.1. Strategies for functional dissection

After detailed anatomical analysis of *fru*+ neurons, we then tried to identify the function of *fru*+ neurons with the VT lines which have a good coverage of *fru* neurons and label subset of them sparsely (Figure 1C and D). We can screen all the VT lines available to manipulate neuronal activity of *fru*+ neurons randomly and infer causality between neurons and behavioral changes, which is similar to the forward genetic approach. Alternatively, we can target specific *fru*+ neurons with select VT lines to manipulate specific *fru*+ neurons and observe the behavioral phenotypes, which is similar to reverse genetic approach. Having a catalog of *fru*+ neurons and VT lines, we could focus on each specific type of *fru*+ neurons and assess their functions with selected VT lines. However, such a “bottom-up” method potentially has several challenges. First, compared to the neuropils responsible for the sensory input, we know very little about higher order processing centers and motor control centers. This could prevent us from estimating their function based on anatomy, thus preventing us from selecting the proper testing paradigm. Second, functional perturbation of one type of neurons can have no behavioral consequence depending on the type of perturbation or the circuit to which the target neuron belongs. Thus, we took a “top-down” approach, screening all the VT lines we collected from the X-gal screening with thermal activation method. We expressed drosophila TRPA1 in various subsets of *fru*+ neurons with *fru*^{FLP} FLP-in system (Hamada et al., 2008; von Philipsborn et al.; Yu et al., 2010). VT lines are crossed to the fly which has *UAS>stop>dtrpA1; fru*^{FLP} and the progeny of the right genotype were subjected to heat application. With this approach, we expect that we can at least elucidate some neuronal components of courtship behavior which in the long-run lead to building the entire courtship circuit.

3.2. Song neurons

See the appendix.

3.3. Bending neurons

3.3.1. Motivation

The final steps of courtship are copulation attempt and copulation, both of which involve bending of the abdomen (Hall, 1994). Through the study of gynandromorphs, neuronal foci that required for copulation attempt were localized in ventral nerve cord (Hall 1979) Feminization of nervous system by the expression of female form of *transformer* suggested that the abdominal ganglion is the key focus (Ferveur and Greenspan, 1998). However, no specific cell type has yet been shown to be functionally involved in the control of copulation attempt or copulation. *fru+* neurons send out thick nerve bundles from abdominal ganglion to abdomen and innervate muscles at multiple segments of abdomen and reproductive organs (Billeter and Goodwin, 2004; Lee et al., 2000). This suggests the presence of *fru+* neurons being involved in the motor control of abdominal bending. In order to identify such neurons and neurons that send the command to them, we carried out thermogenetic screen with the FLP-in system.

3.3.2. Thermal activation Screen for neurons involved in copulation attempt and copulation

We have screened 1324 VT lines which include 1283 VT lines which have confirmed overlap with *fru+* neurons from above mentioned X-gal screen with the FLP-in TRPA1 system. Single *UAS>stop>TRPA1; VT-XXXX/ fru^{FLP}* male was kept in a chamber and then heat is applied from 25°C to 32°C for 10 mins. We scored the bending of the abdomen upon heat application (Figure 4A arrow head). After twice of re-test, we found 125 lines showing abdominal bending (Figure 4A).

3.3.3. Identification and characterization of neurons involved in copulation attempt and copulation

We crossed those 125 lines to *UAS>stop>mCD8GFP; fru^{FLP}* to check which types of *fru+* neurons are labeled. Among those, we focused on the analysis of 78 VT lines with relatively sparse expression. We found 6 neurons (dAB4, dAB5, dAB8, dMT3, dAB7 and vAB2) are labeled repeatedly and sparsely by 60 positive lines (Figure 4B). The remaining 18 lines label some *fru+* neurons in the abdominal ganglion which could not be resolved due to the dense multiple

arborizations in that small neuropil. We did not find any particular neurons shared among those 18 lines.

dAB4, dAB5 and dAB8; potential motor neurons

VT40010 as well as 29 other lines label dAB4 sparsely (Figure 5A). dAB4 has its cell body localized on the dorsal tip or occasionally on ventral side of the abdominal ganglion and arborizes in middle part of abdominal ganglion (Figure 5A'). We also observed that dAB5 is labeled repeatedly (Figure 4B). VT50218 labels dAB5 exclusively (Figure 5B). dAB5 has its cell body on the dorsal tip of the abdominal ganglion and has 2 arbors on the dorsal side of abdominal ganglion (Figure 5B'). dAB8 is labeled by 8 different VT lines (Figure 4B). It has its cell body between the metathoracic ganglion and the abdominal ganglion, arborizes at the dorsal side of the abdominal ganglion (Figure 5C and 5C'). All of these three neurons send efferent projections to the abdomen and can be motor neurons.

dMT3

We found 15 VT lines label dMT3 (Figure 4B). dMT3 has its cell body at the dorsal side of the metathoracic ganglion and send its arbor at the dorsal-anterior part of the abdominal ganglion (Figure 5D and 5D').

dAB7 and vAB2: two ascending neurons

We observed 5 lines including VT19351 that label dAB7 sparsely (Figure 4B). dAB7 is an ascending neuron which has its arbor at dorsal-anterior part of abdominal ganglion in the VNC and at the tritocerebral loop and the arch region in the brain. There are 4 lines labeling vAB2 sparsely among the positive lines (Figure 4B). vAB2 is also an ascending neuron which arborizes at the dorsal-medial part of abdominal ganglion and has arbors at the tritocerebral loop and the arch region in the brain which extensively overlaps with dAB7 arborizations.

The three potential motor neurons dAB4, dAB5, and dAB8 overlaps with each other at the abdominal ganglion (Figure 5G). The two ascending neurons dAB7 and vAB2 overlap with each other at the dorsal side of abdominal ganglion (Figure 5H). dMT3 overlaps with dAB7, dAB4, dAB5, and dAB8 (Figure 5H).

dAB4 and dAB8 is specifically required for copulation, but not for other courtship steps

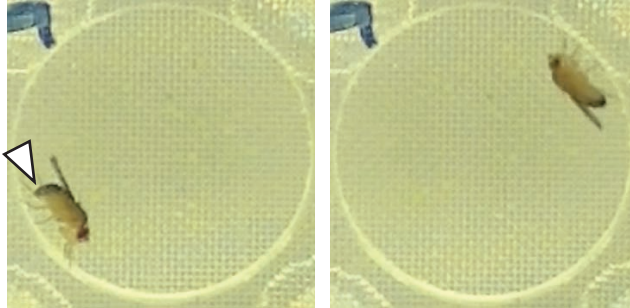
To address if any of these neurons are required for copulation, we crossed two VT lines, VT40010 and VT63450, which labels dAB4 and dAB8 respectively, to *UAS>stop>TNT; fru^{FLP}* in order to block the synaptic transmission in those neurons (Martin et al., 2002). We used inactive form of TNT (*UAS>stop>TNTin*) or *UAS>stop>TNT* without *fru^{FLP}* as controls. *UAS>stop>TNT; VT40010/ fru^{FLP}* males courted virgin females as vigorously as TNTin control males or slightly less vigorous than TNT without *fru^{FLP}* males (Figure 6A). Their success of copulation in 10 min was 0% which is significantly lower than the two controls (Figure 6A'). Similarly, Males with silenced dAB8 (*UAS>stop>TNT; VT63540/ fru^{FLP}*) courted virgin females as vigorously as or slightly less than controls, but their copulation success was significantly reduced (Figure 6B and 6B'). This indicates that dAB4 and dAB5 are necessary for successful copulation but not for courtship. This specific disruption of copulation but not of courtship by the silencing of these two neurons fits well with the idea that these two neurons are motor neurons required for successful copulation.

A

1324 VT lines
(including 1283 Fru+ VT lines) × *fru*^{FLP}
UAS>stop>trpA1



Thermal activation from 25°C to 32°C in ~10 min



2 times of
retest

125
positive VT lines



78 sparse VT lines



1199
negative VT lines

B

	dAB4	dAB5	dAB8	dMT3	vAb7	vAB2
1214						
12301						
7083						
6035						
46785						
2853						
8172						
12759						
13878						
14208						
14430						
14974						
16277						
16371						
17667						
18875						
19059						
25779						
33620						
34628						
38818						
40010						
40576						
40934						
40970						
49481						
50234						
61922						
62257						
999015						
23830						
40564						
1605						
12794						
17557						
31562						
40017						
45663						
47882						
50218						
19758						
8663						
17249						
28544						
32899						
40027						
41688						
63540						
19235						
57463						
6203						
8152						
8277						
11128						
19351						
38450						
17413						
10063						
20731						
25606						
347						
450						
837						
1608						
3285						
4309						
4726						
6415						
7166						
13120						
16275						
21364						
21845						
29305						
43702						
48421						
48866						
50236						

Figure 4

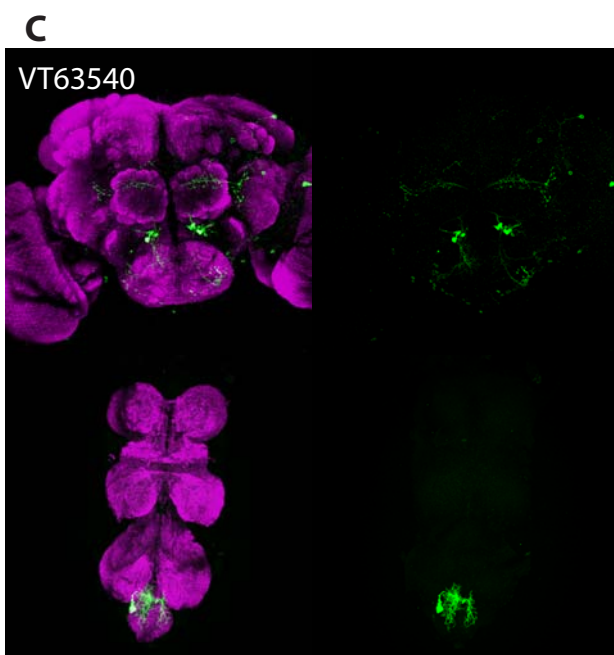
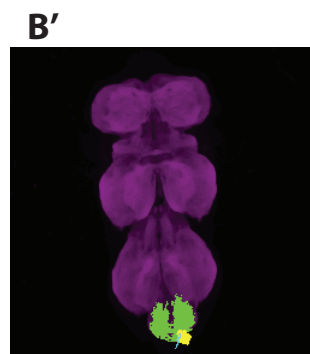
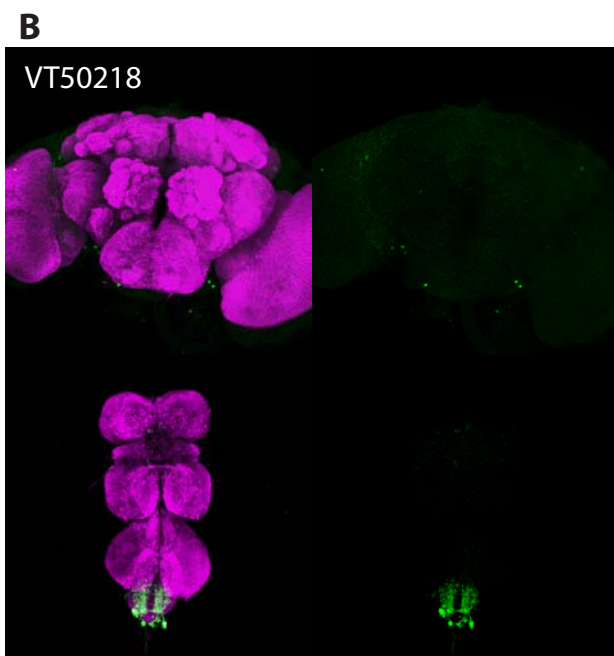
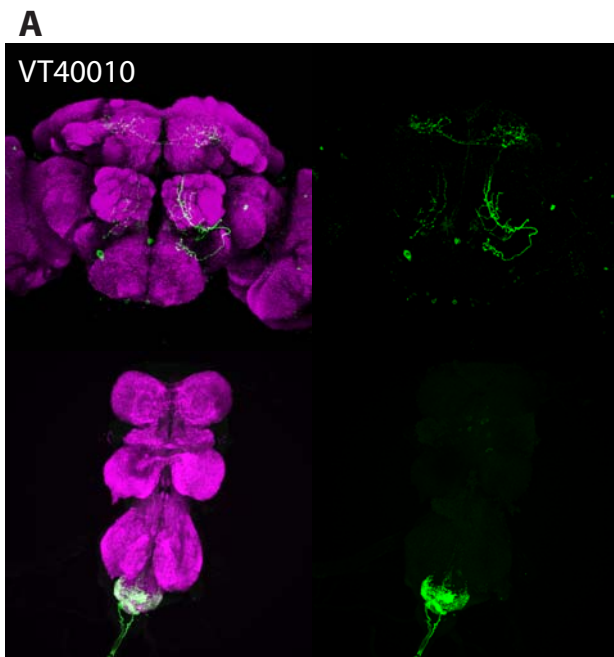


Figure 5

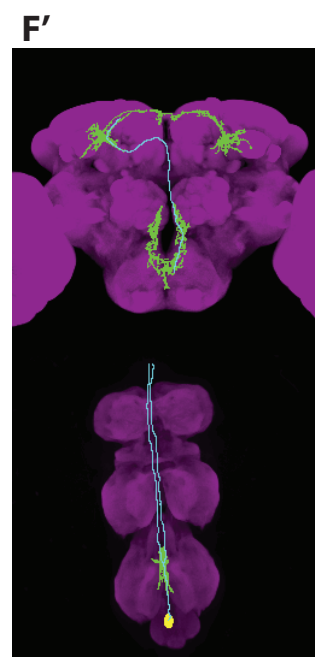
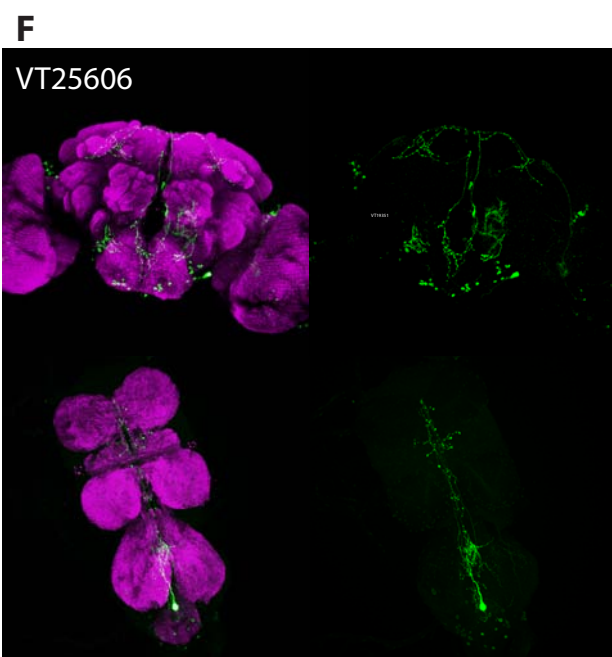
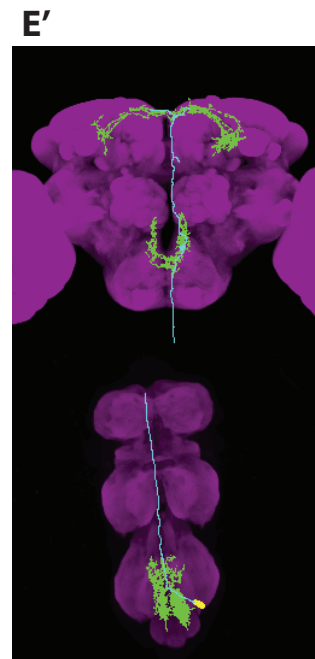
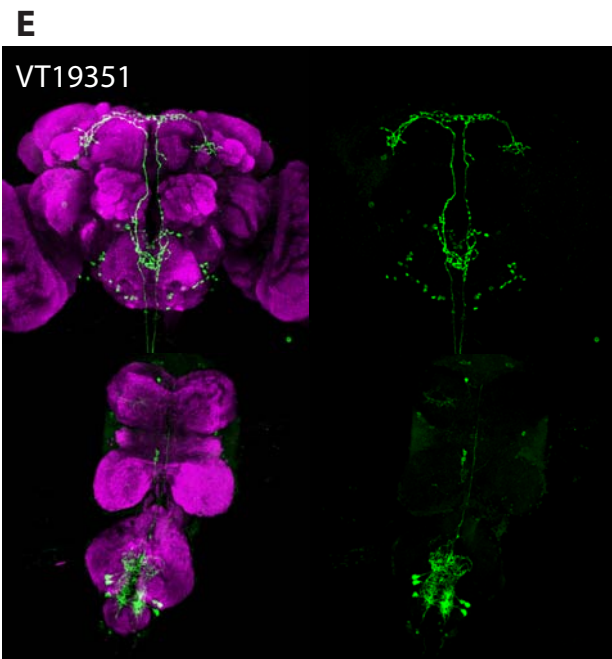
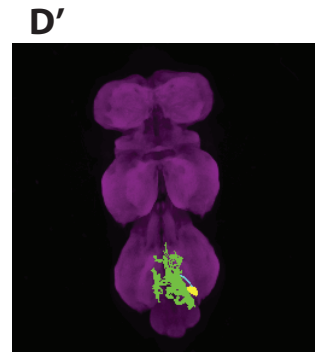
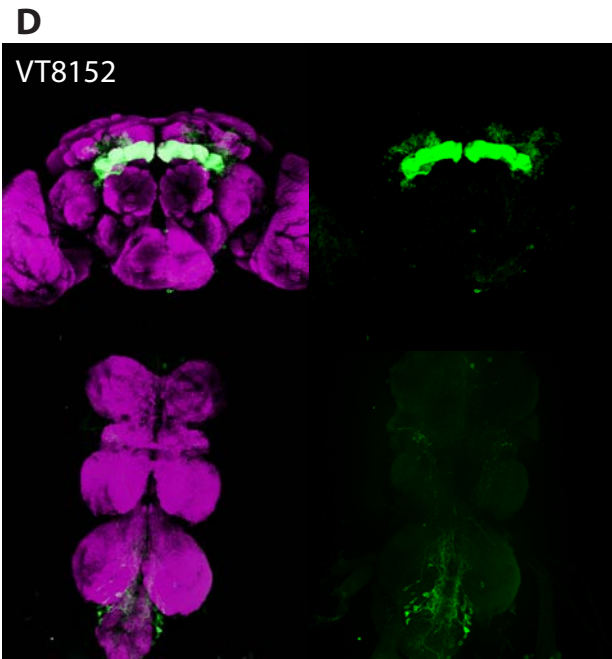


Figure 5

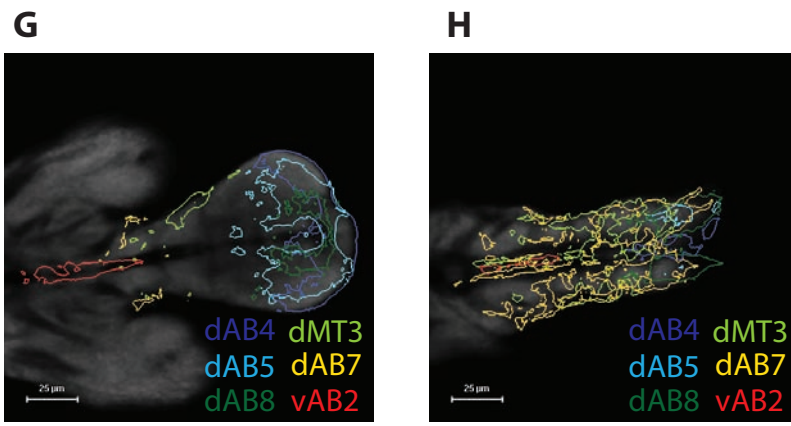


Figure 5

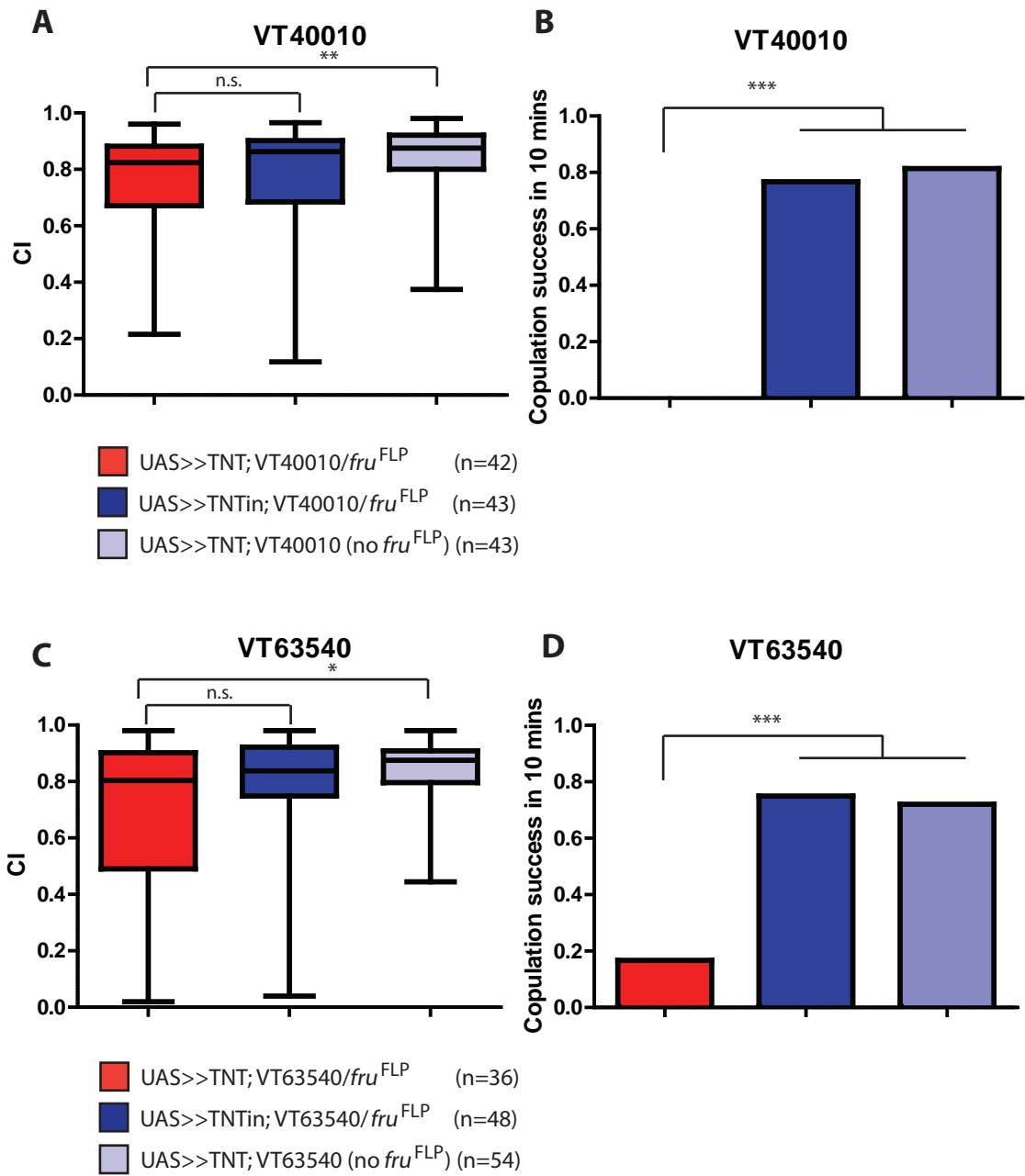


Figure 6

Figure 4. Functional dissection of *fru*+ neurons involved in copulation attempt and copulation
Scheme for screening

Table of VT lines (row) and selected *fru*+ neurons (column). Orange indicates the labeling of the corresponding neuron by each VT line.

Figure 5. Anatomy of bending neurons

Staining with anti-GFP (Green) of *UAS>stop>mCD8GFP; VT-XXX/ fru^{FLP}* A. VT40010 B. VT50218
C. VT63450 D. VT8152 E. VT19351 F. VT2506. Magenta is nc82 staining.

Neuronal representation of A' dAB4, B' dAB5, C' dAB8, D' dMT3, E' dAB7, and F' vAB2.

G. Close-up slice view of ventral side of metathoracic and abdominal ganglion.

H. Close-up slice view of dorsal side of abdominal ganglion.

Figure 6, dAB4 and dAB8 is specifically required for copulation, but not for courtship.

A and C. Courtship index of specified genotype * $p < 0.05$ ** $p < 0.01$. *** $P < 0.001$. Mann-Whitney test.

B and D. Copulation success in 10 minutes. *** $P < 0.001$. Fisher's exact test.

3.4. Courtship-driving neurons

3.4.1 Motivation

What are the neuronal substrates that drive courtship? *fru+ ppk23+* leg afferent neurons (LAN1) have been identified as the chemosensory neurons which sense female aphrodisiac pheromone, 7,11- HD (Lu et al.; Thistle et al., 2012; Toda et al., 2012). Activation of LAN1 through *trpA1* was sufficient to induce courtship toward male, although it does not induce any courtship ritual when there is no target fly (Thistle et al., 2012; Toda et al., 2012). The elevation of courtship toward male is only observed with visual and olfactory cues are provided through target male (Thistle et al., 2012). It has been shown that activation of a subset of P1 together with visual input can elicit following and wing extension toward an artificial target (Pan et al., 2012) These experiments suggest that a neuron that enhances courtship might not elicit any obvious behavior in an isolated fly, but can do so in the presence of additional stimuli. Such a neuron is likely to be a sensory neuron or a neuron relaying the sensory input rather than a neuron involved in motor control. To identify such neurons which drive courtship ritual, we carried out thermal activation screen with two males being paired together.

3.4.2 Thermal activation screen for neurons that drive courtship

We crossed 1324 VT lines and 1 enhancer trap line, NP2631 with *UAS>stop>TRPA1; fru^{FLP}* and paired two flies in a same chamber (Figure 7). We tested 3-10 pairs of males per assay. We rated one male courting the other male when it displayed following, extended wings toward the other male and occasionally attempted copulation (Figure 7). When >50% of the tested pairs showed >3s of such male-male courtship during ~10 min of heating up from 25°C to 32°C, we rated the line as a positive line. Together with paired males, we prepared isolated males to score their wing extension. When the isolated males and paired males showed wing extension at the same temperature, those lines are taken as negative lines during this screen. This is because such lines are likely to label neurons sending courtship song command (*pIP10*) or neurons involved in motor control of courtship song (*dPR1*, *vPR6*, and *vMS11*) which we identified in chapter 3.2 (von Philipsborn et al., 2011). We restored 32 lines after twice of retests (Figure 8A). We have crossed those lines to *UAS>stop>mCD8GFP; fru^{FLP}* to find out

which types of *fru*⁺ neurons are labeled by those VT lines. We focused on the analysis of relatively sparse 28 lines (Figure 8B).

3.4.3 Identification and characterization of neurons that drive courtship

LAN1

The most over-represented neuron among those positive lines was LAN1. We have identified 14 lines that labels LAN1 (Figure 8B). LAN1 is *fru*⁺ and *ppk23*⁺ neurons and its activation as been shown to induce male-male courtship (Thistle et al., 2012; Toda et al., 2012). This indicates that our screen is sensitive enough to pick up sensory modalities which drive the courtship.

P1, pMP4 and pMP4_1

We have recovered 6 lines that label P1 neurons (Figure 8B). This is consistent with previous discoveries that P1 activation with dTRPA1 can elicit courtship song and can elicit following in the presence of target male (Pan et al., 2012; von Philipsborn et al., 2011). Among those, we have found that two VT lines, VT 43068 and VT43137 labels different subtype of P1, pMP4 and pMP4_1 respectively (Figure 9B, 9C and 9D). The sum of arborizations of pMP4 and pMP4_1 matches with P1, suggesting that these two are the only subtypes of P1 (Figure 9B', C' and D'). However, VT43068 labels up to 10 cells of pMP4 per hemisphere and VT43137 labels up to 10 of pMP4_1 per hemisphere, while P1 comprise of 25-30 neurons per hemisphere (7 ± 1.1 per hemisphere by VT43068 and 7.2 ± 0.8 by VT43137. Average \pm SEM) (Kimura et al., 2005). Although there still can be additional cell types that consists of P1, we so far did not anatomically or functionally identify such cell types. Behaviorally, we observed that activation of pMP4 with VT43068 in isolated male can elicit wing extension and courtship song, while activation of pMP4_1 with VT43137 could not (data not shown). This implies different functionality of pMP4 and pMP4_1 in the generation of courtship song. We then questioned the requirement of P1, pMP4 and pMP4_1 during male-female courtship. We crossed NP2631, VT43068, or VT43137 to *UAS>stop>TNT; fru*^{FLP} in order to silence P1, pMP4, and pMP4_1, respectively. The silencing of P1 reduced courtship dramatically, although silencing of pMP4 or pMP4_1 had minor impact or no impact on male-female courtship (Figure 4.11). This suggests pMP4 and pMP4_1 functions in a redundant manner during male- female courtship.

aSP2

Among the positive 28 lines, there are 5 lines labeling aSP2 (Figure 8B). aSP2 has its soma at the anterior- dorsal part of brain and send its arbor to LPC (Figure 9E and E'). Both of P1 and aSP2 innervate LPC and overlaps largely with each other, suggesting their potential connection (Figure 9B' and E'). Anatomical dimorphism of aSP2 was revealed with the staining of female of *UAS>stop>mCD8GFP; VT8657/ fru^{FLP}*, which is consistent of previous report (28.7±0.1 cells per hemisphere in males (n=3) and 11±0.7 cells per hemisphere in female (n=3)). Average ± SEM. Figure 10D, E and F) (Cachero et al., 2010; Yu et al., 2010). Silencing of aSP2 by crossing VT8657 to *UAS>stop>TNT; fru^{FLP}* reduced the courtship toward females dramatically, suggesting its necessity for male-female courtship.

Activation of VT61081+ fru+ neurons elicit following without wing extension

One of the positive lines VT61081 labels both P1 and aSP2 (Figure 8B and S5A). Activation of VT61081+ *fru*+ neurons induced robust male-male courtship (Figure 8A n=27/34 male pairs), but it elicited mainly following and very little oriented wing extension (Figure S5B and S5C) Activation of pMP4, pMP4_1 or aSP2 alone with VT43068, VT43137 and VT8657 respectively elicited robust wing extension during male-male courtship(Figure S5B and S5C). Coactivation of P1 and aSP2 with VT23797 induced as much male-male courtship as with VT61081, but significantly more wing extension than with VT61081. This suggest that the lack of oriented wing extension by activation of VT61081+ *fru*+ neurons is not due to the coactivation of aSP2 and P1 but due to the activation of other neurons labeled by VT61081 such as aSP1 or vMS15.

pip6

We found four lines labeling pip6. One of them is VT19050 which labels only 3 neurons pip6, vPR4 and WAN when it is crossed to *UAS>stop>mCD8GFP; fru^{FLP}*. pip6 has large arbor that overlaps with LPC and sends additional arbor to dorsal posterior side of the brain (Figure 9F and F'). Activation of VT19050+ *fru*+ neurons in isolated male elicits wing extension and courtship song at higher temperature than they initiate male-male courtship (data not shown). The other 3 lines labeling pip6 did not elicit wing extension in isolated males, possibly due to the weaker labeling of pip6. pip6 is a sexually dimorphic neuron. pip6 in female has less cells and thinner arborization (6.9±1.0 cells per hemisphere in males (n=8) and 4±0.9 cells per hemisphere in female (n=6)). Average ± SEM. Figure 10G, H and I). We crossed VT19050 to

UAS>stop>TNT; fru^{FLP} in order to test the necessity of pIP6 during male-female courtship. However, silencing of pIP6 did not impair the courtship (Figure 11).

aSP4

Among the positive 28 lines, three lines labeled aSP4 (Figure 4B). When crossed to *UAS>stop>mCD8GFP; fru^{FLP}*, VT 43700 labels aSP4 and an as yet unresolved *fru+* neuron next to it and VT43708 labels only aSP4 and pMP7. aSP4 has only a single cell per hemisphere and is a sexually dimorphic neuron as was reported before (Figure 10J,K and L) (Yu et al., 2010). Silencing of aSP4 with VT43700 and *UAS>stop>TNT; fru^{FLP}* impairs the courtship slightly but significantly (Figure 11).

aSP21

We found that one of the positive lines VT31392 did not label any of the above mentioned neuron when it was crossed to *UAS>stop >mCD8GFP; fru^{FLP}*. It labeled aSP21 and pMP5. We have no other lines labeling aSP21 restored in anatomical screen, but we restored 6 lines labeling pMP5. Two of the six lines, VT6900 and VT7178 are positive lines with male-male courtship screen but VT6900 labels LAN1, aSP2 and P1 and VT7178 labels P1 in addition to pMP5(Figure 4 A and B, data not shown). 4 of the 6 pMP5 labeling lines did not show male-male courtship during the screen. Collectively, this suggests that activation of aSP21 can elicit courtship, although we cannot exclude the possibility that pMP5 activation has additive effect on the activation of aSP21. aSP21 arborizes in the Lateral horn and arch and lateral junction of LPC(Figure 1). aSP21 resembles the previously described aSP-k (Cachero et al., 2010), where it is reported to be sexually dimorphic. However, we did not observe such a neuron in female *UAS>stop>mCD8GFP; VT31392/ fru^{FLP}* flies (data not shown). In order to test if aSP21 is required for male-female courtship, we crossed VT31392 with *UAS>stop>TNT; fru^{FLP}* and tested male-female courtship. The silencing of VT31392+ *fru+* neurons impaired male-female courtship slightly but significantly, suggesting that aSP21 is required for vigorous courtship but is not essential.

vAB3

There is still another line (VT17933) which did not label any of the neurons mentioned so far. When it was crossed to *UAS>stop>mCD8GFP; fru^{FLP}*, vAB3, LAN2 and AAN1 were labeled in the male (Figure 9I). We identified two more lines (VT18831 and VT19070) labeling LAN2

from the anatomical study. VT18331 is one of the 32 positive lines in this screen but it labels LAN1 as well. *UAS>stop>TRPA1; VT19070/ fru^{FLP}* male do not show any male-male courtship at elevated temperature (n=0/8 male pairs). We identified 14 other VT lines labeling vAB3 and 11 other VT lines labeling AAN1 but none of them was scored positive for male-male courtship in the screen. In summary, we could not yet resolve the responsible neuron for the male-male courtship phenotype of VT17933. However, vAB3 is a strong candidate because of its anatomical features. It is an ascending neuron the arborization of which localizes at the ventral side of prothoracic ganglion and overlaps with LAN1. In the brain, vAB3 arborizes at LPC and overlaps with P1, aSP2, pIP6, aSP4 and aSP21 (Figure 9I').

Neuronal epistasis between P1 and aSP2

The dramatic reduction of courtship upon silencing of P1 and aSP2 raises a question. Which of the neurons functions more down-stream or up-stream? If the activation of aSP2 elicits male-male courtship through triggering P1 activity, silencing of P1 should abolish the male-male courtship induced by aSP2 activation. We first generated a LexA driver combining LexA and Gal4 activation domain (GAD), VT8657.LexAGAD at attP2 (Pfeiffer et al., 2010). This line recapitulated the expression of the original VT8657.Gal4 when it is crossed to *LexAop>stop>mCD8GFP; fru^{FLP}* (Figure S6A). In order to activate aSP2 and silence P1 in the same fly, we used *UAS-TNT LexAop-dTPRA1; tub^P>Gal80> fru^{FLP}* as effector (Gordon and Scott, 2009). This FLP-in strategy allows us to express the TNT under the control of Gal4 and dTRPA1 under the control of LexAGAD only within the *fru+* neurons. To test this FLP-in strategy with *tub^P>Gal80>*, we checked the expression of aSP2 and P1 in *UAS-mCD8RFP, LexAop-mCD8GFP; NP2631; VT8657.LexAGAD/ tub^P>Gal80> fru^{FLP}* males. In this system, VT8657.LexAGAD and NP2631 labeled aSP2 and P1 respectively, but NP2631 drove mCD8RFP expression in more neurons than it does with *UAS>stop>mCD8GFP; fru^{FLP}* (Figure 9B and S6B). This is possibly due to the relative strength of Gal4 expression with NP2631 compared to the suppression with *tub>Gal80>*. When we crossed VT8657.LexAGAD flies to *UAS-TNT LexAop-dTPRA1; tub>Gal80> fru^{FLP}* flies, the progeny with right genotype courted the target male at 30.5°C (Figure 12A). This induced male-male courtship is dramatically impaired when we silenced P1 with NP2631 (Figure 12A).

We also carried the reversed experiment namely silencing of aSP2 on activating P1 by using *LexAop>stop>TNT; UAS>stop>dTPRA1/ fru^{FLP}* as effector. Male-male courtship induced by P1 activation with NP2631 was almost abolished upon aSP2 silencing with VT8657.LexAGAD,

indicating that aSP2 is required for P1-induced male-male courtship (Figure 12B). Here I need to remind that the number of flies tested in these experiments is still low (n=5-9). However, these two sets experiments still suggest aSP2 and P1 works synergistically during courtship rather than work lineally and the activity of both neurons is required for courtship.

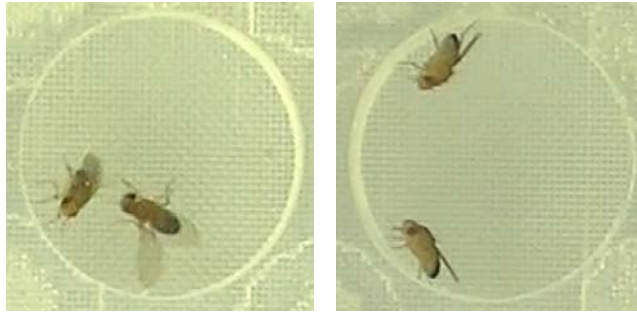
1324 VT lines and NP2631
(including 1283 Fru+ VT lines)

×

fru^{FLP}
UAS>stop>trpA1



Thermal activation from 25°C to 32°C in ~10 min



2 times of
retest



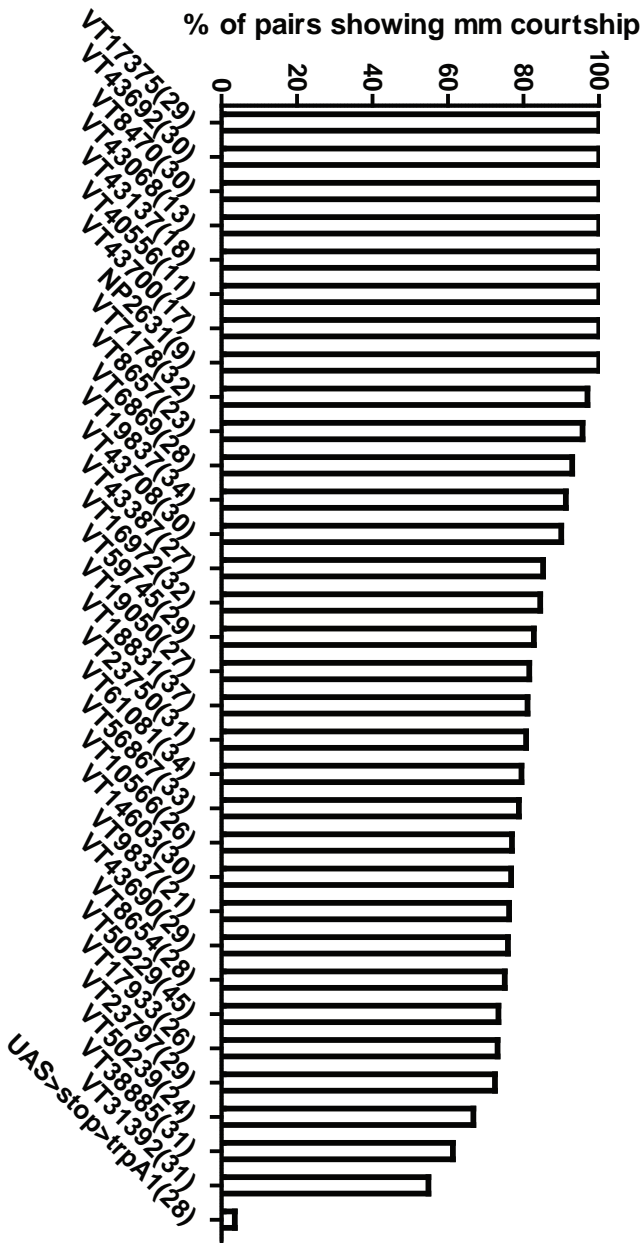
31 positive VT lines
and NP2631



1303 negative VT lines

Figure 7

A



B

VT	sex	LAN1	pMVP4	asp2	pipe	asp4	asp21	adT2	adT4	adT5	adT6	asG9	asp13	asp17	MB	OSN	PSG2	PMPS	DAB4	DAB5	VAB2	VAB3	VMS2	VPR4	HANI	WANI	LAN2	LAN3	LAN4
17375	M	2	0	0	0	0	0	0	0	0	0	0	0	0	0	0	0	0	0	0	0	0	0	0	0	0	0	0	0
7178	M	2	0	2	0	0	0	0	0	0	0	0	0	0	0	0	0	0	0	0	0	0	0	0	0	0	0	0	0
43690	M	2	0	2	0	0	0	0	0	0	0	0	0	0	0	0	0	0	0	0	0	0	0	0	0	0	0	0	0
16972	M	2	0	0	0	2	0	0	0	0	0	0	0	0	0	0	0	0	0	0	0	0	0	0	0	0	0	0	0
50229	M	2	0	0	0	0	0	0	0	0	0	0	0	0	0	0	0	0	0	0	0	0	0	0	0	0	0	0	0
59745	M	2	0	0	0	0	0	0	0	0	0	0	0	0	0	0	0	0	0	0	0	0	0	0	0	0	0	0	0
19837	M	2	0	0	0	0	0	0	0	0	0	0	0	0	0	0	0	0	0	0	0	0	0	0	0	0	0	0	0
43692	M	2	0	0	0	0	0	0	0	0	0	0	0	0	0	0	0	0	0	0	0	0	0	0	0	0	0	0	0
56867	M	2	0	0	0	0	0	0	0	0	0	0	0	0	0	0	0	0	0	0	0	0	0	0	0	0	0	0	0
6869	M	2	0	0	0	0	0	0	0	0	0	0	0	0	0	0	0	0	0	0	0	0	0	0	0	0	0	0	0
38885	M	2	0	0	0	0	0	0	0	0	0	0	0	0	0	0	0	0	0	0	0	0	0	0	0	0	0	0	0
10666	M	2	0	0	0	0	0	0	0	0	0	0	0	0	0	0	0	0	0	0	0	0	0	0	0	0	0	0	0
8470	M	2	0	0	0	0	0	0	0	0	0	0	0	0	0	0	0	0	0	0	0	0	0	0	0	0	0	0	0
18831	M	2	0	0	0	0	0	0	0	0	0	0	0	0	0	0	0	0	0	0	0	0	0	0	0	0	0	0	0
NP2631	M	0	2	0	0	0	0	0	0	0	0	0	0	0	0	0	0	0	0	0	0	0	0	0	0	0	0	0	0
61081	M	0	2	2	0	0	0	0	0	0	0	0	0	0	0	0	0	0	0	0	0	0	0	0	0	0	0	0	0
23750	M	0	2	0	0	0	0	0	0	0	0	0	0	0	0	0	0	0	0	0	0	0	0	0	0	0	0	0	0
43068	M	0	2	0	0	0	0	0	0	0	0	0	0	0	0	0	0	0	0	0	0	0	0	0	0	0	0	0	0
43137	M	0	2	0	0	0	0	0	0	0	0	0	0	0	0	0	0	0	0	0	0	0	0	0	0	0	0	0	0
40556	M	0	1	0	0	0	0	0	0	0	0	0	0	0	0	0	0	0	0	0	0	0	0	0	0	0	0	0	0
22797	M	0	0	2	0	0	0	0	0	0	0	0	0	0	0	0	0	0	0	0	0	0	0	0	0	0	0	0	0
8657	M	0	0	2	0	0	0	0	0	0	0	0	0	0	0	0	0	0	0	0	0	0	0	0	0	0	0	0	0
19050	M	0	0	0	2	0	0	0	0	0	0	0	0	0	0	0	0	0	0	0	0	0	0	0	0	0	0	0	0
50239	M	0	0	0	0	2	0	0	0	0	0	0	0	0	0	0	0	0	0	0	0	0	0	0	0	0	0	0	0
43700	M	0	0	0	0	0	2	0	0	0	0	0	0	0	0	0	0	0	0	0	0	0	0	0	0	0	0	0	0
43708	M	0	0	0	0	0	0	0	0	0	0	0	0	0	0	0	0	0	0	0	0	0	0	0	0	0	0	0	0
31392	M	0	0	0	0	0	0	0	0	0	0	0	0	0	0	0	0	0	0	0	0	0	0	0	0	0	0	0	0
17933	M	0	0	0	0	0	0	0	0	0	0	0	0	0	0	0	0	0	0	0	0	0	0	0	0	0	0	0	0

Figure 8

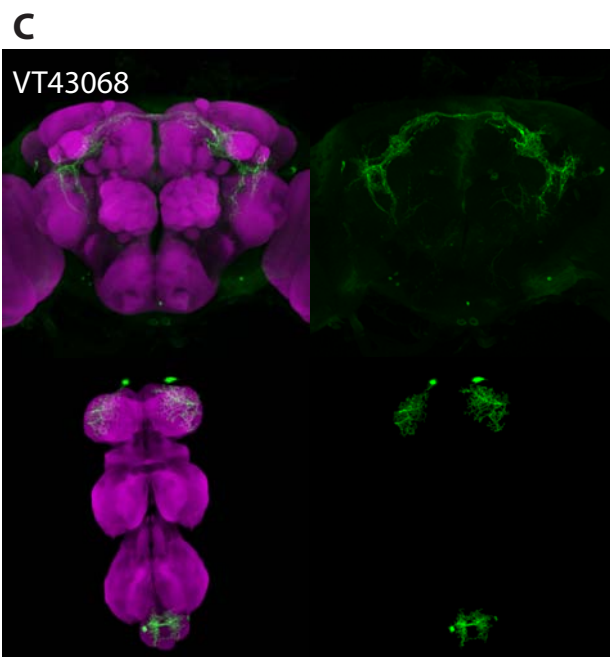
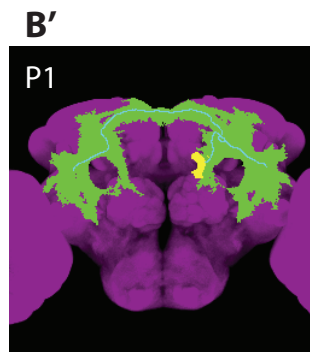
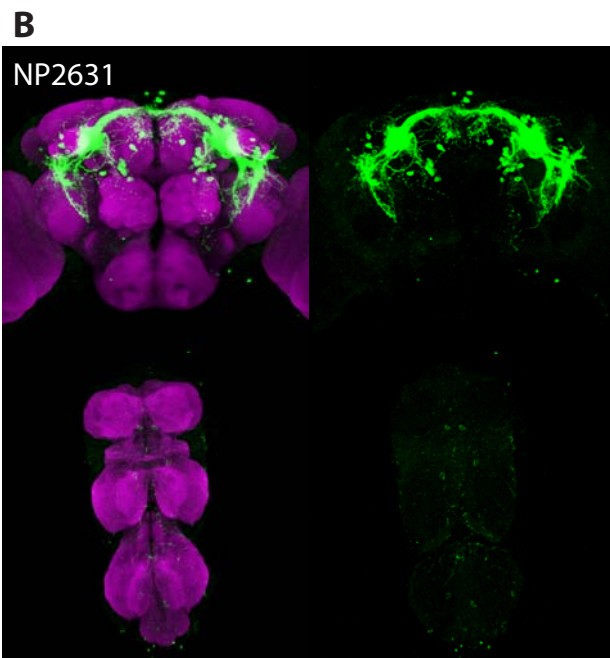
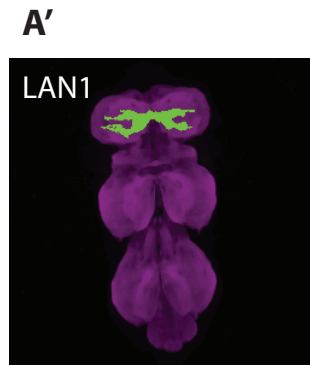


Figure 9

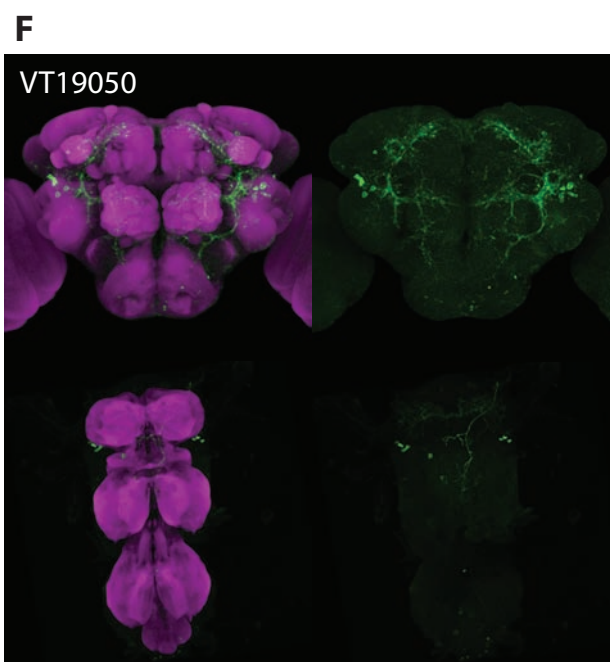
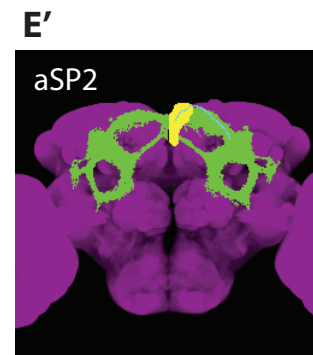
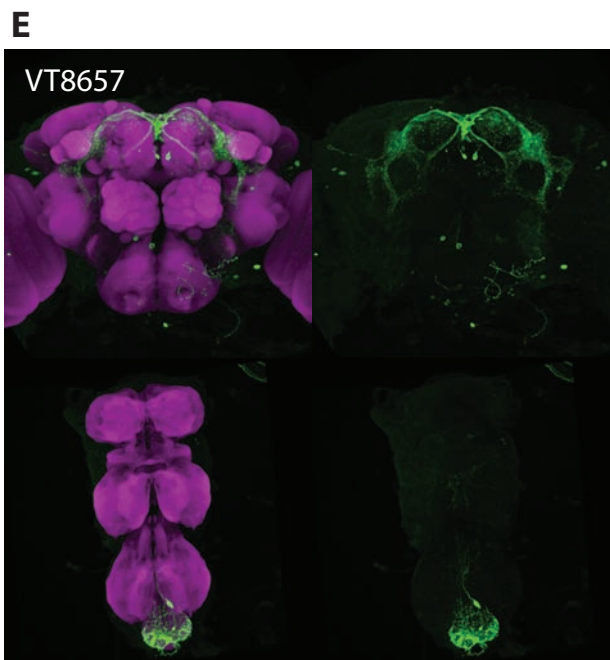
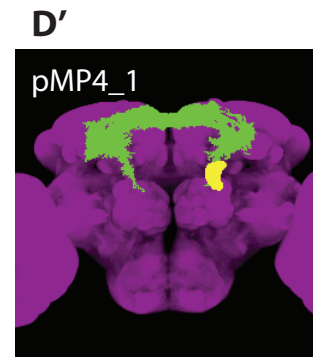


Figure 9

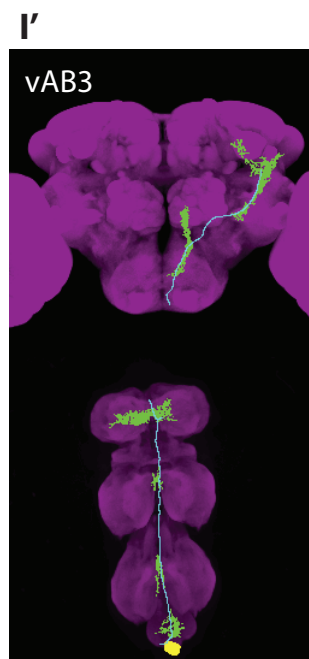
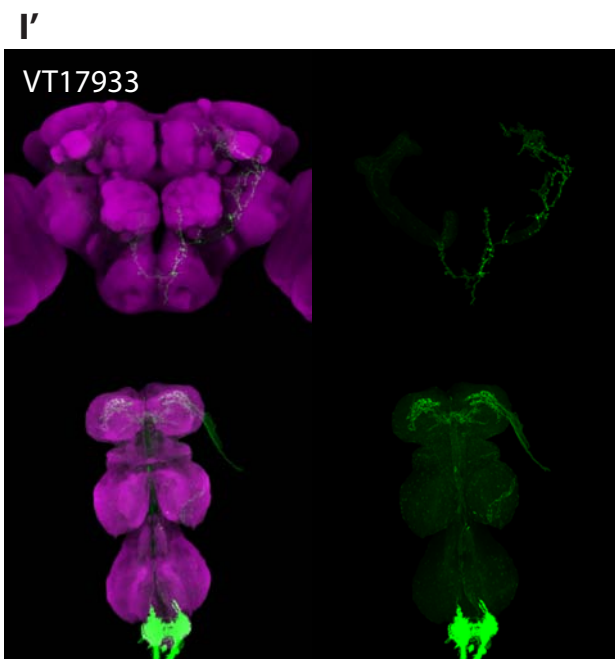
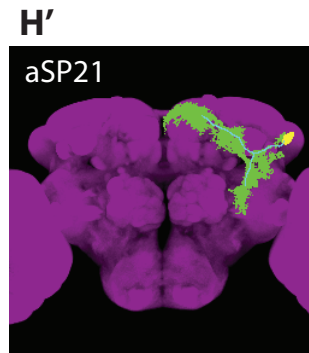
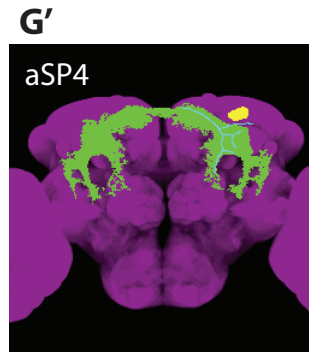
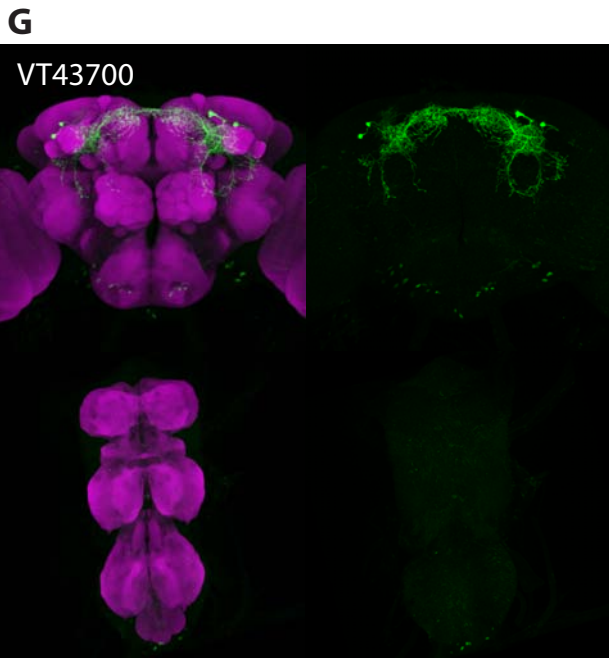


Figure 9

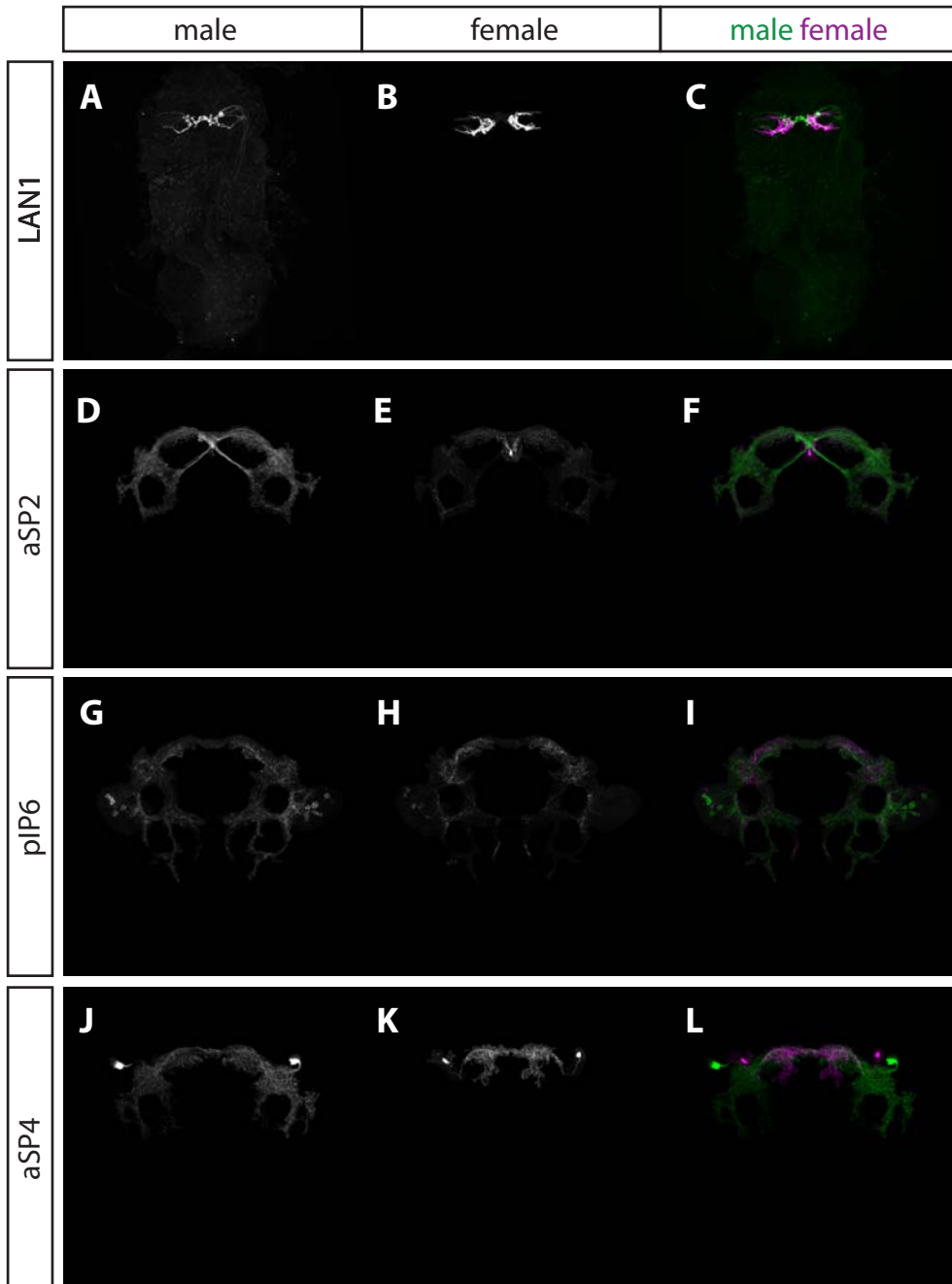


Figure 10

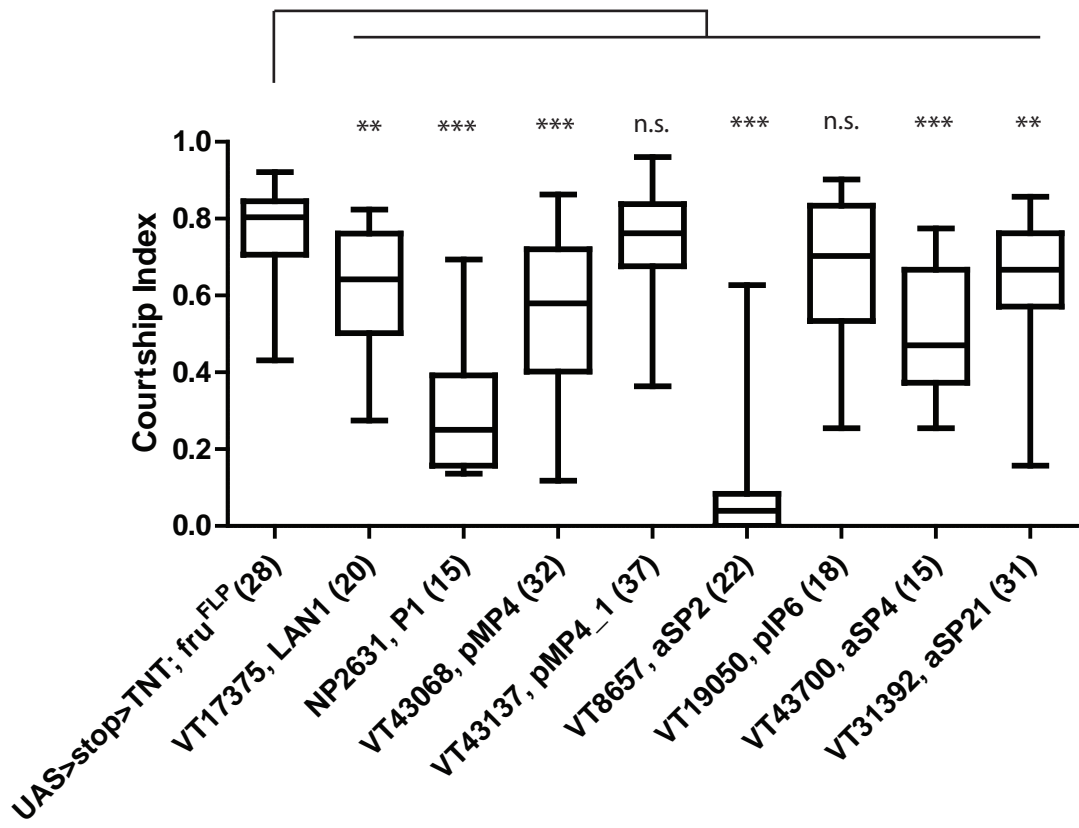


Figure 11

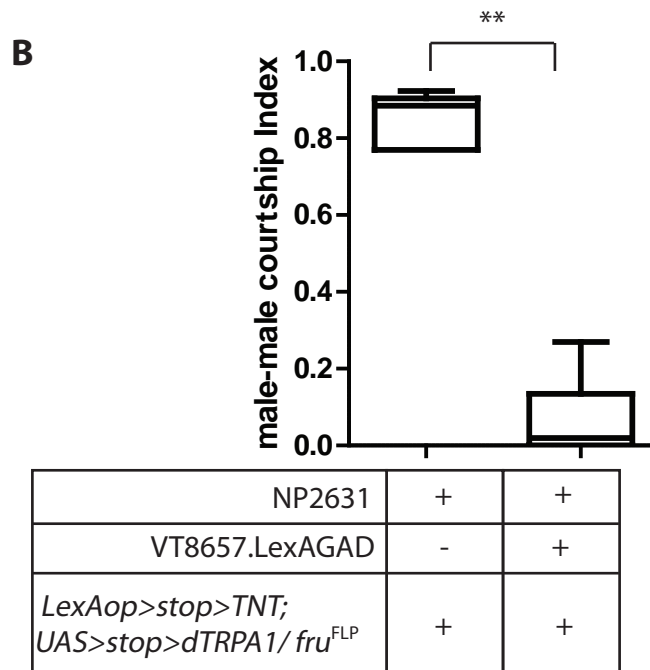
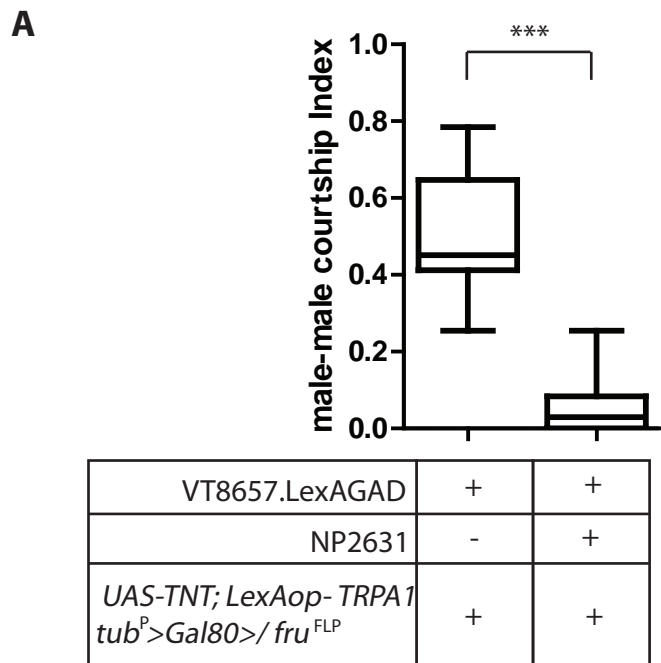


Figure 12

Figure 7. Screening scheme of functional dissection of fru+ neurons which drive courtship

Figure 8. Positive lines from the screen.

The ratio of male-male pairs which showed >3s of male-male courtship during the 10 min of assay. Each VT line was crossed to *UAS>stop>trpA1; Fru^{FLP}*.

Selected VT lines (row) and fru+ neurons (row). All the fru+ neurons which is labeled by more than one VT lines are selected. Dark orange indicates strong labeling and pale orange indicates weak labeling.

Figure 9. Anatomy of courtship driving neurons

Staining with anti-GFP (Green) of *UAS>stop>mCD8GFP; VT-XXX(or NP2631)/ fru^{FLP}* A. VT17375, B. NP2631, C. VT43068, D. V43137, E. VT8657, F. VT19050, G. VT43700, H. 31392 and I VT17933

Neuronal representation of A'. LAN1, B'. P1, C'. pMP4, D'. pMP4_1, E'. aSP2, F'. pIP6, G'. aSP4, H'. aSP21, and I'. vAB3.

Figure 10. Sexual dimorphism of courtship driving neurons

A. D. G. and C. Male

B. E. H. and K. Female

C. F. I. and L. Overlay of male (green) and female (magenta) of each neuron.

Figure 11. Silencing of courtship driving neuron

Courtship index. VT lines are crossed to *UAS>stop>TNT; fru^{FLP}*. VT line and the fru+ neuron it labels are indicated on the X-axis. **p<0.01. *** P<0.001. Mann-Whitney test.

Figure 12. Neuronal epistasis between P1 and aSP2

A. Male-male courtship induced by aSP2 activation is impaired by P1 silencing. *** P<0.001. Mann-Whitney test. (n=9 for left bar and n=8 for the right bar)

B. Male-male courtship induced by P1 activation is impaired by aSP2 silencing. ** P<0.01. Mann-Whitney test. (n=5 for left bar and n=8 for the right bar)

References

- Bidaye, S.S. (2012) Neuronal Basis for directed walking in *Drosophila melanogaster*. Thesis
- Billeter, J.C., and Goodwin, S.F. (2004). Characterization of *Drosophila* fruitless-gal4 transgenes reveals expression in male-specific fruitless neurons and innervation of male reproductive structures. *J Comp Neurol* 475, 270-287.
- Cachero, S., Ostrovsky, A.D., Yu, J.Y., Dickson, B.J., and Jefferis, G.S. (2010). Sexual dimorphism in the fly brain. *Curr Biol* 20, 1589-1601.
- Datta, S.R., Vasconcelos, M.L., Ruta, V., Luo, S., Wong, A., Demir, E., Flores, J., Balonze, K., Dickson, B.J., and Axel, R. (2008). The *Drosophila* pheromone cVA activates a sexually dimorphic neural circuit. *Nature* 452, 473-477.
- Doe, C.Q. (1992). Molecular markers for identified neuroblasts and ganglion mother cells in the *Drosophila* central nervous system. *Development* 116, 855-863.
- Ferveur, J.F., and Greenspan, R.J. (1998). Courtship behavior of brain mosaics in *Drosophila*. *J Neurogenet* 12, 205-226.
- Gordon, M.D., and Scott, K. (2009). Motor control in a *Drosophila* taste circuit. *Neuron* 61, 373-384.
- Groth, A.C., Fish, M., Nusse, R., and Calos, M.P. (2004). Construction of transgenic *Drosophila* by using the site-specific integrase from phage phiC31. *Genetics* 166, 1775-1782.
- Hall, J.C. (1994). The mating of a fly. *Science* 264, 1702-1714.
- Hamada, F.N., Rosenzweig, M., Kang, K., Pulver, S.R., Ghezzi, A., Jegla, T.J., and Garrity, P.A. (2008). An internal thermal sensor controlling temperature preference in *Drosophila*. *Nature* 454, 217-220.
- Jefferis, G.S., Potter, C.J., Chan, A.M., Marin, E.C., Rohlfsing, T., Maurer, C.R., Jr., and Luo, L. (2007). Comprehensive maps of *Drosophila* higher olfactory centers: spatially segregated fruit and pheromone representation. *Cell* 128, 1187-1203.
- Kimura, K., Ote, M., Tazawa, T., and Yamamoto, D. (2005). Fruitless specifies sexually dimorphic neural circuitry in the *Drosophila* brain. *Nature* 438, 229-233.
- Lee, G., Foss, M., Goodwin, S.F., Carlo, T., Taylor, B.J., and Hall, J.C. (2000). Spatial, temporal, and sexually dimorphic expression patterns of the fruitless gene in the *Drosophila* central nervous system. *J Neurobiol* 43, 404-426.
- Lee, T., and Luo, L. (1999). Mosaic analysis with a repressible cell marker for studies of gene function in neuronal morphogenesis. *Neuron* 22, 451-461.
- Lin, S., and Lee, T. (2012). Generating neuronal diversity in the *Drosophila* central nervous system. *Dev Dyn* 241, 57-68.
- Lu, B., LaMora, A., Sun, Y., Welsh, M.J., and Ben-Shahar, Y. ppk23-Dependent chemosensory functions contribute to courtship behavior in *Drosophila melanogaster*. *PLoS Genet* 8, e1002587.
- Martin, J.R., Keller, A., and Sweeney, S.T. (2002). Targeted expression of tetanus toxin: a new tool to study the neurobiology of behavior. *Adv Genet* 47, 1-47.

- Masser C. (2011) Construction of an enhancer library for neuronal circuit dissection in *Drosophila melanogaster* and its employment to identify neurons involved in male courtship behavior. Thesis
- Pan, Y., Meissner, G.W., and Baker, B.S. (2012). Joint control of *Drosophila* male courtship behavior by motion cues and activation of male-specific P1 neurons. *Proc Natl Acad Sci U S A* *109*, 10065-10070.
- Peters, A., Feldman, M., and Saldanha, J. (1976). The projection of the lateral geniculate nucleus to area 17 of the rat cerebral cortex. II. Terminations upon neuronal perikarya and dendritic shafts. *J Neurocytol* *5*, 85-107.
- Pfeiffer, B.D., Jenett, A., Hammonds, A.S., Ngo, T.T., Misra, S., Murphy, C., Scully, A., Carlson, J.W., Wan, K.H., Lavery, T.R., *et al.* (2008). Tools for neuroanatomy and neurogenetics in *Drosophila*. *Proc Natl Acad Sci U S A* *105*, 9715-9720.
- Pfeiffer, B.D., Ngo, T.T., Hibbard, K.L., Murphy, C., Jenett, A., Truman, J.W., and Rubin, G.M. (2010). Refinement of tools for targeted gene expression in *Drosophila*. *Genetics* *186*, 735-755.
- Rohlfing, T., and Maurer, C.R., Jr. (2003). Nonrigid image registration in shared-memory multiprocessor environments with application to brains, breasts, and bees. *IEEE Trans Inf Technol Biomed* *7*, 16-25.
- Strauss, R. (2002). The central complex and the genetic dissection of locomotor behaviour. *Curr Opin Neurobiol* *12*, 633-638.
- Thistle, R., Cameron, P., Ghorayshi, A., Dennison, L., and Scott, K. (2012). Contact chemoreceptors mediate male-male repulsion and male-female attraction during *Drosophila* courtship. *Cell* *149*, 1140-1151.
- Toda, H., Zhao, X., and Dickson, B.J. (2012). The *Drosophila* Female Aphrodisiac Pheromone Activates ppk23(+) Sensory Neurons to Elicit Male Courtship Behavior. *Cell Rep* *1*, 599-607.
- von Philipsborn, A.C., Liu, T., Yu, J.Y., Masser, C., Bidaye, S.S., and Dickson, B.J. Neuronal control of *Drosophila* courtship song. *Neuron* *69*, 509-522.
- von Philipsborn, A.C., Liu, T., Yu, J.Y., Masser, C., Bidaye, S.S., and Dickson, B.J. (2011). Neuronal control of *Drosophila* courtship song. *Neuron* *69*, 509-522.
- Yu, J.Y., Kanai, M.I., Demir, E., Jefferis, G.S., and Dickson, B.J. (2010). Cellular organization of the neural circuit that drives *Drosophila* courtship behavior. *Curr Biol* *20*, 1602-1614.

3. Discussion

3.1 Anatomical analysis of *fru+* neurons

Specific targeting of Fruitless neurons by enhancer tiles

Investigation of neuronal circuits relies on tools to target individual neurons. In *D. melanogaster*, this is mainly achieved through GAL4/UAS system derived from the yeast (Brand and Perrimon, 1993). GAL4 binds to the UAS driving the expression of the reporter downstream of UAS. Large collections of GAL4 drivers were generated through the random insertion of the P-element which contains GAL4 (Hayashi et al., 2002). However such a drive tends to give broad GAL4 expression. This is because the GAL4 expression is under the control of multiple enhancers nearby the insertion site of the P-element. It is especially crucial to gain spatio-temporal control of GAL4 expression in order to investigate the neuronal function. In this study, we used a new collection of GAL4 drivers (VT lines) generated as described before (Pfeiffer et al., 2008; Masser 2011; Bidaye 2012). First, a 2-3 kb of DNA fragment is cloned to regulate GAL4 expression. Then each construct is inserted into the same location through phiC31 site-specific integration (Groth et al., 2004). Such GAL4 drivers achieved restricted expression of GAL4 in the embryo and nervous system of *D. melanogaster* (Pfeiffer et al., 2008). The present study further confirmed the sparser labeling of neurons by this method within the restriction of *fru+* neurons (Figure 1D). The restricted GAL4 expression of VT lines allowed us to further investigate the anatomy of *fru+* neurons. We could resolve the entire arborization and identify more types of neurons (Figure S2 and S3). The thermal activation screen with VT lines allowed us to identify causality between neurons and phenotypes with relative ease.

Functional relevance estimated from anatomical overlap

In this study, we predicted functional relevance based on the anatomical overlap. This is based on Peter's rule derived from the study of mammalian cortices, which infers the occurrence of synaptic targets from the overlap between dendritic and axonal arbors (Binzegger et.al., 2004, Braitenberg and Schüz, 1991). Can we apply this with *fru+* neurons in *D. melanogaster* in order to infer the functional connection? There are still few studies about functional connection between *fru+* neurons. At the lateral horn, electrical stimulation of DA1

projection neurons (aDT3) can induce the transient increase of Ca²⁺ in DC1 (aSP5) and LC1 (aSP8) neurons (Ruta et al., 2010). At AMMC, IVLP-VLP projection neurons responds to various acoustic stimuli including courtship song (Lai et al., 2012). These IVLP-VLP projection neurons are anatomically similar with aIP5 (Figure 3.3). Both of these studies proved the functional connection predicted based on anatomical connection (Yu et. al., 2010). Neurons involved in courtship song generation, in abdominal bending, and in driving of courtship overlap extensively with each other. We have not yet proved direct connection between them, but those are the potential neurons that can further support the Peter's rule in *D. melanogaster*.

Lateral protocerebral complex is an integration center

Neuronal representations of sensory inputs require to be integrated for proper evaluation of the external environment. The integrated information is then processed together with the internal state of the animal to control and execute appropriate motor outputs. Based on the dense innervations of *fru+* neurons in LPC, it was proposed to be the integration center for courtship behavior (Yu et al., 2010). The corresponding region in female fly is smaller (Cachero et al., 2010). These two anatomical studies also revealed the presence of such *fru+* neurons that could mediate various sensory inputs to LPC (Cachero et al., 2010; Yu et al., 2010) . In this study, we reinforced this idea by further anatomical characterization and identification of *fru+* neurons. aSP21 might relay olfactory input to LPC (Figure 3.1). aSP14, aSP16, and pIP2 could mediate visual input from LV to LPC (Figure 3.2B4 and 3.6B1). aIP5 could mediate auditory input to LPC (Figure 3.3B and 3.7B1) dAB2, and dMS6 could mediate gustatory input from gustatory input to LPC (Figure 3.4) We also identified more neurons innervating LPC (Figure 3.5, 3.6, and 3.7).

3.2. Manipulation of a single neuronal class

We have performed a thermogenetic screen to identify neurons involved in generation of courtship song, copulation, and driving of courtship. Although the GAL4 library we used (VT lines) labels a small number of *fru+* neurons on average with the FLP-in system, each VT line rarely labels one single type of *fru+* neurons (Figure 1D). This is also the case with the positive VT lines we collected from the thermogenetic screens. Further genetic dissection is required to exclude the possible involvement of other neurons labeled by the positive VT lines. One

method is the stochastic labeling as we used during the investigation of P1, pIP10, and vMS11 (von Philipsborn et al., 2011). If we can find multiple lines labeling the same neuron, we could use split-GAL4 system to restrict the GAL4 expression to the shared neurons (Luan et al., 2006; Pfeiffer et al., 2010). Combination of split-GAL4 and FLP-in system could potentially allow us to label and manipulate one specific type of neuron. Split-GAL4 system has an advantage of being able to repeatedly access neuron, which is not easy to achieve with stochastic labeling.

3.3. *fru*+ neurons involved in copulation attempt and copulation

In order to investigate the neuronal basis for copulation attempt and copulation, we performed thermogenetic screen of *fru*+ neurons. Abdominal ganglion has been suggested to be required for copulation (Ferveur and Greenspan, 1998). We found six types of neurons (dAB4, dAB5, dAB8, dMT3, dAB7 and vAB2) are labeled repeated in a sparse manner by the positive VT lines restored in the screen. Consistent with the previous study, all the five neurons innervate either anterior or posterior part of the abdominal ganglion (Figure 5G and H).

Motor control by dAB4, dAB5 and dAB8

dAB4, dAB5 and dAB8 send projections into the abdomen, possibly controlling muscles in the abdomen. Which of the muscle is controlled by these three neurons? *fru*+ neurons send thick nerve bundle to the abdomen and innervate the muscles of abdominal segments as well as internal reproductive organs (Lee and Hall, 2001). Detailed observation revealed that *fru*+ neurons innervate the dorsal part of abdominal segment A2 to A6 and ventral part of segment A5 (Billeter and Goodwin, 2004). One intriguing candidate is a sexually dimorphic muscle located at the dorsal segment A5, which is known as muscle of Lawrence (MOL). The formation of MOL requires both Fru^M and the innervations of motor neurons during the development (Currie and Bate, 1995; Gailey et al., 1991). However, MOL is dispensable for male fertility and thus is not an essential component of abdominal bending required for copulation (Gailey et al., 1991). Synaptic silencing of dAB4 and dAB8 with VT40010 and VT63540 respectively prevent the successful copulation within the 10 min of assay. We did not test the success of copulation in longer span (a couple of days) upon silencing of these neurons as was performed in Gailey et al., 1991. This raises the possibility that MOL is actually required for successful copulation in short time and its contraction is controlled by one the potential motor neurons we identified in this study.

The muscular innervation of these neurons can be simply resolved by dissecting the abdomen. There are 18 lines from the bending screen which labels none of the neurons we discussed so far. The dense innervations of multiple fru+ neurons labeled by those 18 lines in the abdominal ganglion prevent us from resolving individual types of fru+ neurons by observing their anatomy. Identification of muscular innervation of those neurons should allow us to resolve their identity.

Signals from or to the brain through dAB7 and vAB2

We found two ascending neurons (dAB7 and vAB2) are labeled repeatedly and sparsely by the positive VT lines from the screen. The functional polarity of these two neurons is yet to be assessed. This can be achieved by expressing GFP-tagged synaptobrevin or DSCAM17.1 as presynaptic or postsynaptic marker respectively.

What can be the signals these two neurons relay from brain or to the brain? Upon the initiation of courtship, the male fly orients and follows the female frequently extending and vibrating its wing unilaterally. Copulation attempts only happen a few seconds to a few minutes after the initiation of courtship (Hall, 1994). This delay is considered to be the time required for the male to assess the female. The close proximity between the male and female fly is also required for copulation attempt. dAB7 or vAB2 arborize at the ring part of LPC, the integration center for courtship, which implies that they can possibly convey the decision made based on the assessment of female or the proximity from the brain to abdominal ganglion. Licking is frequently followed by the copulation attempt (Hall, 1994). Both dAB7 and vAB2 arborize in dorsal part of subesophageal ganglion (SOG) where the gustatory neurons from the proboscis as well as legs send their projections (Stocker, 1994). It might be possible that these two neurons integrate input from LPC and proboscis to make the decision of copulation attempt.

Copulation of *D. melanogaster* lasts for approximately 15-20 min. Although the sperm allocation happens in the first 6-8 min, the extra copulation time is necessary to delay female remating (Gilchrist and Partridge, 2000). One possible function of dAB7 or vAB2 can be to maintain and prolong the copulation. Some sensory input from accessory glands or genitalia, which reflects the progress of copulation, might be conveyed to the abdominal ganglion and then relayed by dAB7 or vAB2 to the brain. Interestingly, dAB7 and vAB2 have similar and overlapping arborization in the brain (Figure 5E' and F'). Thus, it is possible that the copulation

prolonging signal is directly transferred from one neuron to the other to maintain copulation. If this is true, neuronal silencing of dAB7 or vAB2 should not disrupt the initiation of copulation but the continuation.

3.4 *fru*+ neurons that drive courtship

Sensory representations that drive courtship

What kind of sensory stimuli can promote courtship? 7,11-HD and 7,11-ND are female nonvolatile aphrodisiac pheromone which stimulate male courtship (Ferveur, 2005; Jallon, 1984). *ppk23+* and *fru+* gustatory sensory neurons (LAN1) mediate this physiologically and behaviorally (Thistle et al., 2012; Toda et al., 2012). The thermogenetic screen we performed has confirmed the sufficiency of LAN1 activation to drive courtship in the presence of another fly. The target male seems to provide both olfactory and visual input to elicit the courtship behavior (Thistle et al., 2012). We found a line (VT17933) from this screen which labels vAB3. vAB3 is anatomically interesting neurons innervating ventral prothoracic ganglion in the VNC and the lateral junction of LPC. vAB3 thus is a candidate neuron that relays courtship-promoting gustatory input to the LPC, the integration center.

Specific volatile pheromone that stimulates the courtship has not been identified yet. However, two olfactory sensory neurons (OSN) which express *Or47b* or *Ir84a* play important roles in promoting courtship. *Or47b+* OSNs respond to male and female fly extracts and the genetic perturbation of *Or47b+* OSN increases the latency of courtship initiation (Root et al., 2008; van der Goes van Naters and Carlson, 2007). *Ir84a+* OSNs are activated by phenylacetic acid and phenylacetaldehyde, which are widely found in fruit (Grosjean et al., 2012). *Ir84a* mutant males court virgin females less than wild-type males (Grosjean et al., 2012). The olfactory inputs are conveyed from OSNs through projection neurons to mushroom body and lateral horn. From courtship-driving neuron screen, we found a VT line (VT31392) which labels aSP21. aSP21 arborize in the ventral anterior part of lateral horn. Interestingly, projection neurons which innervate the same glomeruli with *Or47b* and *Ir84a* innervate the ventral anterior part of lateral horn (Grosjean et al., 2012). One intriguing hypothesis is that aSP21 mediates the fly odors or the food odors (or both of them) to promote courtship. Interruption of olfactory input delays the courtship initiation but does not completely abolish courtship

behavior (Krstic et al., 2009; Markow, 1987). This is consistent with our observation that aSP21 silencing with VT31392 only partially impairs the courtship behavior (Figure 11).

Visual and auditory input also play important role in courtship behavior. Although blind mutant males have little defect in courtship initiation, they tend to have more frequent breaks during the courtship due to the defect in tracking of females (Cook 1980; Krstic et. al., 2009). When the courtship song is played back to wingless males (mute male), males increase their velocity and court other males episodically (Eberl et al., 1997; von Schilcher, 1976). None of the neuron we identified from our courtship-driving neurons screen has some anatomical features to suggest its relevance to visual or auditory input.

Integration center for driving courtship

In addition to LAN1, vAB3, and aSP21, we have identified P1, two of P1 subtype (pMP4 and pMP4_1), aSP2, pIP6 and aSP4 whose activation can drive courtship in the presence of another fly. All of these neurons innervate LPC extensively where they overlap with vAB3 and aSP21, suggesting that they can be functionally connected with each other and integrate gustatory and olfactory inputs to execute courtship. These neurons can be the core of courtship circuit that drives courtship.

Among them, P1 had been well studied. It has first been identified as male-specific neurons whose masculinization in the female brain can trigger females to follow and extend the wing unilaterally toward target females (Kimura et al., 2005). Thermal activation of P1 with *trpA1* can elicit unilateral wing extension and courtship song (Kohatsu et al., 2011; von Philipsborn et al., 2011). Pan et. al. has reported that male flies with P1 activation even court a moving object as well as wild-type males (Pan et al., 2012). However, they observed only very low level of wing extension in isolated males. The phenotypic difference upon P1 activation can be explained by number of neurons that are targeted in each of these studies. P1 is consists of ~25 cells per hemisphere (Kimura et al., 2005). In the former cases, nearly entire cells of P1 are labeled either by MARCM or NP2631 (Kohatsu et al., 2011; von Philipsborn et al., 2011). In the study of Pan et. al., less than half of P1 neurons were targeted by a Gal4 driver (9.5 ± 1.3 per hemisphere) (Pan et al., 2012). Consistently, when different numbers of P1 neurons were activated through *trpA1* by the stochastic labeling method, the number of activated P1 neurons correlates positively with the amount of induced courtship song and

there seemed to be a minimum number (~10 cells) required for induction of courtship song (von Philipsborn et al., 2011).

With our screen, we found P1 can be subdivided into two types of neurons, pMP4 and pMP4_1 and activation of either of them can elicit courtship toward target males. Activation of pMP4 with VT43068 could also elicit courtship song in isolated males, while activation of pMP4_1 with VT43137 could not, implying functional differences. However, the phenotypic difference between the activation of pMP4 and pMP4_1 can be simply due to the number of pMP4_1 labeled by VT43137 (7.3 ± 0.8). It could also be due to the weaker expression level of GAL4 with VT43137 than VT43068. We need more driver lines which target pMP4_1 to deduct the conclusion.

We identified aSP2 as another courtship-driving neuron. Synaptic silencing of aSP2 with VT8657 almost completely abolished courtship behavior, suggesting that aSP2 is responsible for integrating multiple sensory modalities. We do not know what kind of sensory stimuli aSP2 receives. However, the dramatic reduction of courtship upon silencing of aSP2 suggests it mediates multiple sensory cues rather than one because the ablation of one kind of sensory input affects courtship only in a minor way (Krstic et al., 2009).

The dramatic reduction of courtship behavior upon silencing of P1 and aSP2 made us to question their neuronal hierarchy (Figure 11). We performed neuronal epistasis experiments to either silence P1 upon aSP2 activation or silence aSP2 upon P1 activation. We found that induced courtship towards target males upon aSP2 activation is impaired upon P1 silencing, while induced courtship upon P1 activation is impaired upon aSP2 silencing. We would like to propose that aSP2 and P1 function synergistically during courtship rather than linearly.

Another type of *fru+* neuron that can elicit courtship toward target males is pIP6. Although we found 4 positive VT lines that labels pIP6, only VT19050 could elicit courtship song in isolated male. This might be due to the number of pIP6 neurons labeled by those VT lines as seems to be the case with P1. Although we do not yet know the specific effect of pIP6 silencing on courtship song, males with pIP6 silenced follow male and extend the wing unilaterally as vigorous as control males (Figure 11). pIP6 might be one of the input neurons to P1 which is not necessary for courtship song or serve as a redundant pathway for courtship song generation. It is still too early to deduct any firm conclusion.

The last *fru+* neuron we found from the courtship-driving neuron screen is aSP4. aSP4 might be a dopaminergic neuron since it is labeled by TH-GAL4 which express GAL4 under the

control of *Drosophila* tyrosine hydroxylase promoter (Friggi-Grelin et al., 2003; Yu et al., 2010). Elevated level of dopamine has been shown to promote male arousal and enhance heterosexual and homosexual courtship (Andretic et al., 2005; Kume et al., 2005; Liu et al., 2008). Thus, it is possible that activation of aSP4 mimics the elevated level of dopamine in the fly brain and drives courtship toward target male. Courtship activity is under the control of circadian rhythm through the clock neurons (Fujii and Amrein, 2010; Fujii et al., 2007). One intriguing hypothesis is that these clock neurons regulate directly or indirectly the activity of aSP4 in order to control the courtship activity rhythm.

How is the “command” to court delivered to VNC?

Movement of legs and wings are controlled by CPGs that reside in VNC. The descending input from the brain to CPG is evidently required to perform right motor behavior to make sense of sensory inputs. We still know little about the existence of such descending input in *D. melanogaster*. A small number of neurons, giant fibers, are well studied descending neurons. As its name stands, giant fibers are large interneurons of ~8mm in diameter whose cell bodies are located at the dorsal-medial part of the brain (Koto et al., 1981). They elicit escape behavior through the activation of tergotrochanteral motoneurons that innervate the tergotrochanteral muscle (jump muscle) and the peripherally synapsing interneuron, which outputs to five dorsolongitudinal muscle motoneurons (DLMns) (Tanouye and Wyman, 1980). DLMns supply the large indirect dorsal longitudinal muscles (wing depressors). Another example of descending neurons is pIP10 (or P2B) which is described in this study (see the appendix) (Kohatsu et al., 2011; von Philipsborn et al., 2011). They can be connected to pre-motor neurons dPR1, vRP6, and vMS11 which are potentially part of CPG for courtship song (von Philipsborn et al., 2011; Yu et al., 2010).

What about descending neurons for courtship promotion? pIP10 is a potential candidate. VT40556 which we identified in the song screen is a positive line in the courtship-driving neurons screen as well. However, VT40556 labels a small number of P1 (2-3 cells per hemisphere) and aSP4, both of which were identified in the same screen to promote courtship. Silencing of pIP10 with VT40556 only partially impairs courtship ($UAS>stop>TNT; VT40556/fru^{FLP}$ male, $29.7\pm 1.8\%$. $UAS>stop>TNTinactive; VT40556/fru^{FLP}$ male, $40.7\pm 1.8\%$. the time a male spends on oriented wing extension. average \pm SEM)(von Philipsborn et al., 2011). Thus, pIP10 might function to promote courtship in addition to the production of courtship song, but

does not seem to be the only descending neuron which promotes courtship. However, we could not identify any other descending neurons from our courtship-driving neuron screen.

Orienting toward and following of females are critical steps of courtship ritual. It is not hard to imagine that there are two descending neurons which regulate orienting and following independently. During the courtship, male flies drift sideways in a circle around female, which is known as circling (Dankert et al., 2009). Circling could require different locomotor control and thus potentially be regulated by other descending neurons.

How can we identify those descending inputs? Regulation of orientation and following should require tight temporal control based on the position of females, thus activation of such descending neurons might not induce orientation towards or following of females but only increase the fly locomotor activity or cause turning. Neuronal silencing can be a rather efficient method to identify such neurons, since the lack of either orientation or following ability would lead to reduced courtship.

Orientation and following behavior is observed in females as well (Dankert et al., 2009). This suggests that neuronal basis for this part of courtship ritual is sex monomorphic. If so, then such a circuit might not be under the control of *fruitless*. Taken together, the exploration of descending neurons involved in orientation and following need to be done through neuronal silencing without the restriction of *fruitless* neurons.

Conclusion

~2000 fru+ neurons play key roles in courtship behavior. Anatomical characterization of each types of fru+ neurons and targeted manipulation of them is required to understand the neuronal basis of courtship behavior. In this study, we screened a new collection of GAL4 lines (VT lines) and extended anatomical study, identifying more candidate neurons involved in sensory input, sensory integration, and motor control. Thanks to the sparse labeling of fru+ neurons by the VT lines, thermogenetic activation screen revealed various types of neurons involved in courtship song, copulation attempt, copulation and courtship promotion. Investigation on the input signals they receive and their interaction will provide evidence to understand the neuronal basis of courtship behavior.

References

- Anand, A., Vilella, A., Ryner, L.C., Carlo, T., Goodwin, S.F., Song, H.J., Gailey, D.A., Morales, A., Hall, J.C., Baker, B.S., *et al.* (2001). Molecular genetic dissection of the sex-specific and vital functions of the *Drosophila melanogaster* sex determination gene fruitless. *Genetics* *158*, 1569-1595.
- Andretic, R., van Swinderen, B., and Greenspan, R.J. (2005). Dopaminergic modulation of arousal in *Drosophila*. *Curr Biol* *15*, 1165-1175.
- Billeter, J.C., Atallah, J., Krupp, J.J., Millar, J.G., and Levine, J.D. (2009). Specialized cells tag sexual and species identity in *Drosophila melanogaster*. *Nature* *461*, 987-991.
- Billeter, J.C., and Goodwin, S.F. (2004). Characterization of *Drosophila* fruitless-gal4 transgenes reveals expression in male-specific fruitless neurons and innervation of male reproductive structures. *J Comp Neurol* *475*, 270-287.
- Brand, A.H., and Perrimon, N. (1993). Targeted gene expression as a means of altering cell fates and generating dominant phenotypes. *Development* *118*, 401-415.
- Cachero, S., Ostrovsky, A.D., Yu, J.Y., Dickson, B.J., and Jefferis, G.S. (2010). Sexual dimorphism in the fly brain. *Curr Biol* *20*, 1589-1601.
- Castrillon, D.H., Gonczy, P., Alexander, S., Rawson, R., Eberhart, C.G., Viswanathan, S., DiNardo, S., and Wasserman, S.A. (1993). Toward a molecular genetic analysis of spermatogenesis in *Drosophila melanogaster*: characterization of male-sterile mutants generated by single P element mutagenesis. *Genetics* *135*, 489-505.
- Clyne, J.D., and Miesenbock, G. (2008). Sex-specific control and tuning of the pattern generator for courtship song in *Drosophila*. *Cell* *133*, 354-363.
- Currie, D.A., and Bate, M. (1995). Innervation is essential for the development and differentiation of a sex-specific adult muscle in *Drosophila melanogaster*. *Development* *121*, 2549-2557.
- Dankert, H., Wang, L., Hoopfer, E.D., Anderson, D.J., and Perona, P. (2009). Automated monitoring and analysis of social behavior in *Drosophila*. *Nat Methods* *6*, 297-303.
- Datta, S.R., Vasconcelos, M.L., Ruta, V., Luo, S., Wong, A., Demir, E., Flores, J., Balonze, K., Dickson, B.J., and Axel, R. (2008). The *Drosophila* pheromone cVA activates a sexually dimorphic neural circuit. *Nature* *452*, 473-477.
- Demir, E., and Dickson, B.J. (2005). fruitless splicing specifies male courtship behavior in *Drosophila*. *Cell* *121*, 785-794.
- Doe, C.Q. (1992). Molecular markers for identified neuroblasts and ganglion mother cells in the *Drosophila* central nervous system. *Development* *116*, 855-863.
- Eberl, D.F., Duyk, G.M., and Perrimon, N. (1997). A genetic screen for mutations that disrupt an auditory response in *Drosophila melanogaster*. *Proc Natl Acad Sci U S A* *94*, 14837-14842.
- Ferveur, J.F. (2005). Cuticular hydrocarbons: their evolution and roles in *Drosophila* pheromonal communication. *Behav Genet* *35*, 279-295.
- Ferveur, J.F., and Greenspan, R.J. (1998). Courtship behavior of brain mosaics in *Drosophila*. *J Neurogenet* *12*, 205-226.

- Friggi-Grelin, F., Coulom, H., Meller, M., Gomez, D., Hirsh, J., and Birman, S. (2003). Targeted gene expression in *Drosophila* dopaminergic cells using regulatory sequences from tyrosine hydroxylase. *J Neurobiol* *54*, 618-627.
- Fujii, S., and Amrein, H. (2010). Ventral lateral and DN1 clock neurons mediate distinct properties of male sex drive rhythm in *Drosophila*. *Proc Natl Acad Sci U S A* *107*, 10590-10595.
- Fujii, S., Krishnan, P., Hardin, P., and Amrein, H. (2007). Nocturnal male sex drive in *Drosophila*. *Curr Biol* *17*, 244-251.
- Gailey, D.A., and Hall, J.C. (1989). Behavior and cytogenetics of fruitless in *Drosophila melanogaster*: different courtship defects caused by separate, closely linked lesions. *Genetics* *121*, 773-785.
- Gailey, D.A., Taylor, B.J., and Hall, J.C. (1991). Elements of the fruitless locus regulate development of the muscle of Lawrence, a male-specific structure in the abdomen of *Drosophila melanogaster* adults. *Development* *113*, 879-890.
- Gilchrist, A.S., and Partridge, L. (2000). Why it is difficult to model sperm displacement in *Drosophila melanogaster*: the relation between sperm transfer and copulation duration. *Evolution* *54*, 534-542.
- Goodwin, S.F., Taylor, B.J., Vellella, A., Foss, M., Ryner, L.C., Baker, B.S., and Hall, J.C. (2000). Aberrant splicing and altered spatial expression patterns in fruitless mutants of *Drosophila melanogaster*. *Genetics* *154*, 725-745.
- Gordon, M.D., and Scott, K. (2009). Motor control in a *Drosophila* taste circuit. *Neuron* *61*, 373-384.
- Grosjean, Y., Rytz, R., Farine, J.P., Abuin, L., Cortot, J., Jefferis, G.S., and Benton, R. (2012). An olfactory receptor for food-derived odours promotes male courtship in *Drosophila*. *Nature* *478*, 236-240.
- Groth, A.C., Fish, M., Nusse, R., and Calos, M.P. (2004). Construction of transgenic *Drosophila* by using the site-specific integrase from phage phiC31. *Genetics* *166*, 1775-1782.
- Hall, J.C. (1994). The mating of a fly. *Science* *264*, 1702-1714.
- Hamada, F.N., Rosenzweig, M., Kang, K., Pulver, S.R., Ghezzi, A., Jegla, T.J., and Garrity, P.A. (2008). An internal thermal sensor controlling temperature preference in *Drosophila*. *Nature* *454*, 217-220.
- Hayashi, S., Ito, K., Sado, Y., Taniguchi, M., Akimoto, A., Takeuchi, H., Aigaki, T., Matsuzaki, F., Nakagoshi, H., Tanimura, T., *et al.* (2002). GETDB, a database compiling expression patterns and molecular locations of a collection of Gal4 enhancer traps. *Genesis* *34*, 58-61.
- Ito, H., Fujitani, K., Usui, K., Shimizu-Nishikawa, K., Tanaka, S., and Yamamoto, D. (1996). Sexual orientation in *Drosophila* is altered by the satori mutation in the sex-determination gene fruitless that encodes a zinc finger protein with a BTB domain. *Proc Natl Acad Sci U S A* *93*, 9687-9692.
- Ito, H., Sato, K., Koganezawa, M., Ote, M., Matsumoto, K., Hama, C., and Yamamoto, D. (2012). Fruitless recruits two antagonistic chromatin factors to establish single-neuron sexual dimorphism. *Cell* *149*, 1327-1338.

- Jallon, J.M. (1984). A few chemical words exchanged by *Drosophila* during courtship and mating. *Behav Genet* *14*, 441-478.
- Jefferis, G.S., Potter, C.J., Chan, A.M., Marin, E.C., Rohlfsing, T., Maurer, C.R., Jr., and Luo, L. (2007). Comprehensive maps of *Drosophila* higher olfactory centers: spatially segregated fruit and pheromone representation. *Cell* *128*, 1187-1203.
- Keleman, K., Vrontou, E., Kruttner, S., Yu, J.Y., Kurtovic-Kozaric, A., and Dickson, B.J. (2012). Dopamine neurons modulate pheromone responses in *Drosophila* courtship learning. *Nature* *489*, 145-149.
- Kimura, K., Ote, M., Tazawa, T., and Yamamoto, D. (2005). Fruitless specifies sexually dimorphic neural circuitry in the *Drosophila* brain. *Nature* *438*, 229-233.
- Koganezawa, M., Haba, D., Matsuo, T., and Yamamoto, D. (2010). The shaping of male courtship posture by lateralized gustatory inputs to male-specific interneurons. *Curr Biol* *20*, 1-8.
- Kohatsu, S., Koganezawa, M., and Yamamoto, D. (2011). Female contact activates male-specific interneurons that trigger stereotypic courtship behavior in *Drosophila*. *Neuron* *69*, 498-508.
- Koto, M., Tanouye, M.A., Ferrus, A., Thomas, J.B., and Wyman, R.J. (1981). The morphology of the cervical giant fiber neuron of *Drosophila*. *Brain Res* *221*, 213-217.
- Krstic, D., Boll, W., and Noll, M. (2009). Sensory integration regulating male courtship behavior in *Drosophila*. *PLoS One* *4*, e4457.
- Kume, K., Kume, S., Park, S.K., Hirsh, J., and Jackson, F.R. (2005). Dopamine is a regulator of arousal in the fruit fly. *J Neurosci* *25*, 7377-7384.
- Kurtovic, A., Widmer, A., and Dickson, B.J. (2007). A single class of olfactory neurons mediates behavioural responses to a *Drosophila* sex pheromone. *Nature* *446*, 542-546.
- Lai, J.S., Lo, S.J., Dickson, B.J., and Chiang, A.S. (2012). Auditory circuit in the *Drosophila* brain. *Proc Natl Acad Sci U S A* *109*, 2607-2612.
- Lee, G., Foss, M., Goodwin, S.F., Carlo, T., Taylor, B.J., and Hall, J.C. (2000). Spatial, temporal, and sexually dimorphic expression patterns of the fruitless gene in the *Drosophila* central nervous system. *J Neurobiol* *43*, 404-426.
- Lee, G., and Hall, J.C. (2001). Abnormalities of male-specific FRU protein and serotonin expression in the CNS of fruitless mutants in *Drosophila*. *J Neurosci* *21*, 513-526.
- Lee, T. (2009). New genetic tools for cell lineage analysis in *Drosophila*. *Nat Methods* *6*, 566-568.
- Lee, T., and Luo, L. (1999). Mosaic analysis with a repressible cell marker for studies of gene function in neuronal morphogenesis. *Neuron* *22*, 451-461.
- Lin, S., and Lee, T. (2012). Generating neuronal diversity in the *Drosophila* central nervous system. *Dev Dyn* *241*, 57-68.
- Liu, T., Dartevelle, L., Yuan, C., Wei, H., Wang, Y., Ferveur, J.F., and Guo, A. (2008). Increased dopamine level enhances male-male courtship in *Drosophila*. *J Neurosci* *28*, 5539-5546.
- Lu, B., LaMora, A., Sun, Y., Welsh, M.J., and Ben-Shahar, Y. ppk23-Dependent chemosensory functions contribute to courtship behavior in *Drosophila melanogaster*. *PLoS Genet* *8*, e1002587.

- Luan, H., Peabody, N.C., Vinson, C.R., and White, B.H. (2006). Refined spatial manipulation of neuronal function by combinatorial restriction of transgene expression. *Neuron* 52, 425-436.
- Manoli, D.S., and Baker, B.S. (2004). Median bundle neurons coordinate behaviours during *Drosophila* male courtship. *Nature* 430, 564-569.
- Manoli, D.S., Foss, M., Vilella, A., Taylor, B.J., Hall, J.C., and Baker, B.S. (2005). Male-specific fruitless specifies the neural substrates of *Drosophila* courtship behaviour. *Nature* 436, 395-400.
- Markow, T.A. (1987). Behavioral and sensory basis of courtship success in *Drosophila melanogaster*. *Proc Natl Acad Sci U S A* 84, 6200-6204.
- Martin, J.R., Keller, A., and Sweeney, S.T. (2002). Targeted expression of tetanus toxin: a new tool to study the neurobiology of behavior. *Adv Genet* 47, 1-47.
- Mellert, D.J., Knapp, J.M., Manoli, D.S., Meissner, G.W., and Baker, B.S. (2009). Midline crossing by gustatory receptor neuron axons is regulated by fruitless, doublesex and the Roundabout receptors. *Development* 137, 323-332.
- Pan, Y., Meissner, G.W., and Baker, B.S. (2012). Joint control of *Drosophila* male courtship behavior by motion cues and activation of male-specific P1 neurons. *Proc Natl Acad Sci U S A* 109, 10065-10070.
- Pan, Y., Robinett, C.C., and Baker, B.S. (2011). Turning males on: activation of male courtship behavior in *Drosophila melanogaster*. *PLoS One* 6, e21144.
- Peters, A., Feldman, M., and Saldanha, J. (1976). The projection of the lateral geniculate nucleus to area 17 of the rat cerebral cortex. II. Terminations upon neuronal perikarya and dendritic shafts. *J Neurocytol* 5, 85-107.
- Pfeiffer, B.D., Jenett, A., Hammonds, A.S., Ngo, T.T., Misra, S., Murphy, C., Scully, A., Carlson, J.W., Wan, K.H., Lavery, T.R., *et al.* (2008). Tools for neuroanatomy and neurogenetics in *Drosophila*. *Proc Natl Acad Sci U S A* 105, 9715-9720.
- Pfeiffer, B.D., Ngo, T.T., Hibbard, K.L., Murphy, C., Jenett, A., Truman, J.W., and Rubin, G.M. (2010). Refinement of tools for targeted gene expression in *Drosophila*. *Genetics* 186, 735-755.
- Ritchie, M.G., Halsey, E.J., and Gleason, J.M. (1999). *Drosophila* song as a species-specific mating signal and the behavioural importance of Kyriacou & Hall cycles in *D. melanogaster* song. *Anim Behav* 58, 649-657.
- Rohlfing, T., and Maurer, C.R., Jr. (2003). Nonrigid image registration in shared-memory multiprocessor environments with application to brains, breasts, and bees. *IEEE Trans Inf Technol Biomed* 7, 16-25.
- Root, C.M., Masuyama, K., Green, D.S., Enell, L.E., Nassel, D.R., Lee, C.H., and Wang, J.W. (2008). A presynaptic gain control mechanism fine-tunes olfactory behavior. *Neuron* 59, 311-321.
- Ruta, V., Datta, S.R., Vasconcelos, M.L., Freeland, J., Looger, L.L., and Axel, R. (2010). A dimorphic pheromone circuit in *Drosophila* from sensory input to descending output. *Nature* 468, 686-690.

- Ryner, L.C., Goodwin, S.F., Castrillon, D.H., Anand, A., Vilella, A., Baker, B.S., Hall, J.C., Taylor, B.J., and Wasserman, S.A. (1996). Control of male sexual behavior and sexual orientation in *Drosophila* by the fruitless gene. *Cell* *87*, 1079-1089.
- Schilcher, F.v. (1976). The function of pulse song and sine song in the courtship of *Drosophila melanogaster*. *Animal Behaviour* *24*, 622-625.
- Shorey, H.H. (1962). Nature of the Sound Produced by *Drosophila melanogaster* during Courtship. *Science* *137*, 677-678.
- Sokolowski, M.B. (2001). *Drosophila*: genetics meets behaviour. *Nat Rev Genet* *2*, 879-890.
- Stocker, R.F. (1994). The organization of the chemosensory system in *Drosophila melanogaster*: a review. *Cell Tissue Res* *275*, 3-26.
- Stockinger, P., Kvitsiani, D., Rotkopf, S., Tirian, L., and Dickson, B.J. (2005). Neural circuitry that governs *Drosophila* male courtship behavior. *Cell* *121*, 795-807.
- Strauss, R. (2002). The central complex and the genetic dissection of locomotor behaviour. *Curr Opin Neurobiol* *12*, 633-638.
- Tanouye, M.A., and Wyman, R.J. (1980). Motor outputs of giant nerve fiber in *Drosophila*. *J Neurophysiol* *44*, 405-421.
- Thistle, R., Cameron, P., Ghorayshi, A., Dennison, L., and Scott, K. (2012). Contact chemoreceptors mediate male-male repulsion and male-female attraction during *Drosophila* courtship. *Cell* *149*, 1140-1151.
- Toda, H., Zhao, X., and Dickson, B.J. (2012). The *Drosophila* Female Aphrodisiac Pheromone Activates ppk23(+) Sensory Neurons to Elicit Male Courtship Behavior. *Cell Rep* *1*, 599-607.
- van der Goes van Naters, W., and Carlson, J.R. (2007). Receptors and neurons for fly odors in *Drosophila*. *Curr Biol* *17*, 606-612.
- von Philipsborn, A.C., Liu, T., Yu, J.Y., Masser, C., Bidaye, S.S., and Dickson, B.J. Neuronal control of *Drosophila* courtship song. *Neuron* *69*, 509-522.
- von Philipsborn, A.C., Liu, T., Yu, J.Y., Masser, C., Bidaye, S.S., and Dickson, B.J. (2011). Neuronal control of *Drosophila* courtship song. *Neuron* *69*, 509-522.
- von Schilcher, F. (1976). The role of auditory stimuli in the courtship of *Drosophila melanogaster*. *Animal Behaviour* *24*, 18-26.
- Yu, H.H., Chen, C.H., Shi, L., Huang, Y., and Lee, T. (2009). Twin-spot MARCM to reveal the developmental origin and identity of neurons. *Nat Neurosci* *12*, 947-953.
- Yu, J.Y., Kanai, M.I., Demir, E., Jefferis, G.S., and Dickson, B.J. (2010). Cellular organization of the neural circuit that drives *Drosophila* courtship behavior. *Curr Biol* *20*, 1602-1614.
- Zollman, S., Godt, D., Prive, G.G., Couderc, J.L., and Laski, F.A. (1994). The BTB domain, found primarily in zinc finger proteins, defines an evolutionarily conserved family that includes several developmentally regulated genes in *Drosophila*. *Proc Natl Acad Sci U S A* *91*, 10717-10721.

Material and methods

Fly stock

All the VT lines used in this study were created in the Lab as described in Masser, 2011 and Bidaye 2012. *VT8657.LexAGAD* was generated by replacing GAL4 with LexAGAD and phi31 site-specific integration to attP2 site as described in Pfeiffer et. al. (2010). NP2631 was obtained from the *Drosophila Genetics Resource Centre*, Japan. *UAS>stop>TNT* and *UAS>stop>TNTinactive* are described in Stockinger et. al.(2005). *fru^{FLP}*, *UAS>stop>tauLacZ* and *UAS>stop>mCD8GFP* are as described in Yu. et. al. (2010). *UAS-trpA1* and *UAS>stop>trpA1* is described in von Philipsborn et. al. (2011). *UAS-TNT* was obtained from Sweeney et. al. (1995). *tub^P>Gal80>* was provided by K. Scott lab (Gordon and Scott, 2009). Virgin females used as targets for courtship assays were from *Conton S* stock. Males used as targets for male-male courtship assays were from *w¹¹¹⁸* stock.

Screening of VT lines with X-gal staining and immunostaining

UAS>stop>tauLacZ; VT-XXXX/ fru^{FLP} males and females were dissected at the age of 4-6 days. Their brains and VNCs are subjected to X-gal staining. The overlapping neurons of VT-XXXX and fruFLP are labeled in blue color. We have screened 2383 lines with this method and identified 1283 lines which has overlap with fruFLP. Among those, we selected 473 lines based on the sparseness of X-gal staining to further analysis. They are crossed to *UAS>stop>mCD8GFP; fruFLP* and the male and female progenies of the right genotype were dissected and subjected to immunostaining at the age of 4-6 days. We dissected 2-4 brains and 2-4 VNCs for each sex to obtain a representation of each type of fru+ neurons.

Immunostaining and image registration

Fly brains and VNCs were dissected in PBS and fixed with 4% paraformaldehyde in PBST (PBS with 0.3% Triton X-100). After washing with PBST, the tissues were blocked in 10% normal goat serum in PBST for 3-4 hours at room temperature. The primary and secondary antibodies incubated for 48-72 hours at 4°C. After each antibody incubation, the tissues were washed with PBST. They were incubated at 4°C for overnight after the wash of secondary antibody. They were mounted in Vectashield (VectorLabs) for image acquisition.

Antibodies used were: rabbit polyclonal anti-GFP (1: 6000, Torri Pines); mouse nc82 (1:20, Hybridoma Bank); rabbit anti-myc (1:6000 or 1:12,000, abcam); secondary Alexa-488, -568, -647 antibodies (1: 1000, Invitrogen).

Confocal stacks of stained brains and VNCs were obtained with a Zeiss LSM510 or Zeiss LSM710 with a Multi Immersion Plan NeoFluor 25x/0.8 objective. Nonrigid registration, segmentation, analysis of overlap, and image preparation were performed with Amira software (Visage Imaging) as described before (Yu et al., 2010).

Thermal activation experiments

trpA1-expressing flies were reared at 22°C. Males were collected shortly after eclosion and aged in groups of 10-20 for 10-15 days at 22°C. As a primary screen, we tested 5-10 isolated males or 3-5 male pairs per genotype which were aspirated into chambers of 10 mm in diameter placed on a heating plate. Temperature was raised from 25°C to 32-33°C during a 10 min video recording. We tested 10-15 isolated males for abdominal bending neuron screen and 5-10 pairs of males for courtship-driving neurons screen at secondary and tertiary test. Paired males which show continuous engagement of following or oriented courtship for >3s during a 10 min video recording were scored as a positive pair. When >50% of male pairs were positive pairs, we scored the VT lines as positive.

Courtship index (CI) and wing extension index (WI) in Figure S5 were scored when the male flies are heated from 30°C to 32°C. While CI represents the frequency of following and oriented wing extension, WI represents the frequency of oriented wing extension. Scoring of the events was done every 12s.

For neuronal epistasis experiments (Figure 12), Male flies were aged individually for 10-12 days. The target males were *w¹¹¹⁸* males which were age 6-10 days at 22°C in groups. Male-male courtship behavior was tested in 10 mm chamber in diameter at a constant temperature 30.5°C for 10 min. Male-male courtship index was generated by scoring following and oriented wing extension toward the target male every 12s.

Neuronal silencing experiments

Flies were reared at 25°C. Males were collected shortly after eclosion and aged individually for 6-7 days at 25°C. Single males were paired with a 3-5 days old Canton S virgin female and courtship and copulation were recorded for a 10 min. 10 mm chamber in diameter was used for Figure 6 and 18mm chamber in diameter was used for Figure 11. Courtship index (CI) was manually scored every 12s for 10 min. CI includes following of females, oriented wing extension towards females and copulation attempt.

References

- Gordon, M.D., and Scott, K. (2009). Motor control in a *Drosophila* taste circuit. *Neuron* *61*, 373-384.
- Stockinger, P., Kvitsiani, D., Rotkopf, S., Tirian, L., and Dickson, B.J. (2005). Neural circuitry that governs *Drosophila* male courtship behavior. *Cell* *121*, 795-807.
- von Philipsborn, A.C., Liu, T., Yu, J.Y., Masser, C., Bidaye, S.S., and Dickson, B.J. (2011). Neuronal control of *Drosophila* courtship song. *Neuron* *69*, 509-522.
- Yu, J.Y., Kanai, M.I., Demir, E., Jefferis, G.S., and Dickson, B.J. (2010). Cellular organization of the neural circuit that drives *Drosophila* courtship behavior. *Curr Biol* *20*, 1602-1614.
- Sweeney, S.T., Broadie, K., Keane, J., Niemann, H., and O’Kane, C.J. (1995). Targeted expression of tetanus toxin light chain in *Drosophila* specifically eliminates synaptic transmission and causes behavioral defects. *Neuron* *14*, 341–351.

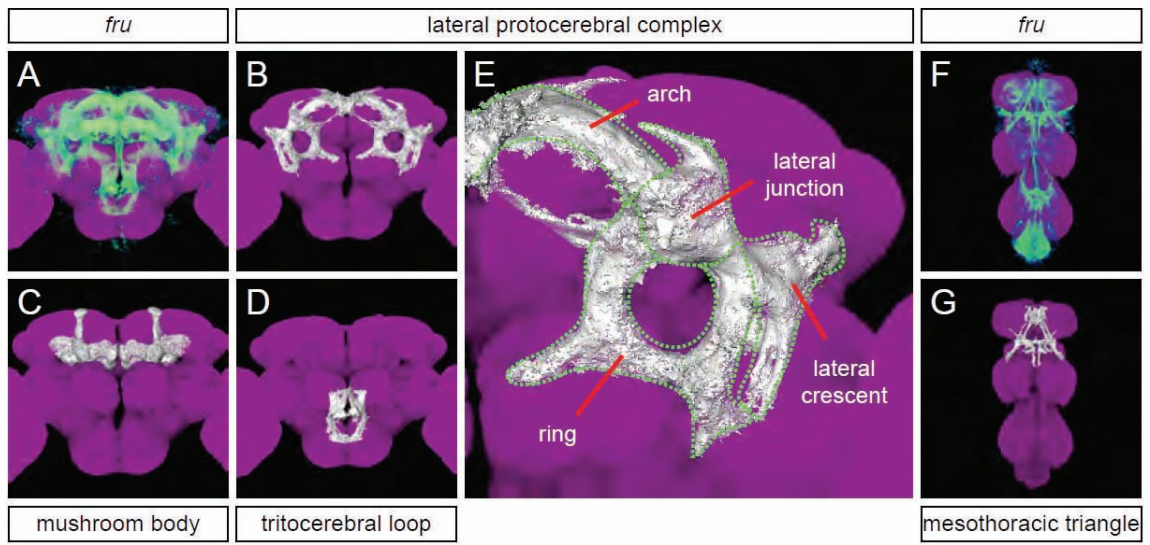


Figure S1

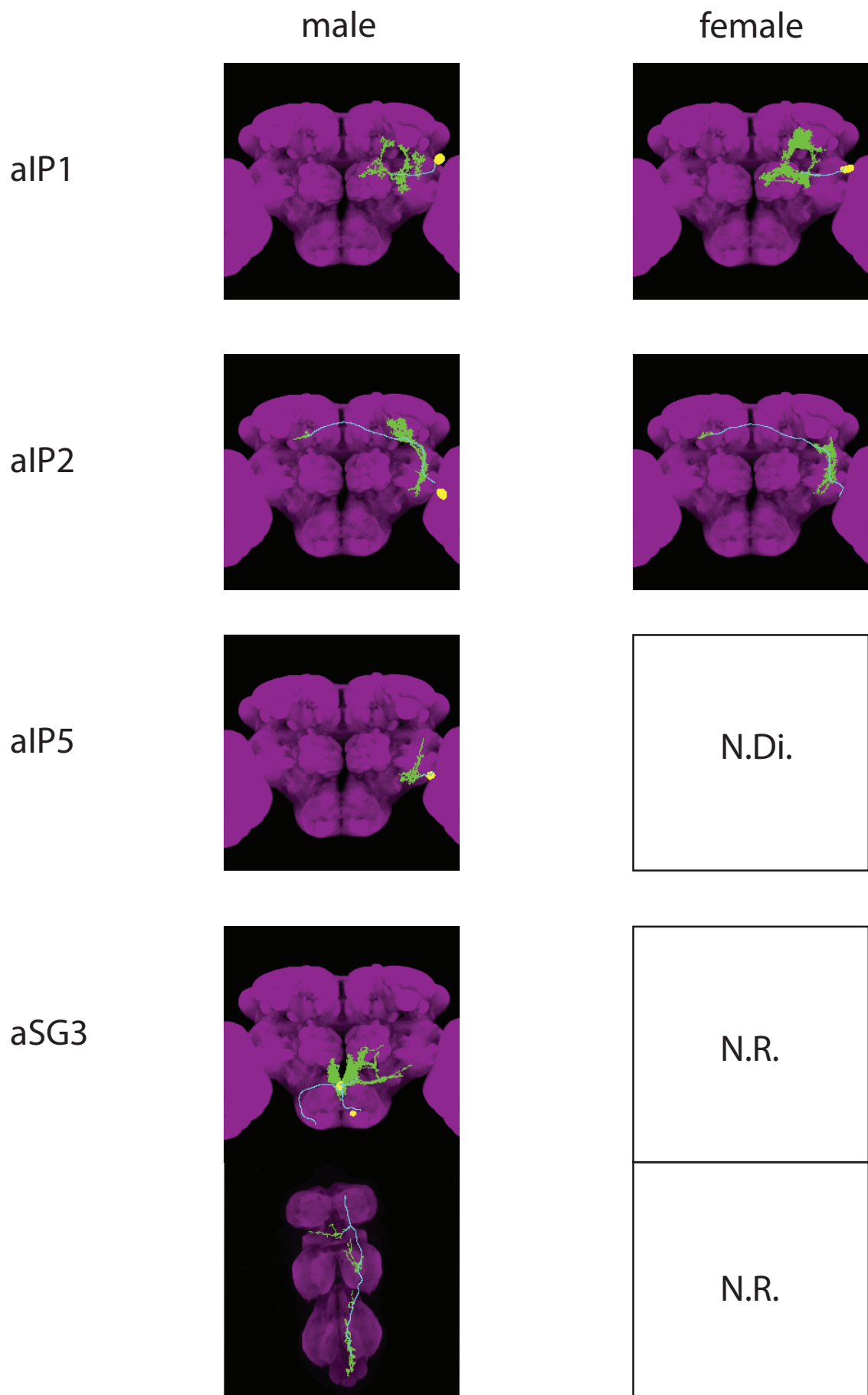


Figure S2

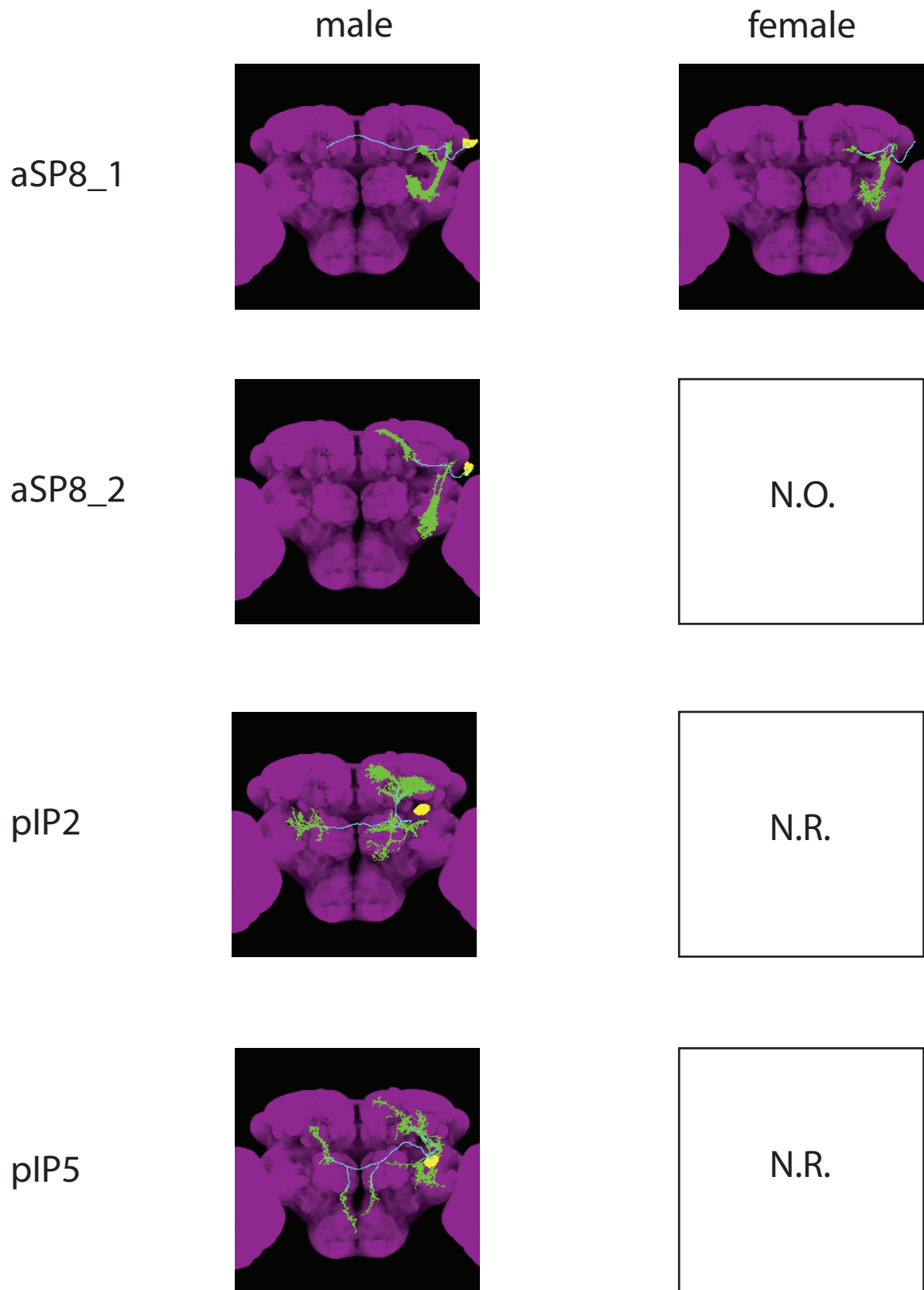


Figure S2

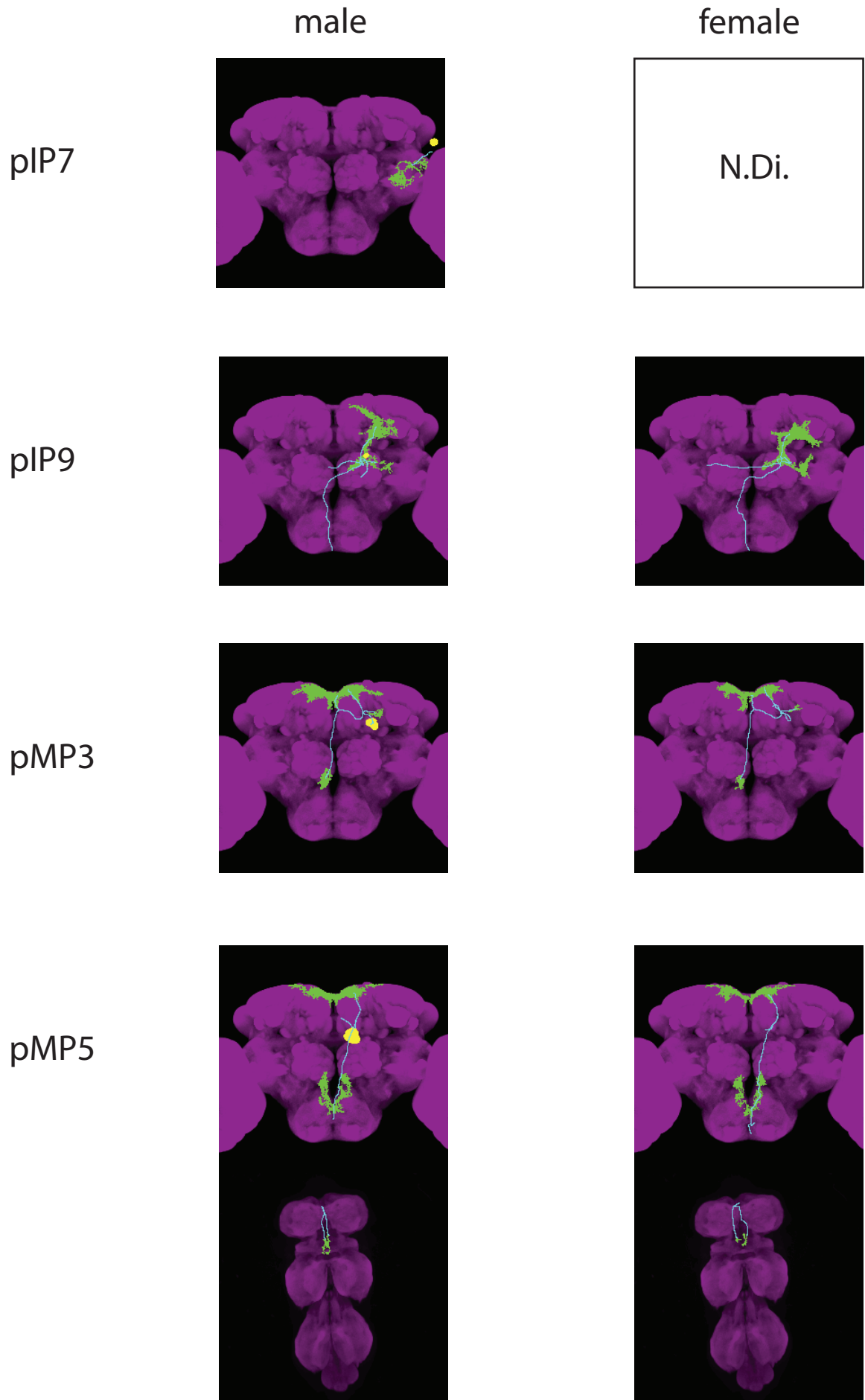


Figure S2

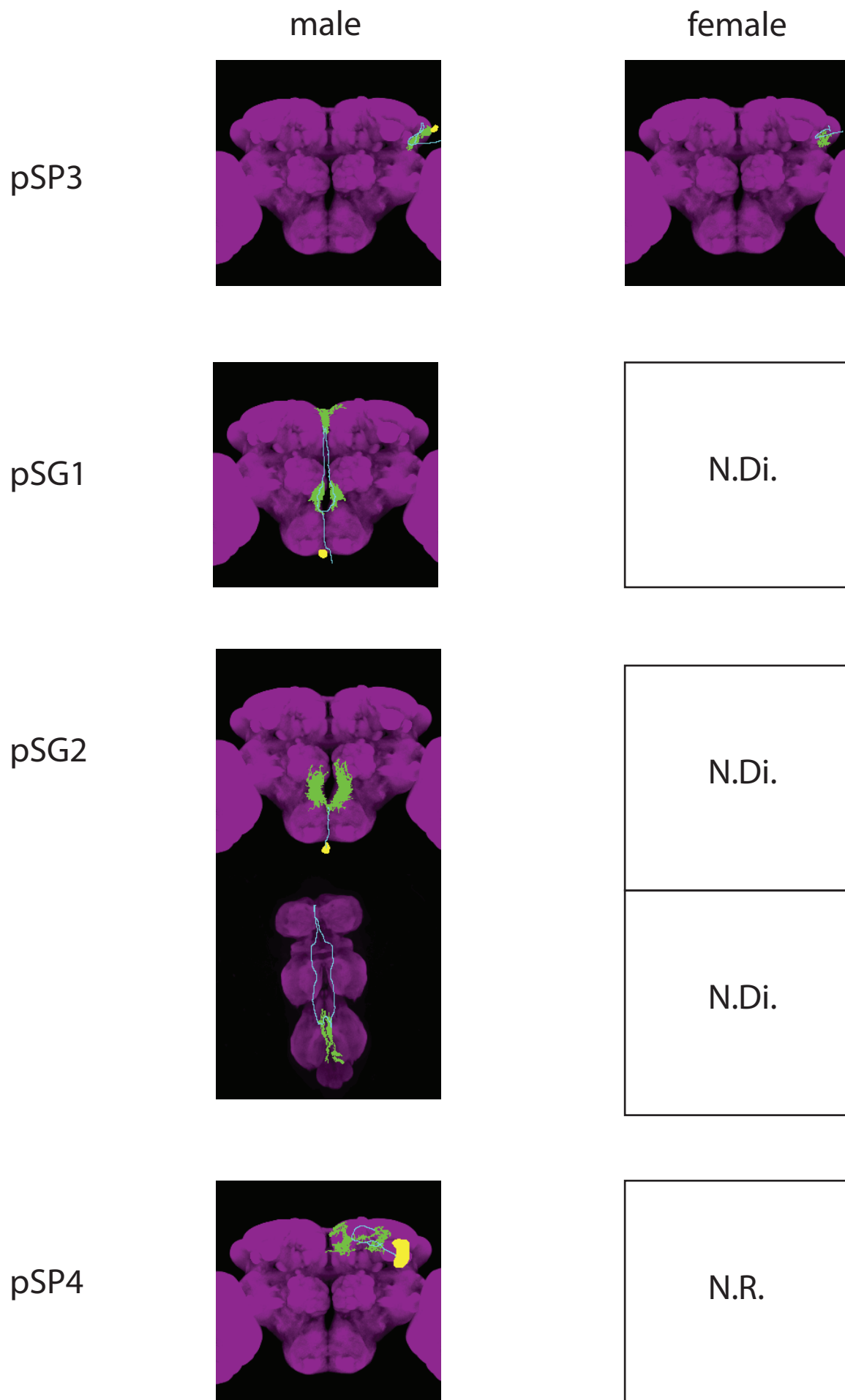


Figure S2
88

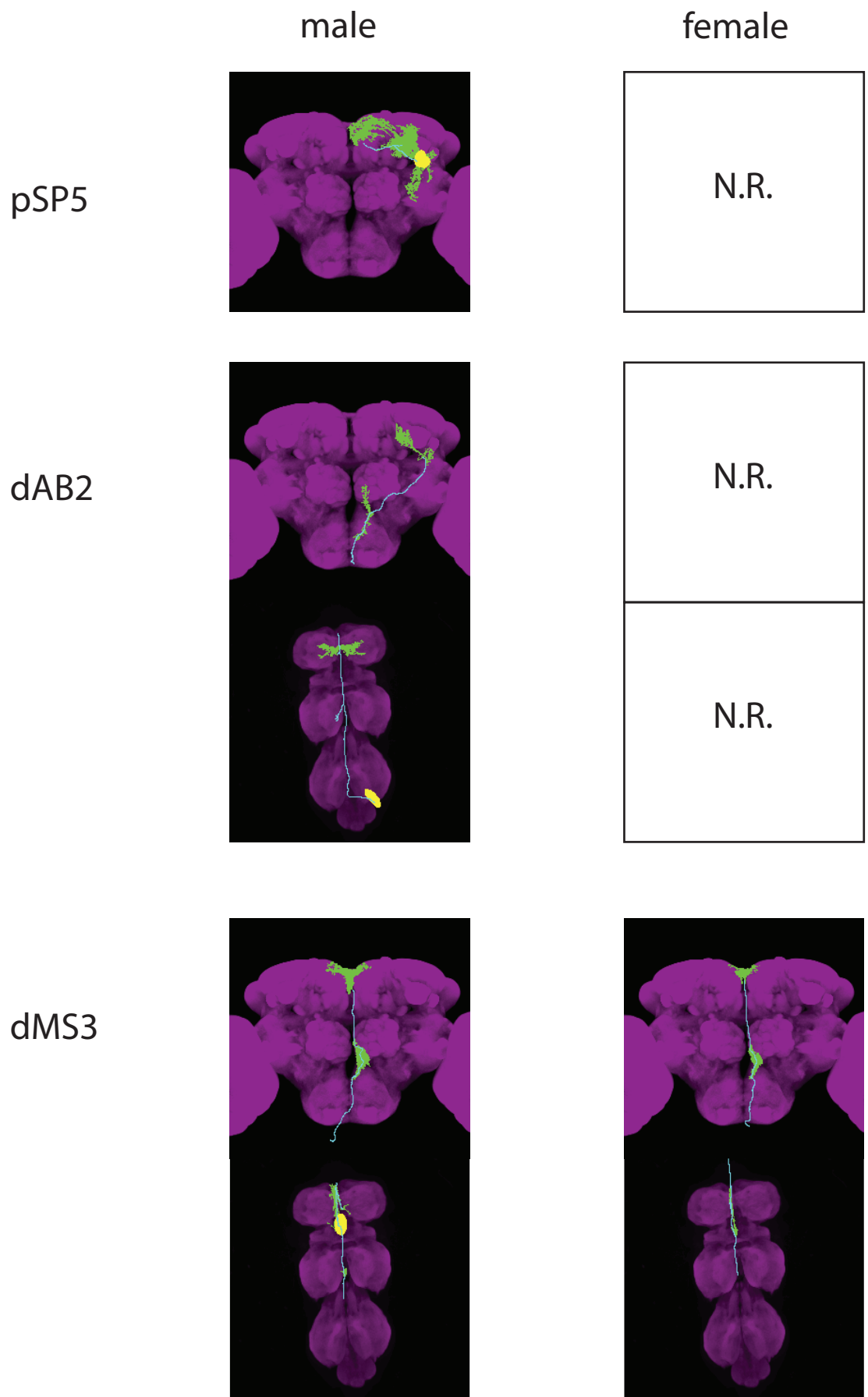
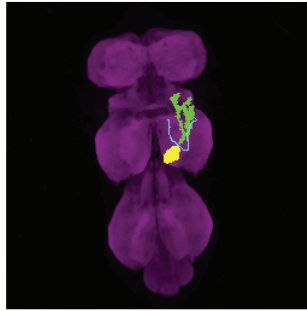


Figure S2

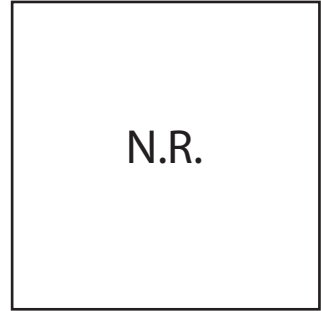
male

female

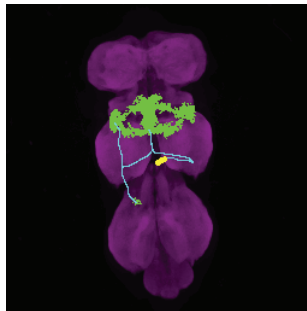
dMS4



N.R.



dMS5



dMS6

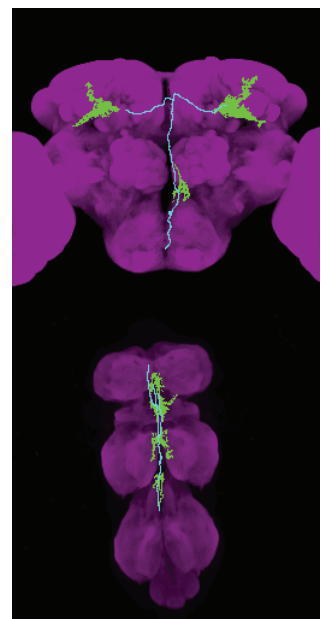
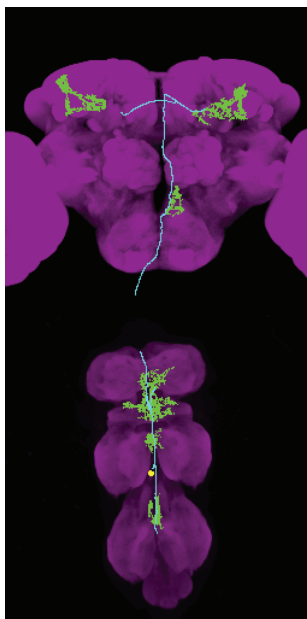


Figure S2

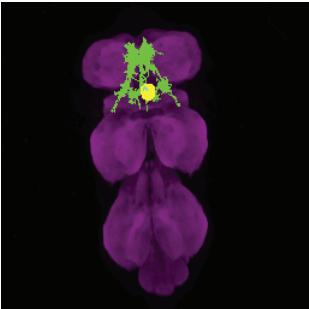
	male	female
vAB2		N.Di.
vPR9		N.O.

Figure S2

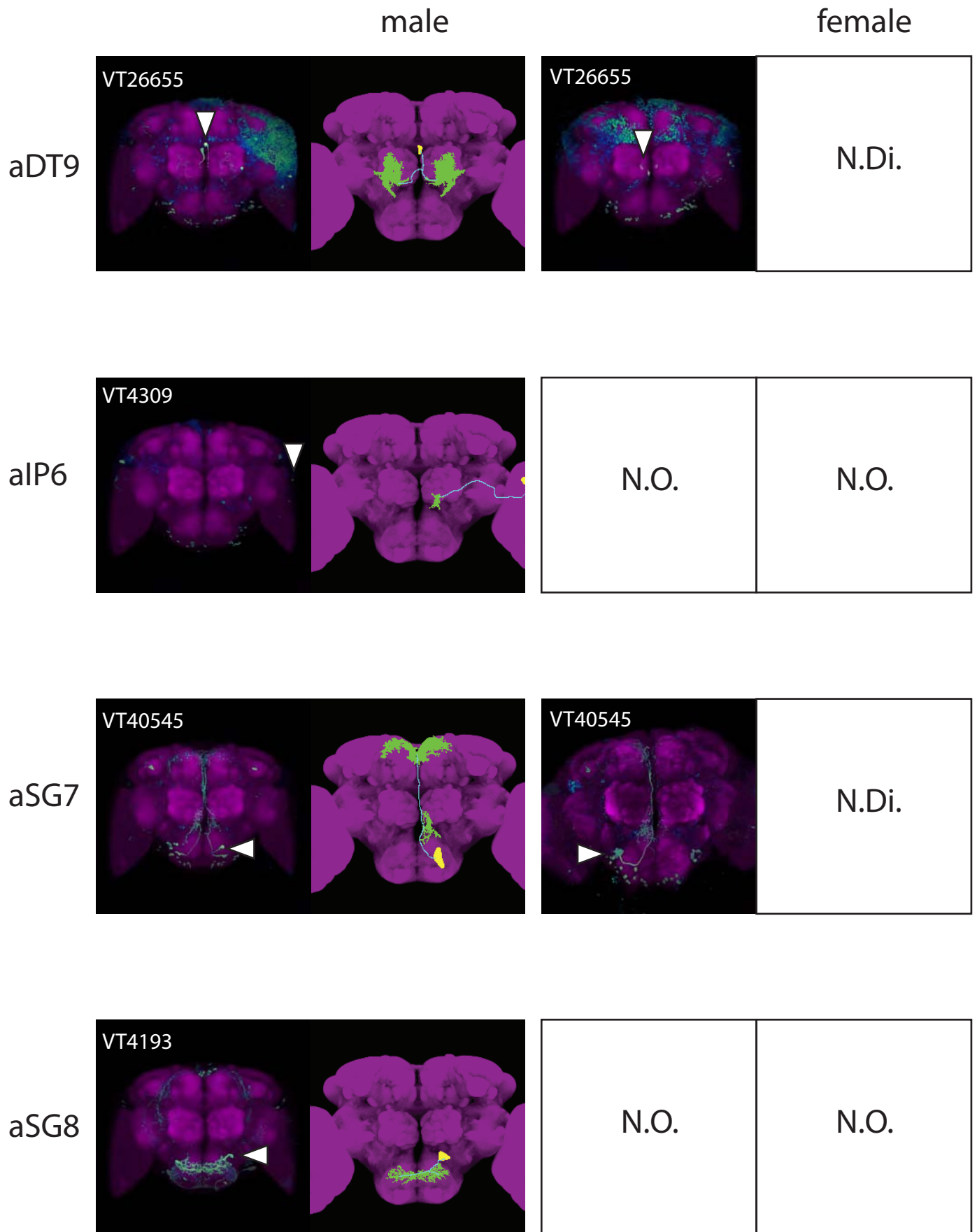


Figure S3

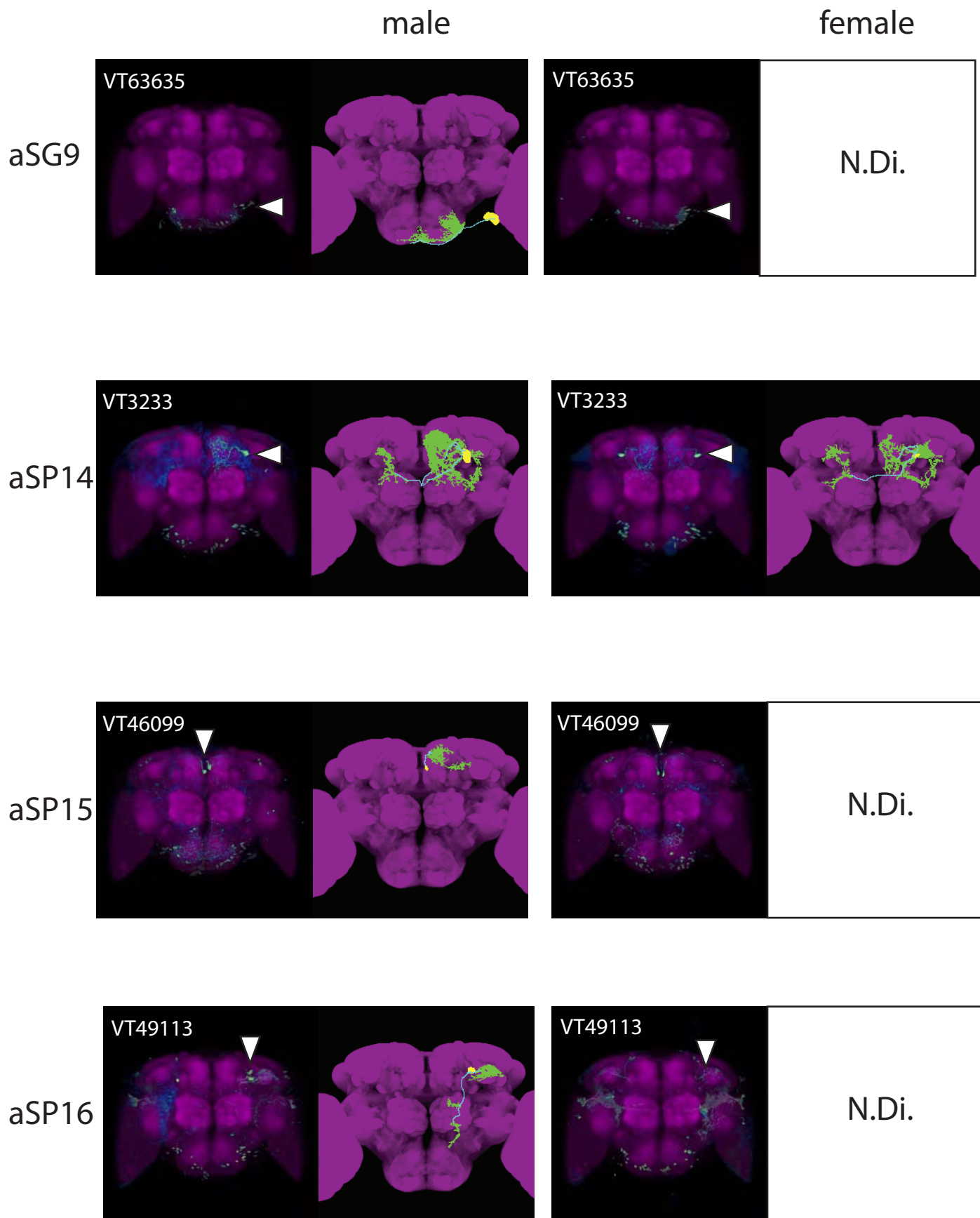


Figure S3

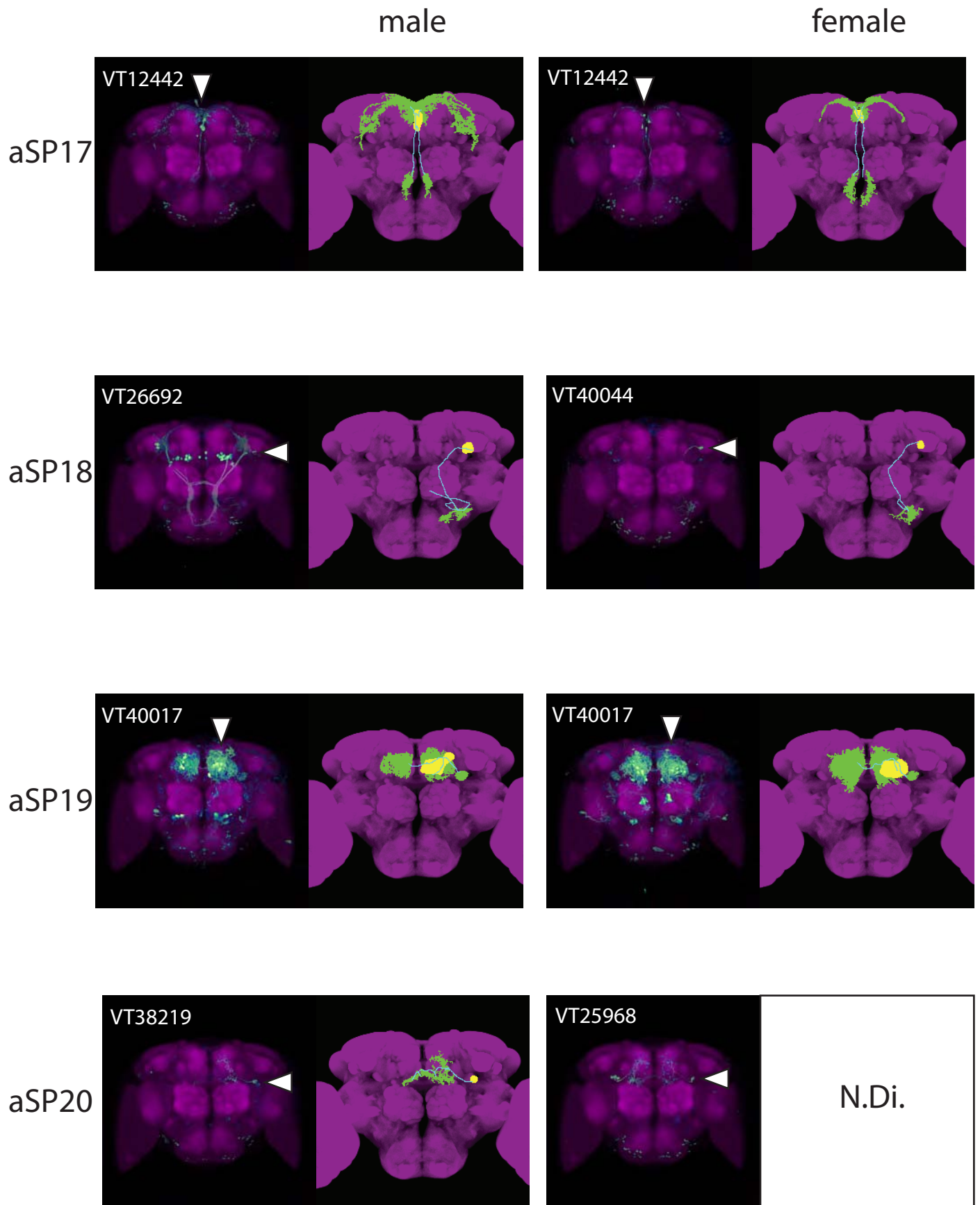


Figure S3

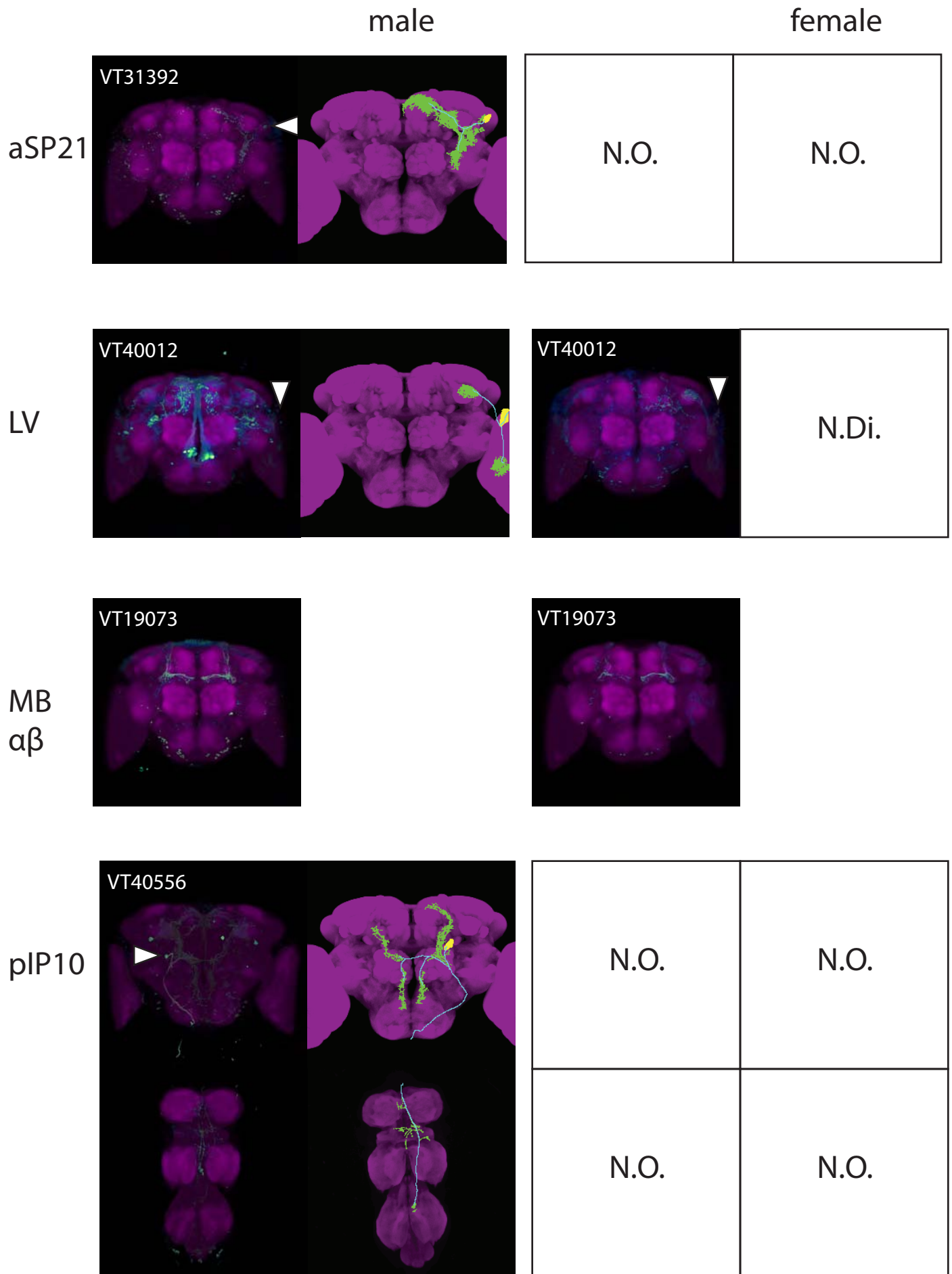


Figure S3
95

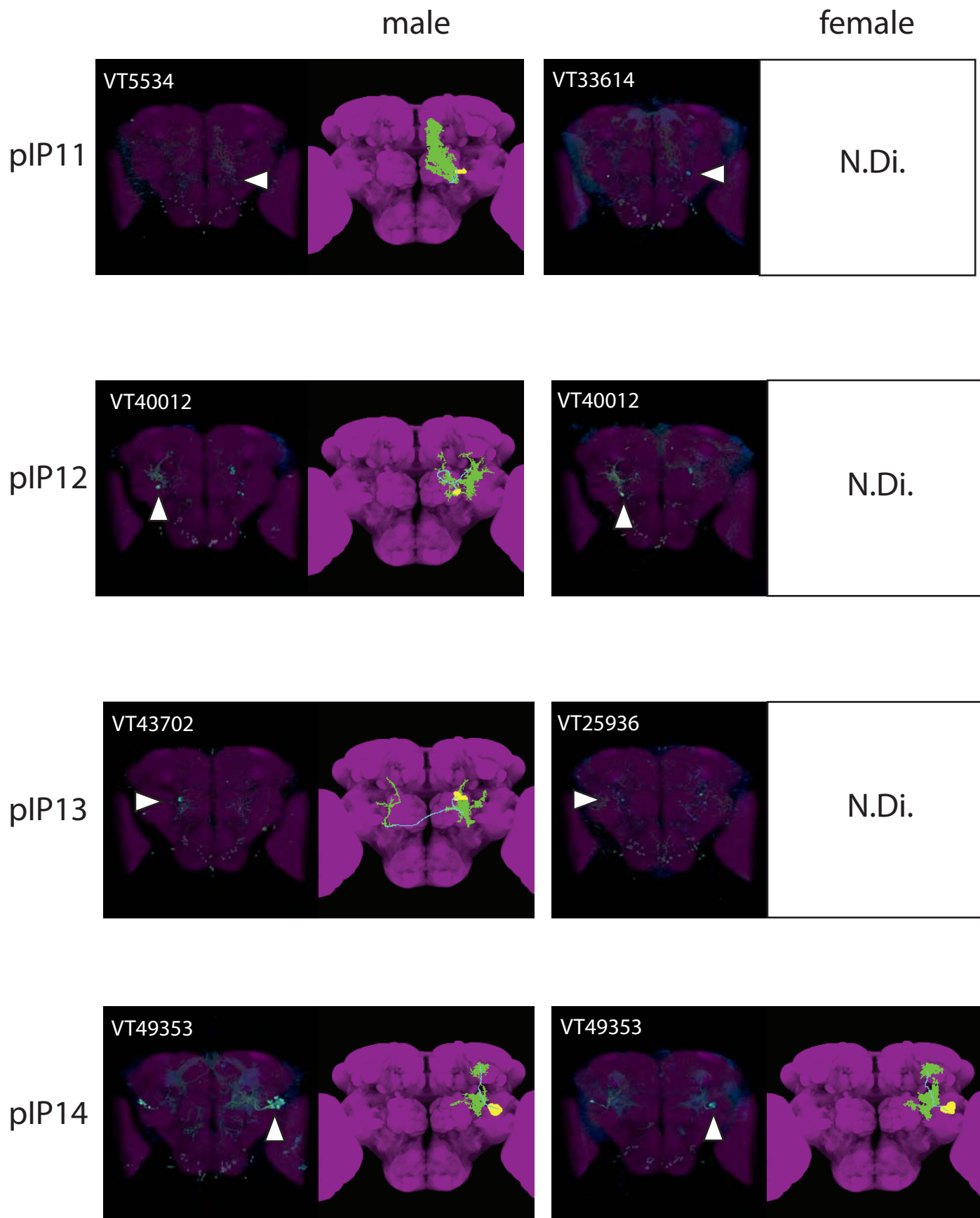


Figure S3

male

female

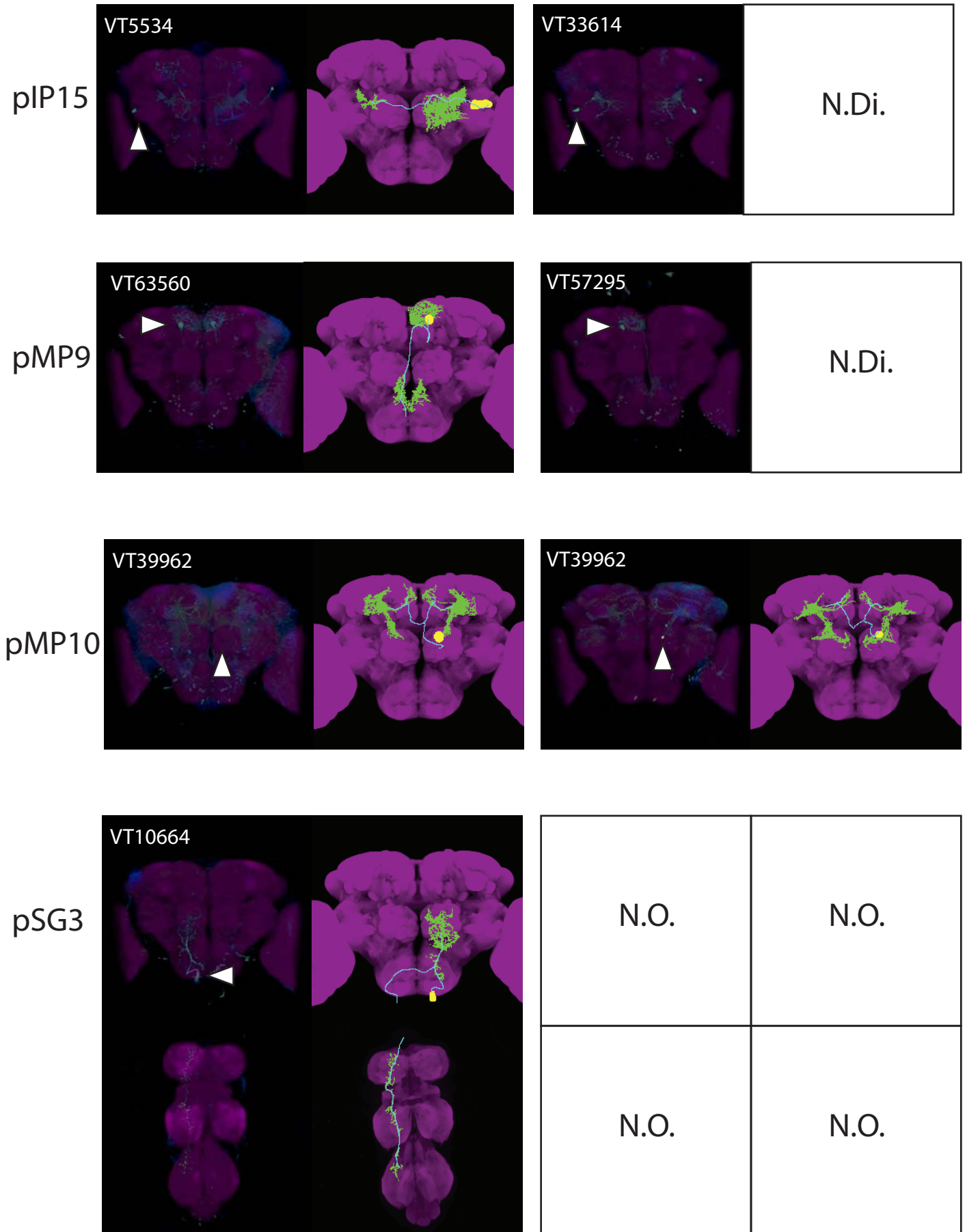


Figure S3

male

female

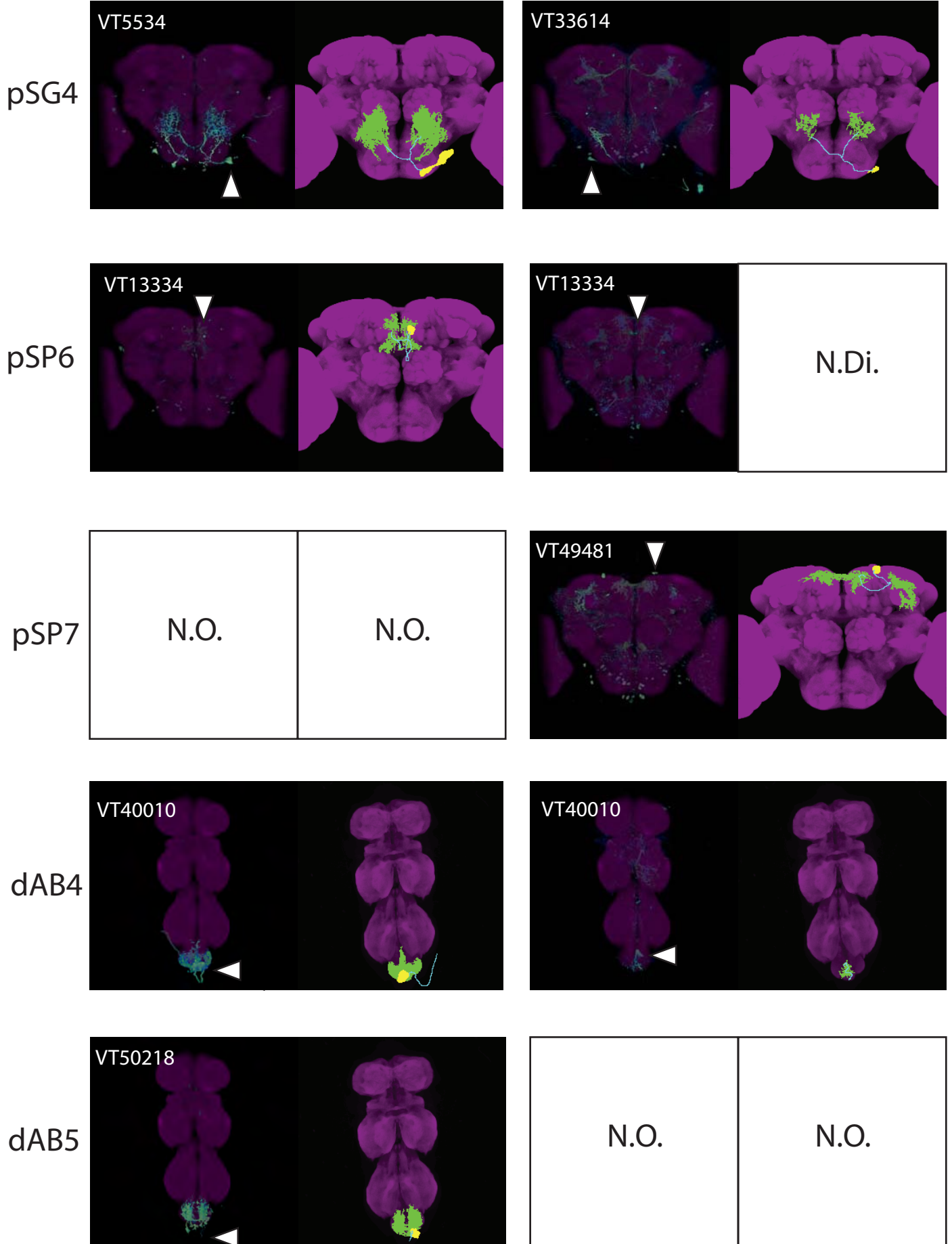


Figure S3

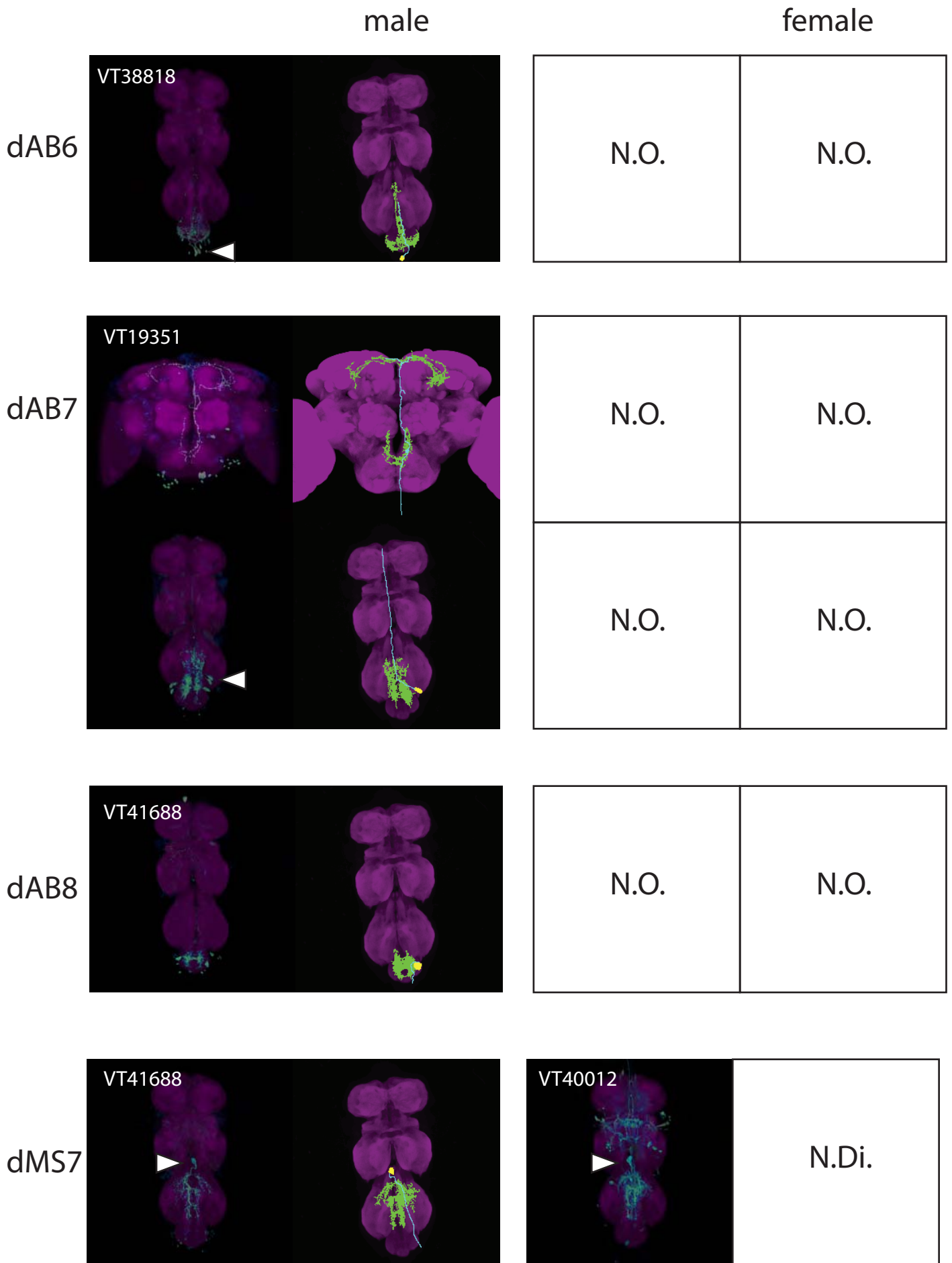


Figure S3

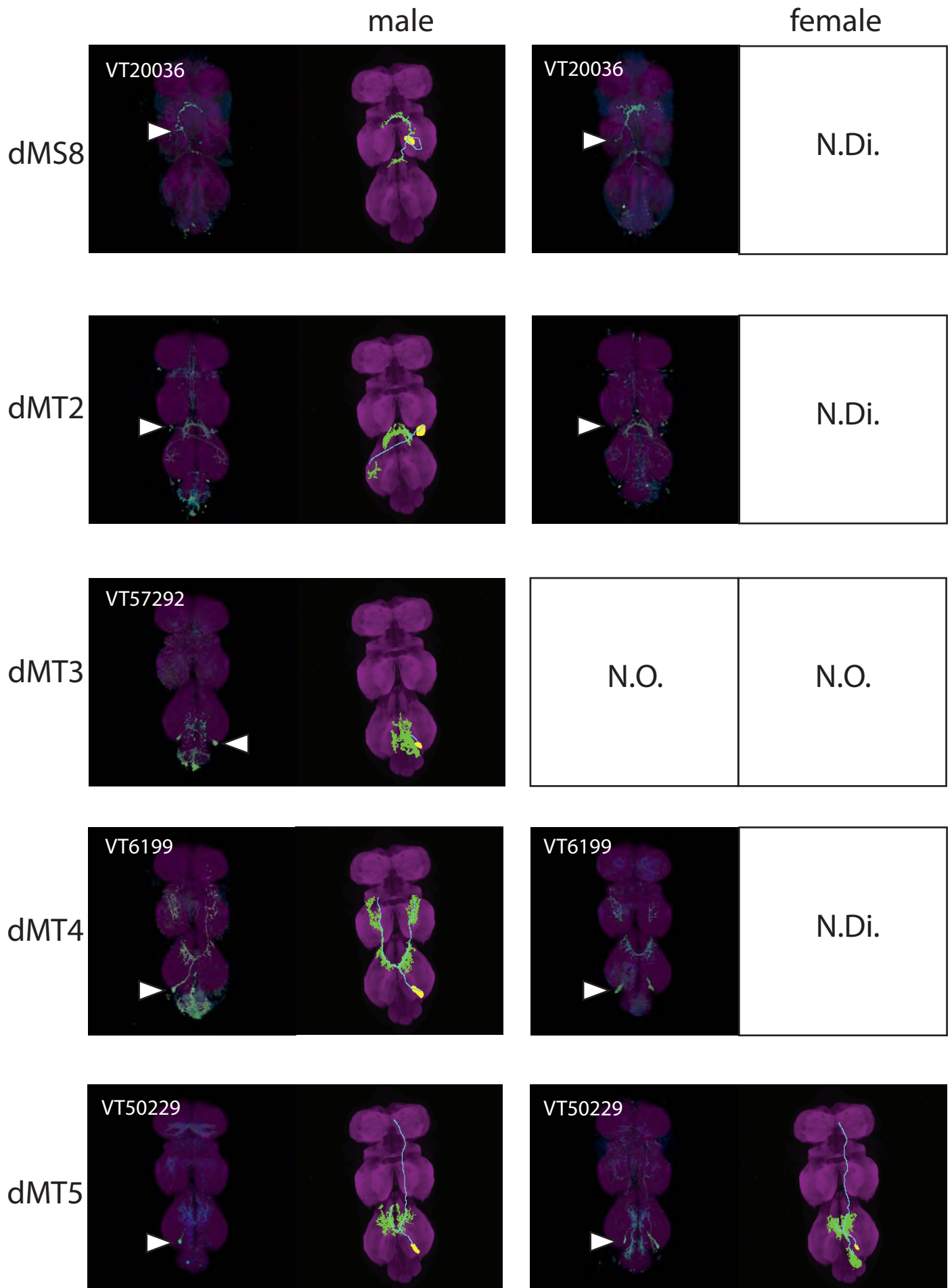


Figure S3

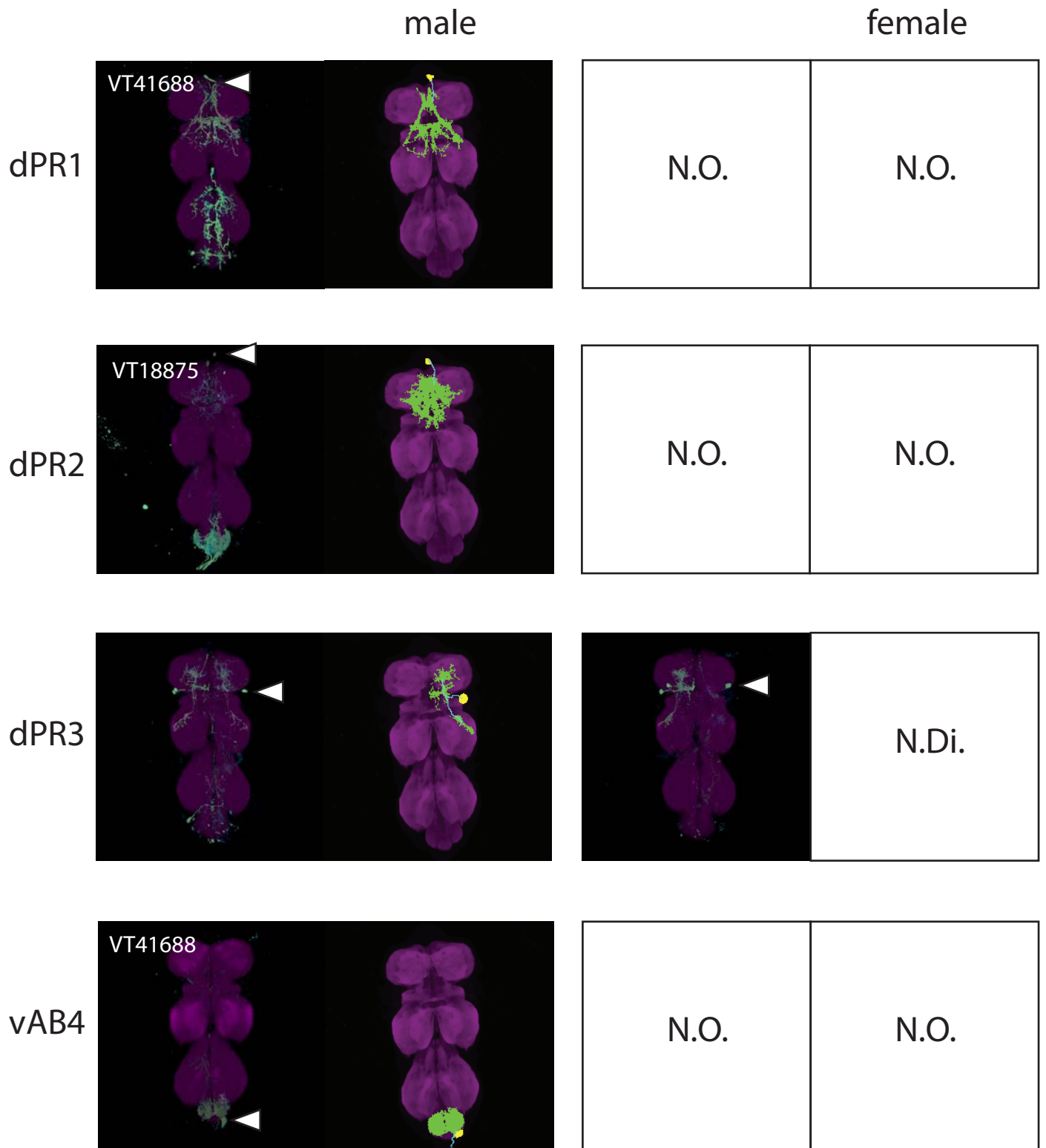


Figure S3
101

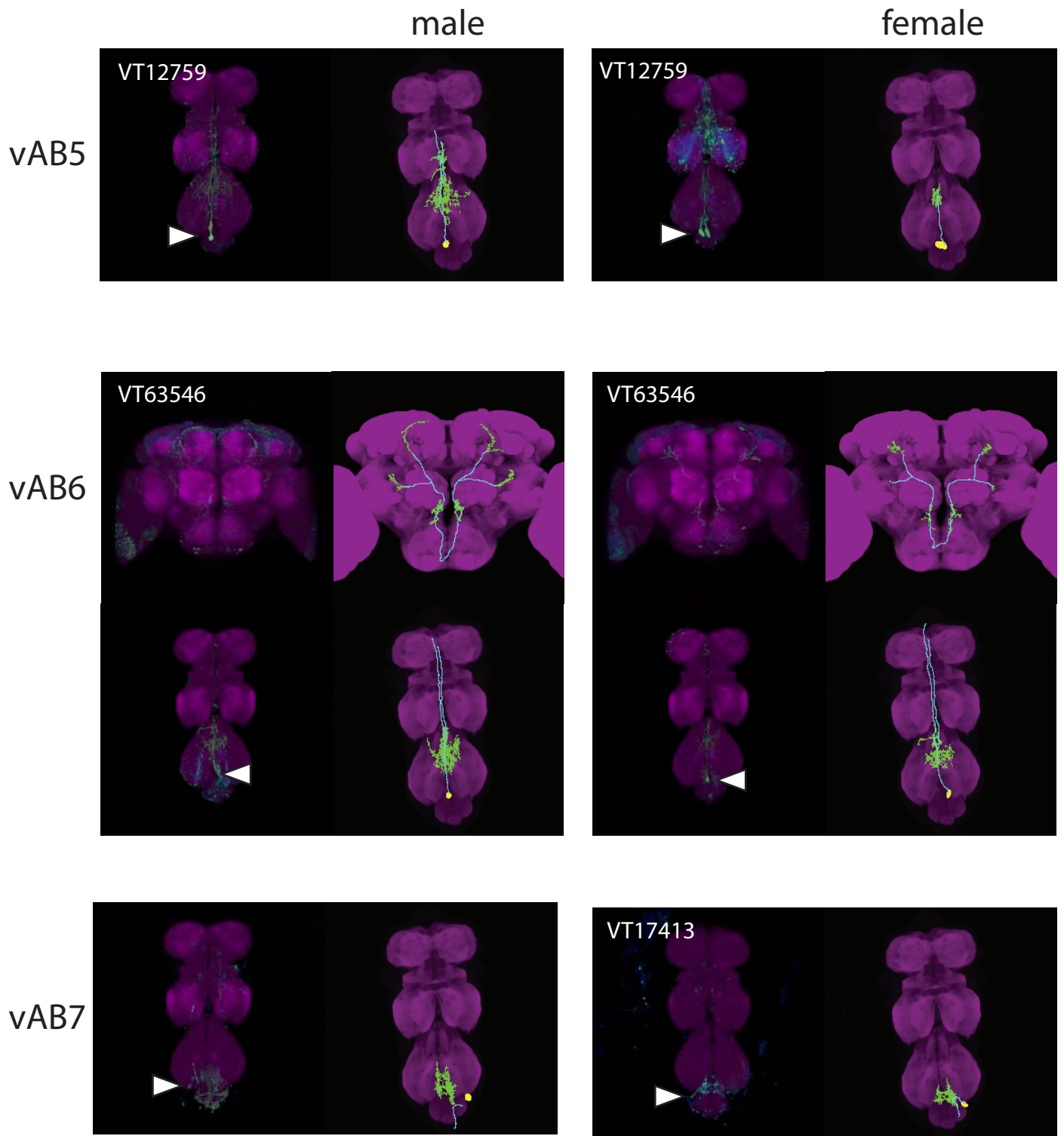
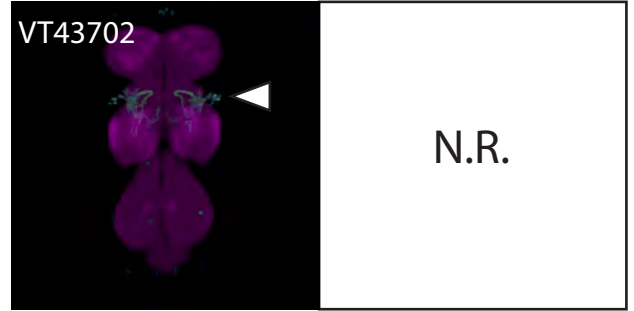
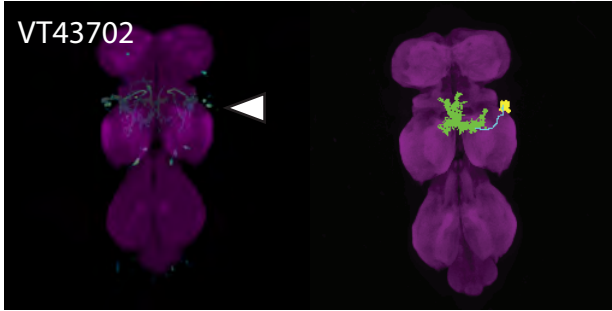


Figure S3

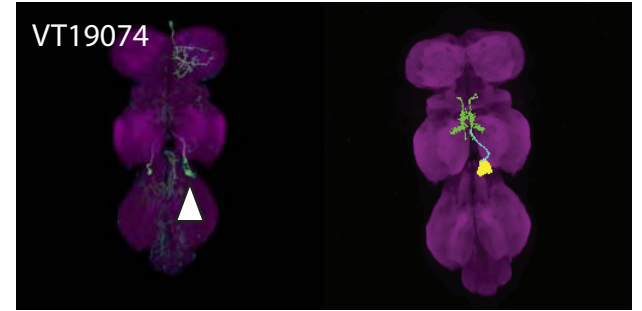
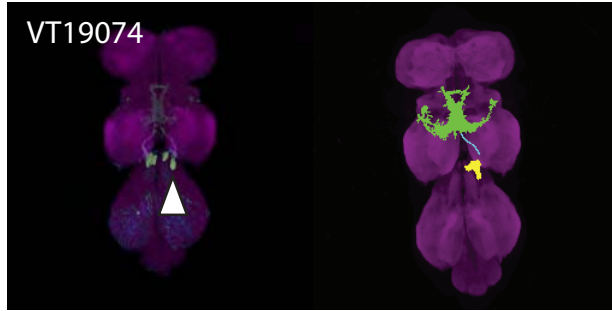
male

female

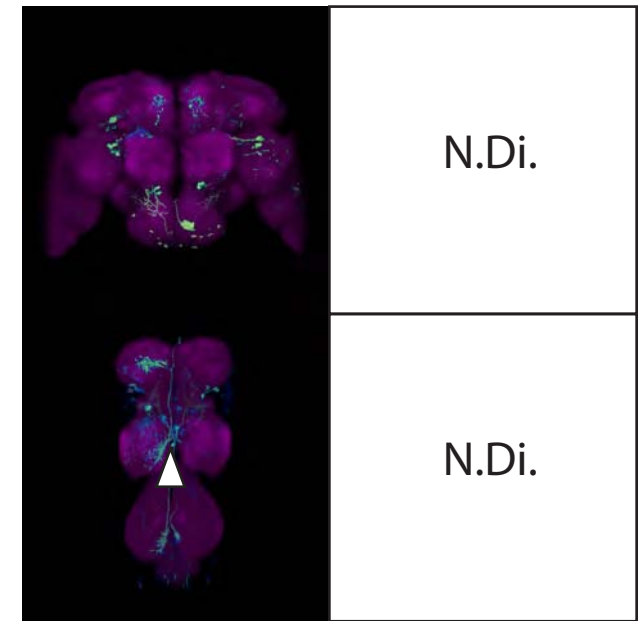
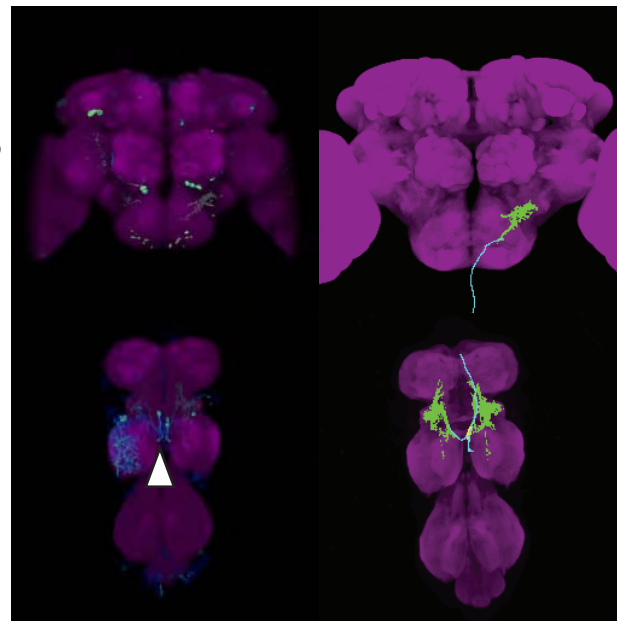
vMS11



vMS12



vMS13



vMS14

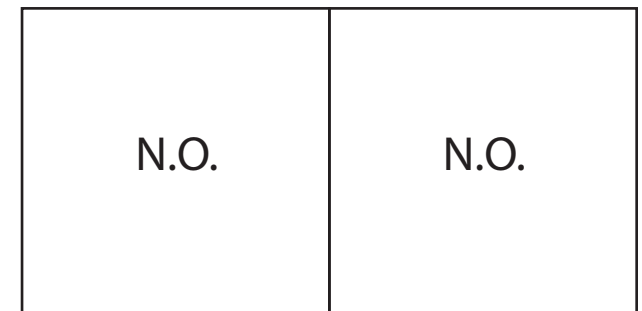
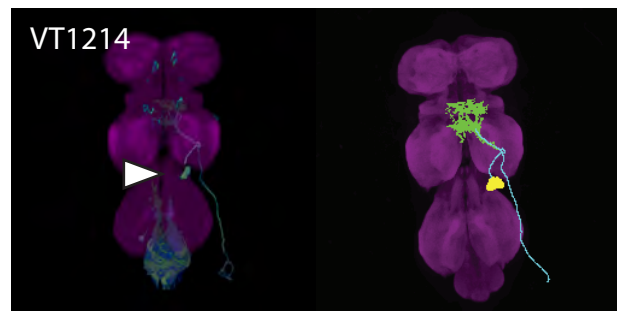


Figure S3

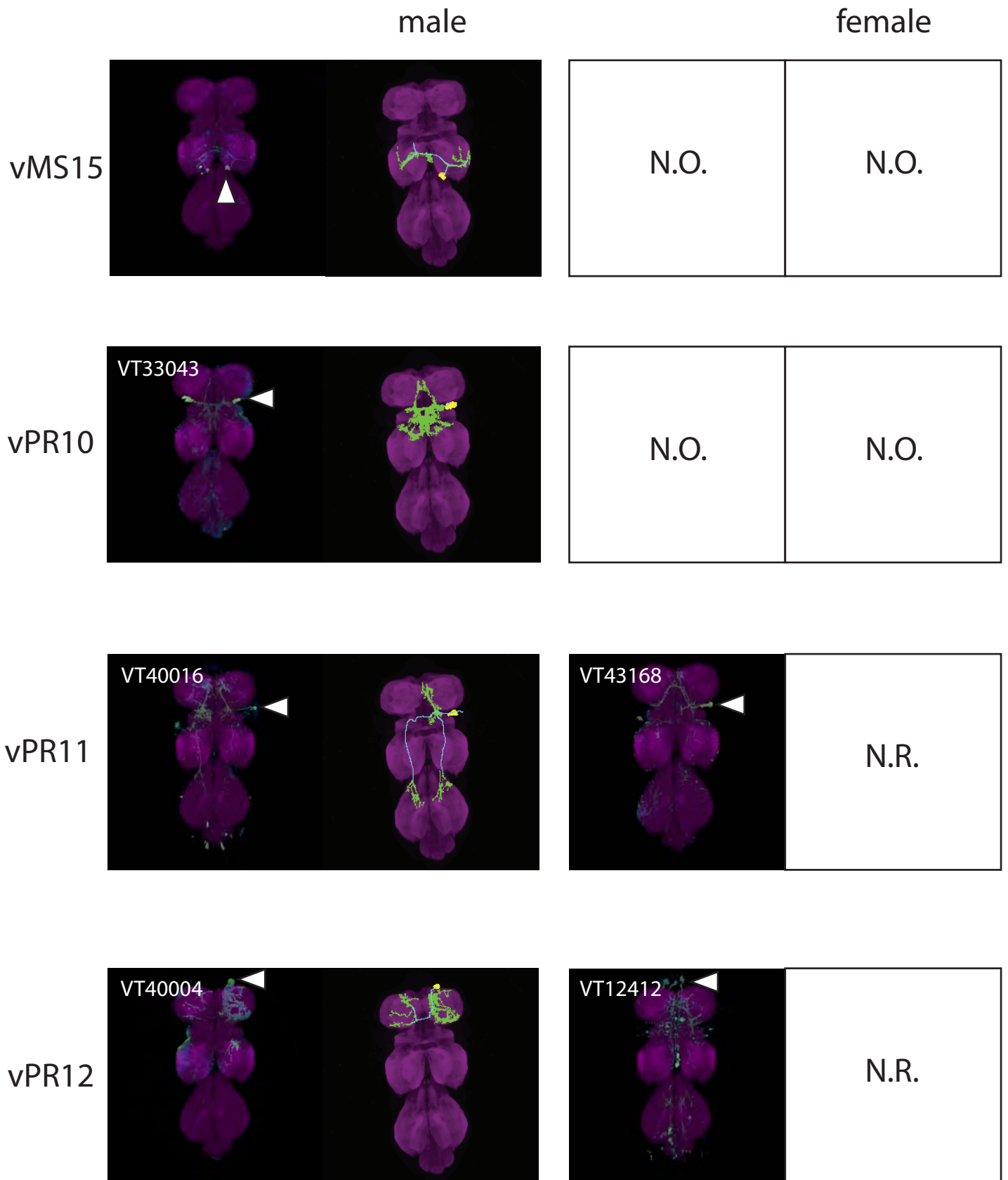
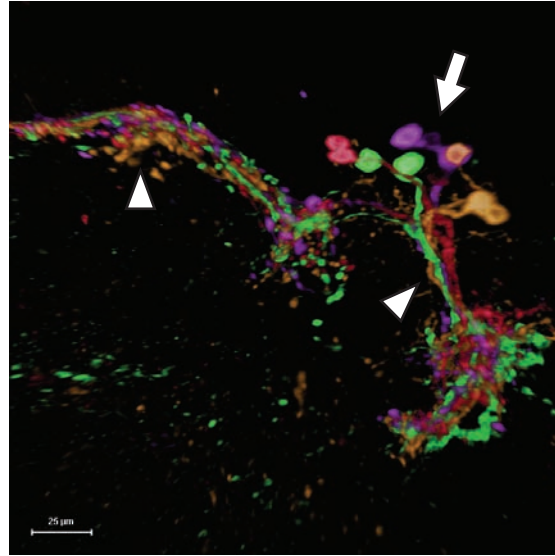
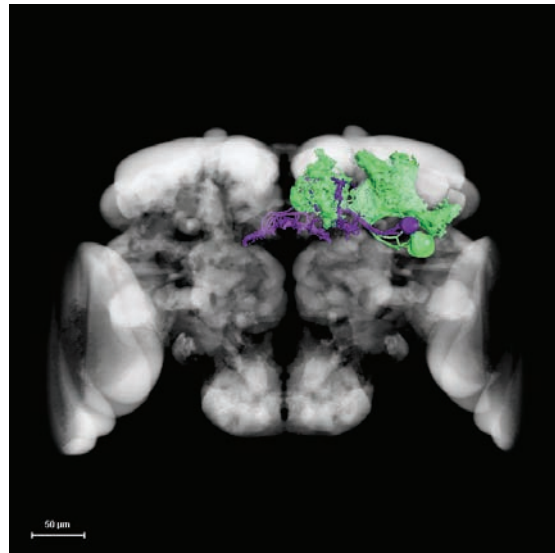


Figure S3

A



B



C

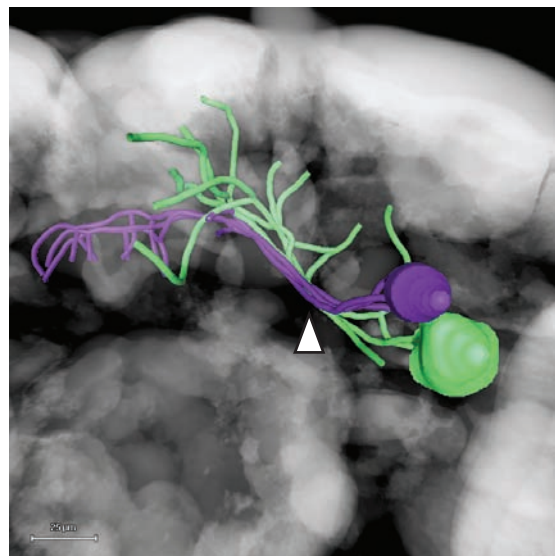
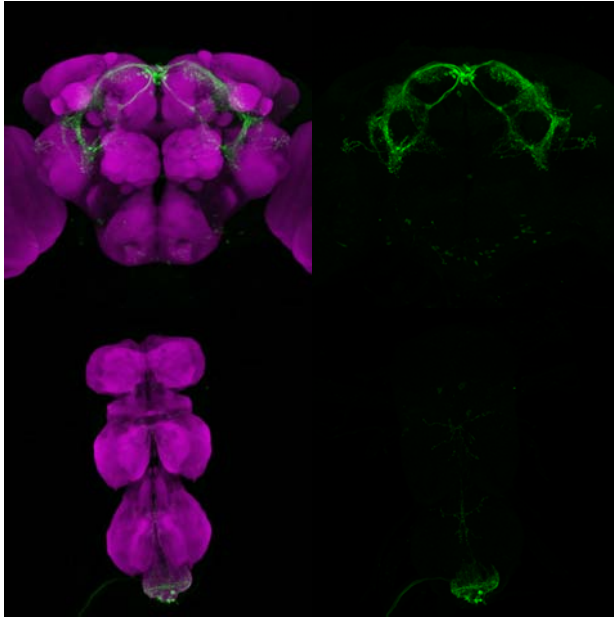


Figure S4

A

LexAop>stop>mCD8GFP; VT8657.lexAGAD/fru^{FLP}



B

UAS-mCD8RFP LexAop-mCD8GFP; NP2631; VT8657.LexAGAD/ tub>stop> fru^{FLP}

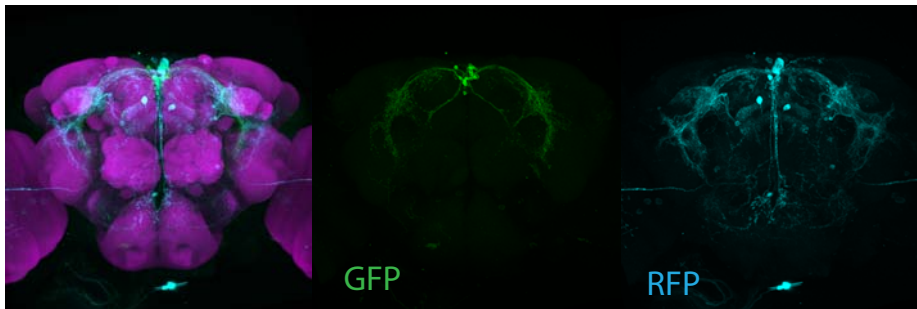
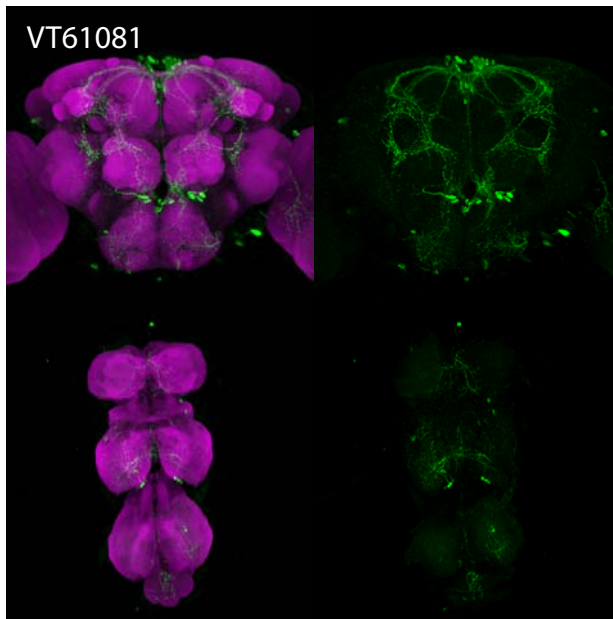
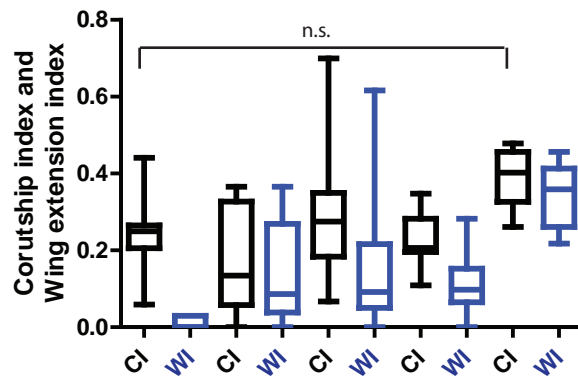


Figure S5

A

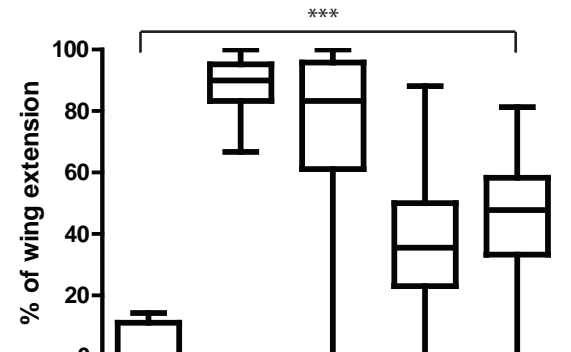


B



VT	61081	43068	43137	8657	23797
pMP4	+	+	-	-	+
pMP4_1	+	-	+	-	+
aSP2	+	-	-	+	+

C



VT	61081	43068	43137	8657	23797
pMP4	+	+	-	-	+
pMP4_1	+	-	+	-	+
aSP2	+	-	-	+	+

Figure S6

Supplementary figure legends

Figure S1. Prominent Regions of fru+ neurons innervations

A and F. of *UAS>stop>mCD8-GFP; nsyb-GAL4/ fru^{FLP}* male is stained with anti-GFP (green) and nc82 (magenta).

B-E and G Demarcation of mushroom body lateral protocerebral complex (B), mushroom body (C), tritocerebral loop (D), and mesothoracic triangle (G). E is the close-up view of E. grey indicates the surface representation of each region and magenta is nc82 staining. (adapted from Yu et. al., 2010)

Figure S2. Catalog of newly resolved from Yu et. al., 2010

Neuronal representation is shown. Cell body in yellow, projection in gray and arborizations in green. When there is no anatomical dimorphism, N.Di. (“not dimorphic”) is used. When the neuron was never observed in female, N,O, (“not observed”) is used. When the arborization of the neuron is not resolved, N.R. (“not resolved”) is used.

Figure S3. Catalog of newly identified neurons in this study

Anti-GFP (green) and nc82 staining (magenta) of *UAS>stop>mCD8GFP; VT-XXXX/ fru^{FLP}* is shown on left side and neuronal representation is shown on the right side. Left half is male and right half is female. Cell body in yellow, projection in gray and arborizations in green. When there is no anatomical dimorphism, N.Di. (“not dimorphic”) is used. When the neuron was never observed in female, N,O, (“not observed”) is used. When the arborization of the neuron is not resolved, N.R. (“not resolved”) is used.

Figure S4. Anatomical features used to discriminate neuronal types

- A. Overlay of four registered images from the same driver line (VT40016) which labels aSP5. The cell body location varies (arrow), but the axon tracts hardly vary (arrow head).
- B. Neuronal representations (cell body, projection, and arborization) of aSP12(light green) and aSP20(purple). The cell body of aSP12 and 20 are close and the axon tract are shared, but their arborization clearly differ.

C. Close up of C.

Figure S5. Staining and activation phenotype of VT61081

- A. Anti-GFP (green) and nc82 (magenta) staining of *UAS>stop>mCD8GFP; VT61081/fru^{FLP}* male.
- B. Courtship index (CI, black) and wing extension index (WI, blue) of each VT line during gradual shift of temperature from 30-32 degree. VT line are crossed to *UAS>stop>trpA1; fru^{FLP}*. The fru+ neurons which each VT line labels are described in the table. While CI represents the frequency of following and oriented wing extension, WI represents the frequency of oriented wing extension.
- C. Wing extension index is divided by courtship index.

Figure S6. Staining of VT8657.LexAGAD

- A. Anti-GFP (green) and nc82 (magenta) staining of *LeAop>stop>mCD8GFP; VT8657.LexAGAD/fru^{FLP}* male.
- B. Anti-GFP (green), anti-RFP (cyan) and nc82 (magenta) staining of *UAS-mCD8GFP LexAop-mCD8RFP; NP2631; VT8657.LexAGAD/tub^P>stop>fru^{FLP}* male.

Appdendix

Neuronal Control of *Drosophila* Courtship Song

Anne C. von Philipsborn,¹ Tianxiao Liu,¹ Jai Y. Yu,¹ Christopher Masser,¹ Salil S. Bidaye,¹ and Barry J. Dickson^{1,*}

¹Research Institute of Molecular Pathology, Dr. Bohrgasse 7, A-1030 Vienna, Austria

*Correspondence: dickson@imp.ac.at

DOI 10.1016/j.neuron.2011.01.011

SUMMARY

The courtship song of the *Drosophila* male serves as a genetically tractable model for the investigation of the neural mechanisms of decision-making, action selection, and motor pattern generation. Singing has been causally linked to the activity of the set of neurons that express the sex-specific *fru* transcripts, but the specific neurons involved have not been identified. Here we identify five distinct classes of *fru* neuron that trigger or compose the song. Our data suggest that P1 and pIP10 neurons in the brain mediate the decision to sing, and to act upon this decision, while the thoracic neurons dPR1, vPR6, and vMS11 are components of a central pattern generator that times and shapes the song's pulses. These neurons are potentially connected in a functional circuit, with the descending pIP10 neuron linking the brain and thoracic song centers. Sexual dimorphisms in each of these neurons may explain why only males sing.

INTRODUCTION

Many animals use acoustic signals to coordinate their social behaviors. Among these are the songs that males of various insect species, including grasshoppers, crickets, and cicadas, produce to attract or arouse females. These mating calls are astonishing in their diversity and, often, their volume. Male crickets, for example, rub their front wings together to produce a calling song that attracts females from a distance, and a courtship song that stimulates them during mating behavior (Hedwig, 2006). *Drosophila melanogaster* males produce their courtship song by extending and vibrating one wing (Bennet-Clark and Ewing, 1967). Although not as spectacular as the songs of crickets and cicadas, the *Drosophila* song offers an ideal opportunity to apply molecular genetic approaches to the investigation of the neural mechanisms of acoustic communication.

The courtship song of *Drosophila melanogaster* consists of two components: sine song and pulse song (von Schilcher, 1976). The sine song is a humming sound with a fundamental frequency of 140–170 Hz; it has been proposed to prime the female for the pulse song (von Schilcher, 1976). The pulse song consists of a train of 2–50 pulses, each containing one to three cycles (cycles per pulse, or CPP) with a carrier frequency of 150–300 Hz. Pulses are separated by a pause that lasts an

average of ~35 ms (the interpulse interval, or IPI). The pulse song is a key factor in mating success, with the IPI providing a critical signature for song and species recognition (Bennet-Clark and Ewing, 1969; Kyriacou and Hall, 1982).

Normally only male flies sing. Initial attempts to map the neural centers responsible for song production thus relied on the construction of sex mosaics, or gynandromorphs, in order to delineate the parts of the nervous system that must be male for a fly to sing. These studies demonstrated that a region of the dorsal posterior brain must be male to initiate singing (Hall, 1977; von Schilcher and Hall, 1979), while regions of the mesothoracic ganglia need to be male to ensure the correct song structure (von Schilcher and Hall, 1979). Accordingly, fly song is thought to rely on a neural architecture in which a local and largely autonomous central pattern generator (CPG) produces rhythmic motor patterns subject to the control of descending “command” neurons in the brain. Such an architecture has been documented in crickets, for example, with the identification of command neurons that activate a thoracic CPG for stridulation (Hedwig, 1994, 2000; Howse, 1975).

More recent studies have begun to exploit molecular genetic approaches to map the fly's song circuitry more precisely. These studies have also been guided by the fact that only males sing, and thus focused on the two genes that control almost all aspects of sexual differentiation in *Drosophila*: *fruitless* (*fru*) and *doublesex* (*dsx*). Of these, *fru* plays the predominant role in the sexual differentiation of the nervous system and behavior, including song production. Male-specific *fru* isoforms (*fru*^M) are essential for males to sing (Ryner et al., 1996; Vilella et al., 1997), and, if produced aberrantly in females, are sufficient to enable them to sing (Demir and Dickson, 2005). The songs of *fru*^M females are not, however, perfect renditions of the male song, but become so if male-specific *dsx* isoforms are also present (Rideout et al., 2007). Male *dsx* isoforms on their own are neither necessary nor sufficient for pulse song (Taylor et al., 1994; Vilella and Hall, 1996).

fru^M is expressed in ~2000 neurons distributed in small clusters throughout the male central nervous system (CNS) (Lee et al., 2000). Genetic access to these neurons has been gained through targeted insertion of sequences encoding the GAL4 or *lexA* transcriptional activators, or the FLP recombinase, into the *fru* locus (Manoli et al., 2005; Mellert et al., 2010; Stockinger et al., 2005; Yu et al., 2010). These genetic reagents can now be used to target the expression of genetically encoded activity modulators specifically to the *fru*-expressing neurons in males or their counterparts in females. Silencing these neurons in males impairs courtship performance, including song production (Manoli et al., 2005; Stockinger et al., 2005). Conversely, light-triggered activation of the *fru* neurons in beheaded flies of

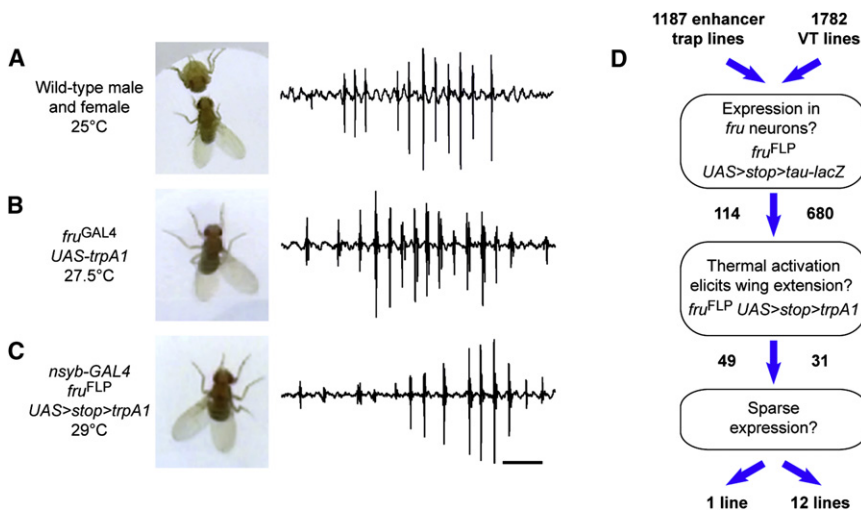


Figure 1. Thermal Activation of *fru* Neurons with TrpA1 Evokes Courtship Song

(A–C) Wing extension (left) and pulse song production (right) of (A) a wild-type male courting a female, (B) an isolated *fru^{GAL4} UAS-trpA1* male at 27.5°C (see also Movies S1 and S2), and (C) an isolated *nsyb-GAL4 fru^{FLP} UAS>stop>trpA1* male at 29°C (see also Movies S3 and S4). Scale bar: 100 ms. (D) Overview of thermal activation screen to identify sparsely expressed GAL4 lines capable of driving wing extension in combination with *fru^{FLP}* and *UAS>stop>trpA1*. Initial identification of lines expressed in *fru* neurons is according to Yu et al. (2010) and our unpublished results (VT lines).

either sex elicits singing and other aspects of the courtship ritual (Clyne and Miesenböck, 2008). These experiments have established a causal link between the activity of the *fru* neurons and song production. The specific neurons involved have not been identified.

We have recently used the *fru^{FLP}* allele in an intersectional genetic approach to subdivide the set of *fru* neurons into some 100 distinct neuronal classes (Yu et al., 2010). This work not only provided a cellular resolution map of the *fru* network, but also the genetic tools needed to selectively express activity modulators in small subsets of these neurons. Here, we use these tools, together with a thermal activation strategy (Hamada et al., 2008; Pulver et al., 2009), to identify and functionally characterize specific neurons involved in pulse song production. We identify two types of neuron in the brain, P1 (pMP4) and pIP10 neurons, that are capable of eliciting an authentic song. The pIP10 neuron is a descending neuron with axonal termini in the mesothoracic ganglia, and P1 is likely to be one of its inputs. Three other types of neuron in the thoracic ganglia, dPR1, vPR6, and vMS11, appear to control distinct features of wing extension and pulse song. We propose that dPR1, vPR6, and vMS11 neurons are components of a thoracic CPG for pulse song, controlled by signals from P1 and the pIP10 command neuron. The P1, pIP10, and dPR1 neurons are all male specific, potentially explaining why only males can sing.

RESULTS

Thermal Activation of *fru* Neurons with TrpA1 Elicits Pulse Song

Photoactivation of the *fru* neurons using *fru^{GAL4}* and the P2X₂ system (Lima and Miesenböck, 2005) elicits courtship song in isolated flies (Clyne and Miesenböck, 2008). Similarly, we found that thermal activation with TrpA1 also induced singing, often together with other courtship behaviors such as abdominal bending (Figures 1A and 1B and Movie S1, available online). One important difference, however, is that robust singing with the P2X₂ system was only observed with beheaded flies (Clyne

and Miesenböck, 2008), whereas thermal activation also triggered singing in intact flies. Aside from this exception, the two activation methods gave similar results, in that both produced pulse songs with

somewhat longer IPIs than normal (55.7 ± 1.5 ms for thermal activation at 27.5°C, $n = 14$), and elicited singing in females as well as males. For both methods, greater input energy was required to induce females to sing (for thermal activation, above $\sim 28.5^\circ\text{C}$ for females and $\sim 26^\circ\text{C}$ for males), and female pulse songs had even longer IPIs (72.8 ± 1.6 ms at 29°C, $n = 14$) and were more often polycyclic ($11\% \pm 4\%$ of pulses in female songs had more than two cycles, $n = 5$ flies, compared with $2\% \pm 1\%$ of male songs, $n = 5$ flies; $p = 0.012$, Mann-Whitney test). Whereas photoactivated and thermally activated males generally extended only one wing, as in natural songs, females often extended both wings simultaneously, and to a lesser degree (Movie S2).

We obtained qualitatively similar results when we used *fru^{FLP}* and the panneuronal driver *nsyb-GAL4* to thermally activate the *fru* neurons, in this case using a combinatorial *UAS>stop>trpA1* transgene (Figure 1C and Movies S3 and S4; “>stop>” indicates a transcriptional stop cassette flanked by FLP recombinase target [FRT] sites, and thus excised only in the cells that express *fru^{FLP}*). This intersectional approach required slightly higher activation temperatures (above $\sim 28.5^\circ\text{C}$ for males and $\sim 31.5^\circ\text{C}$ for females) than the direct *fru^{GAL4} UAS-trpA1* strategy, possibly due to differences in TrpA1 expression levels from the two transgenes. Despite this minor difference, thermal activation of *fru* neurons using *fru^{FLP}* also produced songs with pulses that were more widely spaced than those of natural songs, and which were often polycyclic in females (IPIs of 51.2 ± 1.9 ms in males at 29°C, $n = 10$; 64.7 ± 2.2 ms in females at 32°C, $n = 8$; $64\% \pm 6\%$ of pulses polycyclic in females, $n = 5$, $1.0\% \pm 0.0\%$ in males, $n = 5$).

The robust song response of thermally activated *fru^{FLP}* flies, together with the intersectional genetic approach *fru^{FLP}* enables (Yu et al., 2010), provided an efficient and reliable assay for a thermogenetic screen to identify specific neurons involved in song production (Figure 1D). To this end, we screened a set of 794 GAL4 lines known to drive expression in one or more subclasses of *fru* neuron, consisting of 114 enhancer trap lines (Yu et al., 2010) and 680 molecularly defined enhancer-GAL4

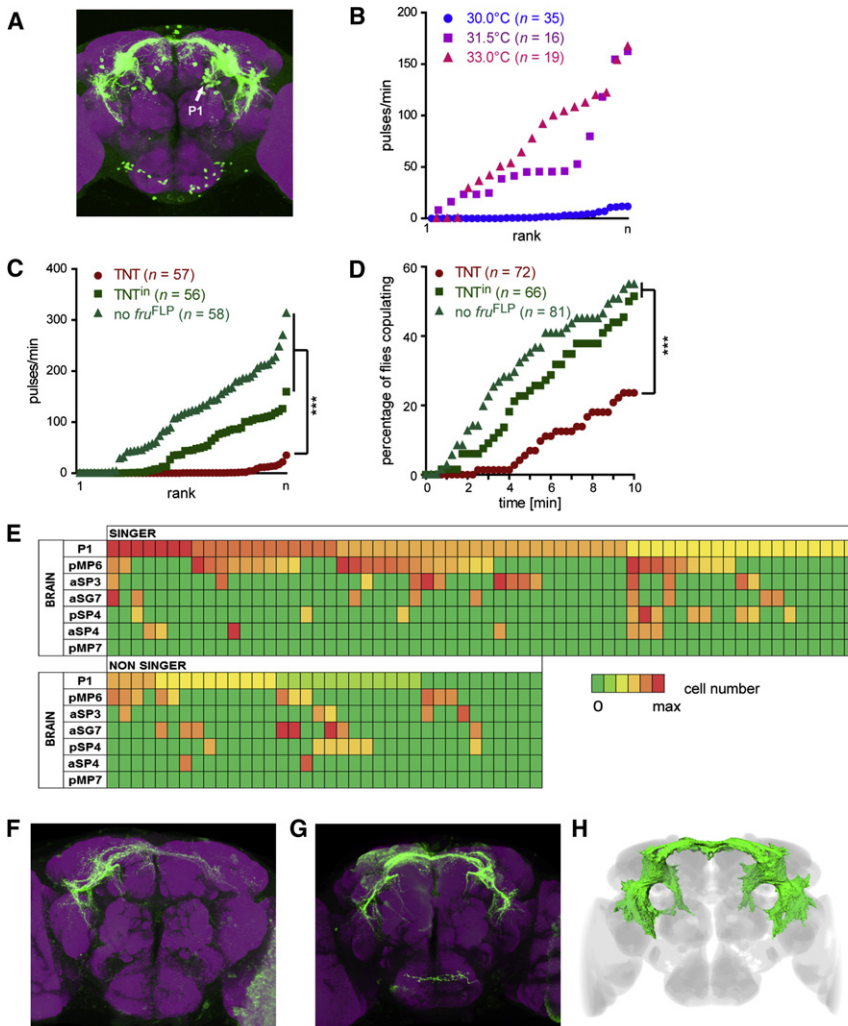


Figure 2. P1: A Brain Neuron that Triggers Pulse Song

(A) Brain of an *NP2361 fru^{FLP} UAS>stop>mCD8-GFP* male stained with anti-GFP (green) and the synaptic marker mAb nc82 (magenta).

(B) Song production of isolated *NP2361 fru^{FLP} UAS>stop>trpA1* males at different temperatures. Each data point represents a single fly, ranked by the amount of pulse song (see also Movie S5).

(C) Song production of *NP2361 fru^{FLP} UAS>stop>TNT* (TNT), *NP2361 fru^{FLP} UAS>stop>TNTⁱⁿ* (TNTⁱⁿ), and *NP2361 UAS>stop>TNT* (no *fru^{FLP}*) males paired with wild-type virgin females. Each data point represents a single fly, ranked by the amount of pulse song. ****p* < 0.0001, Mann-Whitney test.

(D) Copulation success of males of the same genotypes as in (C). ****p* < 0.0009, Fisher's exact test.

(E) *TrpA1^{myc}* expression in each of the *NP2361⁺ fru^{FLP}* neuronal classes in 62 singing and 36 non-singing *NP2361 hs-mFLP5 fru^{FLP} UAS>stop>stop>trpA1^{myc}* males subjected to a brief heat shock during development. Each vertical column represents one fly; each row, one cell type. Color-coding indicates the approximate number of cells labeled, with maxima (red) of 40+ for P1, 10 for pMP6 and aSP3, 2 for aSG7, 6 for pSP4, and 5 for aSP2. Green indicates no labeling. The six different shades for P1 indicate bins of 0, 1–10, 11–20, 21–30, 31–40, and over 40 cells, respectively, from green to red. pMP7 was never labeled. Neuronal classes are as described previously (Yu et al., 2010) and as in Figure S1A.

(F) Male brain with unilateral *TrpA1^{myc}* expression in P1 neurons, as visualized with anti-myc (green) and mAb nc82 counterstain (magenta).

(G) Male brain with bilateral *TrpA1^{myc}* expression in P1 neurons, stained as in (F).

(H) Segmented arborization of the P1 class.

transgenes (VT lines; C.M., S.B., T.L., V. Belyaeva, M. Kinberg, and B.J.D., unpublished data; Pfeiffer et al., 2008). Each line was crossed into the *fru^{FLP} UAS>stop>trpA1* background, and four to eight isolated male progeny were gradually warmed from 25°C to ~32°C during a 10 min video recording. Lines in which the majority of flies showed unilateral wing extension and/or vibration were scored as positive. Of 80 such lines recovered in the screen, we restricted our further analysis to 13 lines with relatively sparse expression in the CNS.

P1: A Brain Neuron that Triggers Pulse Song

The one positive GAL4 enhancer trap line from our screen was *NP2361*, which labels seven classes of *fru* neuron in the brain and none in the ventral nerve cord (VNC) (Yu et al., 2010; Figures 2A and S1A available online). In video and audio recordings, we found that *NP2361 fru^{FLP} UAS>stop>trpA1* males sang reliably at temperatures between 30°C and 33°C (Figure 2B and Movie S5), producing monocyclic pulses organized into distinct trains that were indistinguishable from those of natural courtship songs (Table 1). Moreover, in contrast to the extended IPIs of songs

produced upon activation of all *fru* neurons using *nsyb-GAL4*, the IPIs of songs elicited at 30°C using the *NP2361* driver were comparable to those of natural song at the same temperature (Table 1). Artificial activation of one or more of the *NP2361⁺ fru^{FLP}* neurons in the brain is thus sufficient to trigger a pulse song very close to the natural rendition.

To test whether the activity of these neurons is also required for normal song production, we combined *NP2361* and *fru^{FLP}* with a *UAS>stop>TNT* transgene. *TNT* encodes tetanus toxin light chain (TeTxLC), which cleaves synaptobrevin and thereby inhibits synaptic transmission (Sweeney et al., 1995). Males were paired with wild-type virgin females for either a 3.5 min recording session to monitor song production or a 10 min video assay to assess copulation success. Compared to control males that either expressed an inactive TeTxLC protease (*TNTⁱⁿ*) or lacked *fru^{FLP}*, test males sang less often and with fewer pulse trains (Figure 2C and Table S1 available online). They were also less successful in their courtship attempts (Figure 2D and Table S1).

These data suggest that the activity of one or more of the seven classes of *NP2361⁺ fru^{FLP}* neuron in the brain is both

Table 1. Pulse Songs Elicited by Thermal Activation of Specific *fru* Neurons

Neuronal Class	GAL4 Line	Temperature	Singers (%)	n	Pulses/Min	n	IPI (ms)	n	CPP	n
P1	NP2361	30.0°C	63	35	4.2 ± 0.8	22	28.4 ± 0.7	11 (311)	1.01 ± 0.01	8 (207)
		31.5°C	100	16	57.9 ± 11.4	16	29.4 ± 0.4	16 (1850)	1.00 ± 0.00	6 (712)
		33.0°C	89	19	84.2 ± 10.7	17	33.7 ± 0.6	16 (2567)	1.00 ± 0.00	6 (872)
pIP10	VT40556	29.0°C	100	20	25.1 ± 4.9	20	33.3 ± 0.6	14 (722)	1.01 ± 0.01	5 (335)
		31.5°C	100	16	245.8 ± 29.9	16	34.1 ± 0.7	14 (6965)	1.09 ± 0.02	5 (945)
		33.0°C	100	15	285.7 ± 26.8	15	35.4 ± 0.7	15 (6875)	1.13 ± 0.06	5 (999)
dPR1	VT41688	31.5°C	43	35	21.3 ± 4.9	15	46.3 ± 0.9	10 (522)	1.01 ± 0.00	6 (453)
		33.0°C	63	35	34.8 ± 7.0	22	45.7 ± 1.0	16 (1308)	1.01 ± 0.00	6 (635)
vPR6	VT19579	27.5°C	95	20	30.4 ± 5.1	19	63.1 ± 0.7	16 (1381)	1.31 ± 0.05	6 (540)
		29.0°C	100	16	105.7 ± 16.5	16	59.0 ± 0.7	16 (4420)	1.19 ± 0.02	5 (625)
		31.5°C	100	15	168.1 ± 23.9	15	43.5 ± 0.8	15 (7360)	1.18 ± 0.02	5 (754)
	VT5534	29.0°C	100	16	123.0 ± 21.8	16	60.1 ± 0.5	16 (4962)	1.36 ± 0.07	6 (755)
		31.5°C	100	16	144.5 ± 19.7	16	40.5 ± 0.7	16 (6164)	1.22 ± 0.02	6 (795)
		33.0°C	100	16	118.0 ± 17.5	16	59.1 ± 1.1	16 (4606)	1.13 ± 0.04	6 (719)
	VT57239	29.0°C	100	15	98.6 ± 13.1	15	60.6 ± 0.7	15 (3923)	1.29 ± 0.03	5 (596)
		31.5°C	100	15	246.4 ± 19.2	15	43.0 ± 0.8	15 (10677)	1.32 ± 0.05	5 (721)
		33.0°C	100	17	78.0 ± 11.7	17	36.2 ± 0.7	16 (3354)	1.23 ± 0.03	5 (576)
	VT46099	29.0°C	95	22	15.7 ± 5.1	21	68.3 ± 1.2	14 (632)	1.18 ± 0.05	5 (261)
		31.5°C	94	17	44.4 ± 12.2	16	60.6 ± 0.9	16 (3936)	1.18 ± 0.03	5 (629)
		33.0°C	100	18	122.9 ± 18.5	18	47.7 ± 1.1	16 (6185)	1.31 ± 0.05	5 (614)
	VT17258	30.0°C	72	25	10.8 ± 2.7	18	67.9 ± 1.3	11 (523)	1.13 ± 0.03	6 (312)
		31.5°C	100	16	104.6 ± 23.7	16	61.5 ± 0.8	16 (4744)	1.23 ± 0.04	6 (709)
		33.0°C	100	16	118.0 ± 17.5	16	59.1 ± 1.1	16 (4606)	1.13 ± 0.04	6 (719)
n/a	wild-type courtship	27.5°C	–	–	–	–	30.9 ± 0.5	11 (645)	1.02 ± 0.01	6 (784)
		30.0°C	–	–	–	–	27.9 ± 0.4	11 (692)	1.01 ± 0.01	6 (740)
		33.0°C	–	–	–	–	25.5 ± 0.4	8 (606)	1.01 ± 0.00	6 (892)

Values for pulses/min are mean ± SEM of n flies that sang. Values for IPI and CPP are grand mean ± SEM, i.e., the mean of the mean per fly, for n flies. Numbers in parentheses indicate the total number of IPIs and pulses, respectively. Wild-type courtship indicates songs recorded from a Canton S male courting a virgin Canton S female.

necessary and sufficient to trigger pulse song. We used a stochastic approach to identify the specific neuronal type(s) involved. As each neuronal class is represented by multiple cells, we feared that cellular redundancy might preclude the identification of these neurons by stochastic silencing of single neurons. In contrast, activation of single or few neurons in a given class may be sufficient to trigger song production. To enable such a stochastic activation approach, we thus modified the *UAS>stop>trpA1* transgene to tag the TrpA1 protein with a *c-myc* epitope, and in addition, inserted a second transcriptional stop cassette flanked by mutant FRT sites (mFRT71, denoted here as “≥”). These mutant FRT sites are not recognized by the wild-type FLP protein, but are efficiently excised by a mutant FLP protein, mFLP5 (Hadjieconomou et al., 2011; Voziyanov et al., 2003). In this tripartite strategy, the canonical *>stop>* cassette is excised, as before, with *fru*^{FLP}, while the additional *≥stop≥* cassette is removed using *hs-mFLP5*. Thus, by subjecting *NP2361 hs-mFLP5 fru*^{FLP} *UAS>stop>≥stop≥trpA1*^{myc} males to a brief heat shock during larval development, we could restrict TrpA1^{myc} expression to a random subset of the *NP2361*⁺ *fru*^{FLP+} cells. After testing individual adult males for song, we dissected and stained their brains to identify these cells.

From a total of 98 flies tested, 62 produced pulse song and 36 did not (Figure 2E). In all 62 singers, neurons of the P1 class were labeled, and in 16 of them these were the only labeled cells (Figures 2E and 2F). None of the other six classes of neuron were consistently labeled in singers. P1 neurons were also labeled in 25 of the 36 flies that did not sing, but these flies generally had fewer labeled P1 cells than the singers (Figure 2E). The P1 class comprises 15–20 individual, and possibly heterogeneous, neurons per hemisphere (Yu et al., 2010). P1 neurons are male specific, and their ectopic presence in female gynandromorphs correlates with male-like courtship behavior (Kimura et al., 2008). Clusters of at least 10 individual P1 neurons were labeled in all of the singers (62/62), but few of such clusters (14/36) were labeled in the nonsingers. Moreover, the number of labeled P1 cells in singers positively correlated with the amount of produced pulse song (Figure S1B). The pMP6 neurons were also more often labeled in singers (34/62) than in nonsingers (11/36, p = 0.02). However, as pMP6 was not labeled in all singers, and among the singers pMP6 labeling did not correlate with the amount of song produced (Figure S1C), we infer that P1 neurons alone are primarily responsible for the song production observed with *NP2361*, and that a threshold number of P1

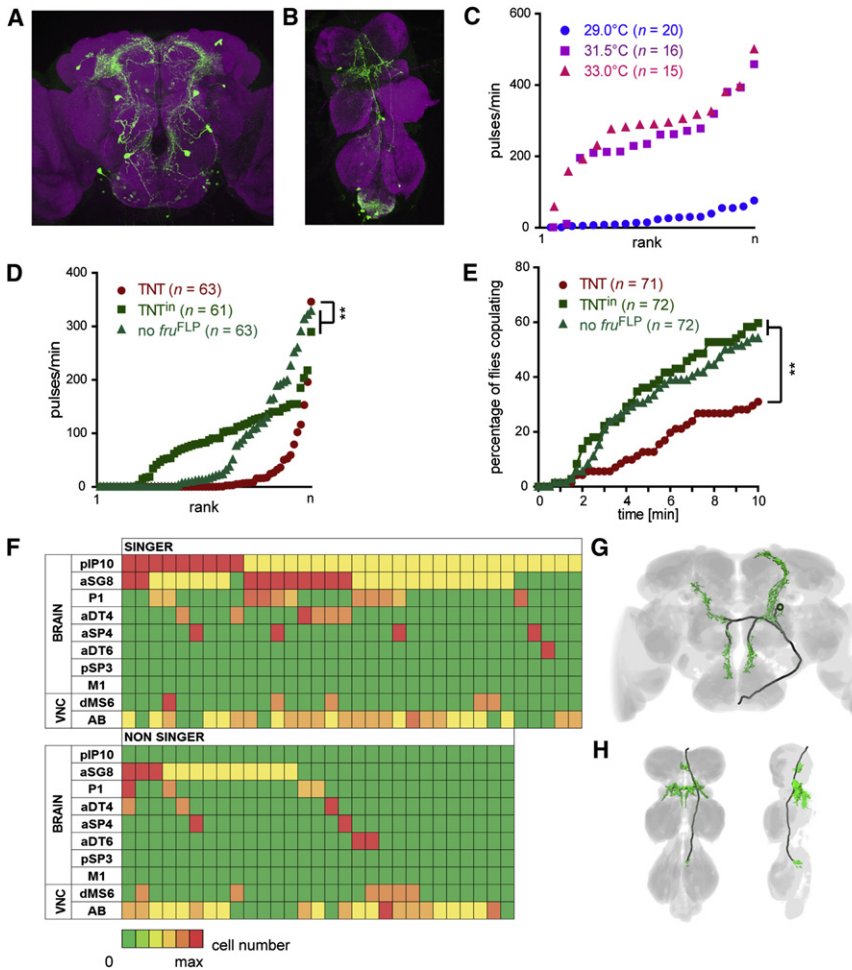


Figure 3. pIP10: A Descending Command Neuron for Pulse Song

(A and B) Brain (A) and VNC (B) of a *VT40556 fru^{FLP} UAS>stop>mCD8-GFP* male stained with anti-GFP (green) and the synaptic marker mAb nc82 (magenta).

(C) Song production of isolated *VT40556 fru^{FLP} UAS>stop>trpA1* males at different temperatures. Each data point represents a single fly, ranked by the amount of pulse song (see also *Movie S6*).

(D) Song production of *VT40556 fru^{FLP} UAS>stop>TNT* (TNT), *VT40556 fru^{FLP} UAS>stop>TNTⁱⁿ* (TNTⁱⁿ), and *VT40556 UAS>stop>TNT* (no fru^{FLP}) males paired with wild-type virgin females. Each data point represents a single fly, ranked by the amount of pulse song. **p < 0.002, Mann-Whitney test.

(E) Copulation success of males of the same genotypes as in (D). **p < 0.007, Fisher's exact test.

(F) TrpA1^{myc} expression in each of the *VT40556⁺ fru^{FLP}* neuronal classes in 34 singing and 29 non-singing *VT40556 hs-mFLP5 fru^{FLP} UAS>stop>stop>trpA1^{myc}* males subjected to a brief heat shock during development. Each vertical column represents one fly; each row, one cell type. Color-coding indicates the approximate number of cells labeled, with maxima (red) of two for pIP10, aSG8, aDT4, and dMS6, four for P1 and AB, and one for aSP4 and aDT6. Green indicates no labeling. pSP3 and M1 were never labeled. Neuronal classes are as described previously (Yu et al., 2010) and as in *Figure S2A*.

(G and H) Segmented arborization of the pIP10 class, showing the brain (G) and the ventral (H, left) and lateral (H, right) views of the VNC.

neurons, or possibly a specific subtype, must be activated to trigger song.

To assess whether unilateral activation of P1 neurons preferentially leads to song generation with one or the other wing, we analyzed the wing extensions of six flies with unilateral expression of TrpA1 in P1 neurons (*Figure 2F*), as well as 12 with bilateral expression (*Figure 2G*). In almost all cases (5/6 and 11/12, respectively), flies variously extended either the ipsilateral or contralateral wing, but never both simultaneously. P1 neurons evidently do not control the laterality of wing extension.

In summary, we infer from these data that activity of P1 neurons (*Figure 2H*) is necessary and sufficient to trigger song production, and that song structure and wing choice are under the control of subordinate neural circuits.

pIP10: A Descending Neuron that Triggers Pulse Song

Another GAL4 line from our initial screen that elicited seemingly natural pulse songs was *VT40556* (*Figures 3A* and *3B*). As with *NP2361*, the thermally induced pulse songs obtained using *VT40556* consisted of monocyclic pulses organized in trains with IPIs in the natural range (33.3 ± 0.6 ms at 29°C to 35.4 ± 0.7 ms at 33°C; *Figure 3C*, *Table 1*, and *Movie S6*). To test

whether activity of *VT40556⁺ fru^{FLP}* neurons is also required for song, we silenced these neurons with *UAS>stop>TNT* and tested these males for song production and copulation success in pairings with wild-type virgin females. These *VT40556* test males sang less and copulated less than each of the corresponding controls (*Figures 3D* and *3E* and *Table S1*).

To identify the specific subset of *fru* neurons labeled by *VT40556*, we replaced *UAS>stop>trpA1* with a *UAS>stop>mCD8-GFP* transgene, inserted at the same genomic location. Staining brains and VNCs from these animals with anti-GFP revealed expression in eight classes of *fru* neuron in the brain and in two *fru* clusters in the VNC (*Figures 3A*, *3B*, and *S1B*). The P1 neurons were among those cells labeled in the brain. However, *VT40556* labels only 2.7 ± 0.2 P1 neurons per hemisphere (n = 12). Judging from the results of our stochastic activation experiments using *NP2361*, this could be too few P1 cells to account for song production in *VT40556* flies. We therefore suspected that some other cell type might be responsible for eliciting songs in these flies.

As previously with *NP2361*, we used the stochastic activation approach with *VT40556* to identify the specific cell type responsible, recovering in this case 34 males that sang and 29 that did

not (Figure 3F). One cell type was labeled in all singers and in none of the nonsingers: the pIP10 neurons (Figure 3E, $p < 0.0001$, Fisher's exact test). P1, in contrast, was no more often labeled in singers than in nonsingers (Figure 3E, $p = 0.14$). aSG8 neurons were slightly more frequently labeled in singers (27/34) than in nonsingers (13/29, $p = 0.008$). However, in contrast to pIP10, aSG8 was labeled in many nonsingers and not labeled in all singers. Furthermore, more pulse song was consistently produced by flies with bilateral labeling of pIP10 than those with unilateral labeling ($p = 0.009$, Figure S2B), whereas no such effect was observed with aSG8 ($p = 0.37$, Figure S2C). We conclude therefore that the pIP10 neurons alone account for song production in thermal activation experiments with VT40556.

The pIP10 neuron has its soma located in the medial posterior brain (Figure 3G). In VT40556 *fru*^{FLP} *UAS>stop>mCD8-GFP* males we observed just a single pIP10 neuron either bilaterally (14 of 18 males) or unilaterally (4 of 18 males). A corresponding cell type was never seen in females ($n = 8$). pIP10 extends neurites bilaterally, branching ventrally to innervate the periesophageal region and dorsally to innervate the lateral protocerebral complex. Both of these regions are richly innervated by fibers of other *fru*⁺ neurons, including the P1 neurons in the lateral protocerebral complex (Yu et al., 2010). Another long process descends to the VNC, where it arborizes extensively within the wing neuropil of the anterior mesothoracic ganglia (Figure 3H). The pIP10 neuron was not characterized in our previous genetic dissection of the *fru*^{FLP} neurons (Yu et al., 2010), presumably because it is not targeted by any of the enhancer trap GAL4 lines in our collection. pIP10 is however similar to a cell type observed within the male-specific clone pIP-a in a MARCM analysis of the *fru*^{GAL4} neurons (Cachero et al., 2010).

We selected 20 singers for analysis of wing usage, 13 with unilateral labeling of pIP10 and 7 with bilateral labeling. In almost all cases (10/13 and 6/7, respectively), flies variously extended either the left or the right wing only. In the case of those flies with unilateral expression of *TrpA1*^{myc}, there was no obvious bias for the ipsilateral or contralateral wing.

In summary, we conclude that activity of pIP10 neurons, just like P1 neurons, is necessary and sufficient to trigger song production, but also does not encode specific features of the song.

dPR1: A Prothoracic Song Neuron

As none of the remaining positive lines from our screen labeled either P1 or pIP10, the singing observed with these lines was presumably due to activation of some other class of *fru* neuron. One of these, VT41688, labels three distinct clusters of *fru* neuron in the VNC: dPR1, dMS7, and a heterogeneous set of cells in the abdominal ganglia (AB; Figure 4A). It does not label any *fru* neurons in the brain. Typically, ~50% of VT41688 *fru*^{FLP} *UAS>stop>trpA1* males produced pulse songs when warmed above ~31.5°C (Figure 4B, Movie S7, and Table 1). Like natural songs, these were organized into distinct trains of monocyclic pulses, but with significantly longer IPIs (46.3 ± 0.9 ms at 31.5°C, $n = 10$, and 45.7 ± 1.0 ms at 33.0°C, $n = 16$, $p = 0.0001$). Conversely, silencing these neurons with *UAS>stop>TNT* significantly reduced both the song production ($p < 0.0001$,

Figure 4C and Table S1) and copulation success ($p < 0.0004$, Figure 4D) when males were paired with wild-type virgins. The frequency of wing extension was however similar in both test and control males ($p < 0.1$, Mann-Whitney test, Table S1), suggesting that males with silenced VT41688⁺ *fru*^{FLP+} neurons extend their wings but do not produce pulse song.

To determine which VT41688⁺ *fru*^{FLP+} neurons are involved in song production, we took advantage of the fact that the expression in each cell type is somewhat stochastic in VT41688⁺ *fru*^{FLP+} flies. This inherent stochasticity may explain why not all flies sang in the thermal activation experiments, and some still did in the silencing experiments. Using *UAS>stop>trpA1*^{mCherry} and *UAS>stop>trpA1*^{myc} transgenes, we sorted individual flies into singers ($n = 57$) and nonsingers ($n = 54$) and then dissected and stained their VNCs (Figure 4E). dPR1 was labeled in all 57 singers but only 37 of the 54 nonsingers ($p < 0.0001$, Fisher's exact test). Moreover, dPR1 labeling was bilateral in 52/57 singers but only in 7/54 nonsingers ($p < 0.0001$). In contrast, neither dMS7 nor AB neurons were more frequently labeled in singers versus nonsingers ($p < 0.66$). These data strongly suggest that dPR1 neurons are responsible for pulse song production in thermally activated VT41688 flies.

The morphology of dPR1 is consistent with a role in song production (Figures 4A and 4F). In VT41688 *fru*^{FLP} *UAS>stop>mCD8-GFP* males we typically observed one or two cell bodies located medially in the anterior region of the prothoracic ganglion. Processes of these neurons extended bilaterally to innervate the wing neuropil of the anterior mesothoracic segment. We have not observed this neuron in VT41688 *fru*^{FLP} *UAS>stop>mCD8-GFP* females ($n = 10$), implying that it is either absent or does not express GAL4 in VT41688 females. The former is consistent with data from the MARCM study (Cachero et al., 2010): dPR1 is likely contained within the dPR-b clone, which in females lacks the arborization that we attribute to dPR1 in males. The location and dimorphism of dPR1 further suggest that it may correspond to a subtype of the *dsx*⁺ TN2 neurons (Rideout et al., 2010). In support of this, double stainings with anti-Fru^M and anti-Dsx^M revealed that dPR1 neurons are Dsx⁺ (Figure S3A).

vPR6: A Mesothoracic Neuron that May Encode the IPI

Of the remaining 10 positive GAL4 lines from the *trpA1* screen, 9 are expressed in the vPR6 neurons of the thoracic ganglia. As vPR6 is the only class of *fru* neuron common to all nine lines, these neurons are most likely responsible for song production within each of these lines. We focused our further analysis on the five lines with the most restricted expression patterns: VT19579, VT5534, VT57239, VT40699, and VT17258 (Figures 5A and S4). When combined with *fru*^{FLP} and *UAS>stop>mCD8-GFP*, each of these lines consistently labeled two to five vPR6 cells per hemisphere. These neurons are located laterally near the border of the prothoracic and mesothoracic ganglia, and extend processes medially and posteriorly within the wing neuropils (Figures 5A and 5B). In some cases, we also observed weakly stained processes that extended anteriorly and may also arise from these cells. Similar cells were not observed in females with four of these GAL4 lines ($n = 4-7$); VT17258 additionally labels a similar but probably distinct cell type in both sexes.

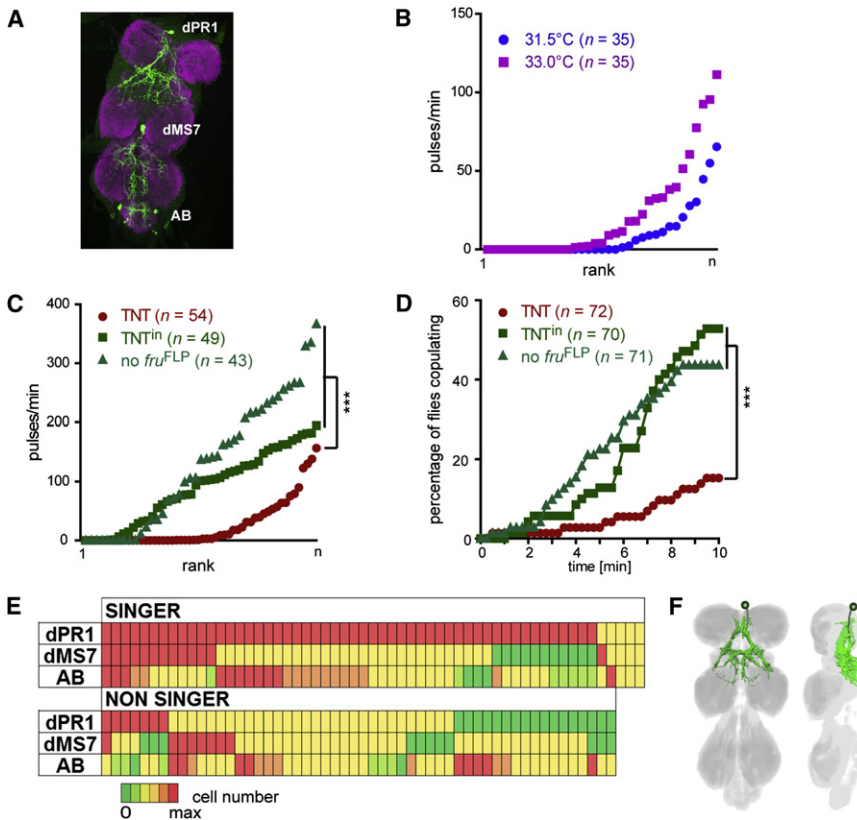


Figure 4. dPR1: A Prothoracic Song Neuron

(A) VNC of a *VT41688 fru^{FLP} UAS>stop>mCD8-GFP* male stained with anti-GFP (green) and the synaptic marker mAb nc82 (magenta).

(B) Song production of isolated *VT41688 fru^{FLP} UAS>stop>trpA1* males at 31.5°C and 33.0°C. Each data point represents a single fly, ranked by the amount of pulse song (see also [Movie S7](#)).

(C) Song production of *VT41688 fru^{FLP} UAS>stop>TNT* (TNT), *VT41688 fru^{FLP} UAS>stop>TNTⁱⁿ* (TNTⁱⁿ), and *VT41688 UAS>stop>TNT* (no *fru^{FLP}*) males paired with wild-type virgin females. Each data point represents a single fly, ranked by the amount of pulse song. ****p* < 0.0001, Mann-Whitney test.

(D) Copulation success of males of the same genotypes as in (C). ****p* < 0.0004, Fisher's exact test.

(E) Expression of tagged TrpA1 in each of the *VT41688⁺ fru^{FLP}⁺* neuronal classes in 57 singing and 54 nonsinging *VT40556 fru^{FLP} UAS>stop>trpA1^{mCherry}* or *UAS>stop>trpA1^{myc}* males. Each vertical column represents one fly; each row, one cell type. Color-coding indicates the number of cells labeled. Red, yellow, and green indicate 2, 1, and 0 cells, respectively, for dPR1 and dMS7, and 4, 2, and 0, respectively, for AB.

(F) Segmented arborization of the dPR1 class, showing ventral (left) and lateral (right) views of the VNC.

The location, morphology, and sexual dimorphism of vPR6 neurons suggest that they may represent a subclass of the *dsx⁺ TN1* neurons (Rideout et al., 2010). Double stainings for *Fru^M* and *Dsx^M* confirmed that vPR6 neurons are indeed *Dsx⁺* (Figure S3B).

Songs were reliably induced with *fru^{FLP} UAS>stop>trpA1* and each of the five selected vPR6 GAL4 lines (Figure 5C, [Movie S8](#), and [Table 1](#)). Songs were generally produced in the temperature range of 27.5°C–33°C, but the five lines varied in their optimal activation temperature ([Table 1](#)). For example, *VT19579* and *VT5534* flies began to sing above 27.5°C, and did so most robustly around 29°C–31°C. *VT17258* flies, on the other hand, only began to sing above 30°C and were most active around 33°C. Within their respective temperature ranges, songs from all lines were consistently organized into distinct trains of predominantly monocyclic pulses ([Table 1](#)).

We used the two most restricted GAL4 lines, together with *fru^{FLP}* and *UAS>stop>TNT*, to test whether synaptic activity of vPR6 neurons might also be essential for normal song production and courtship success. With both *VT19579* and *VT5534*, fewer flies sang when paired with virgin females, and those that did so sang less than the corresponding controls (Figures 5D and 5E and [Table S1](#)). The test males were also less successful in mating (Figures 5F and 5G and [Table S1](#)). The simplest interpretation of these data is that activity of vPR6 neurons is both necessary and sufficient for robust song production.

In the thermal activation experiments, IPIs decreased markedly with temperature for all five vPR6 GAL4 lines tested (Figures 5H and 5I and [Table 1](#)). Overall, mean IPIs decreased at a rate of 5.4 ± 0.7 ms/°C. The mean IPI of natural song also decreases slightly with temperature (Shorey, 1962), but only at a rate of 1.0 ms/°C within this temperature range (Figure 5I and [Table 1](#)). Moreover, IPIs did not decrease with temperature with any of the GAL4 lines that trigger songs by activating neurons other than vPR6 ([Table 1](#)). This is particularly notable in the case of dPR1 (*VT41688*), which elicits songs with IPIs in a similar range. The shortening of IPIs with increasing temperature is also not a trivial consequence of increased song at higher temperature, as mean IPI did not in general correlate with the number of pulses an individual fly produced ([Table S2](#)). We therefore conclude that the temperature dependence of IPI observed with all of the GAL4 lines expressed in vPR6 specifically reflects a tight inverse coupling between vPR6 activity and the IPI.

vMS11: A Regulator of Wing Extension and CPP

The final GAL4 line that we selected for detailed analysis, *VT43702*, differed from the others in that thermal activation elicited wing extension but not wing vibration (only two pulses recorded from 45 flies; [Movie S9](#)). Moreover, these wing extensions were often bilateral or, if unilateral, persistently involved one or the other wing (Figure 6A). The persistent use of one wing was even observed across repeated trials of the same fly.

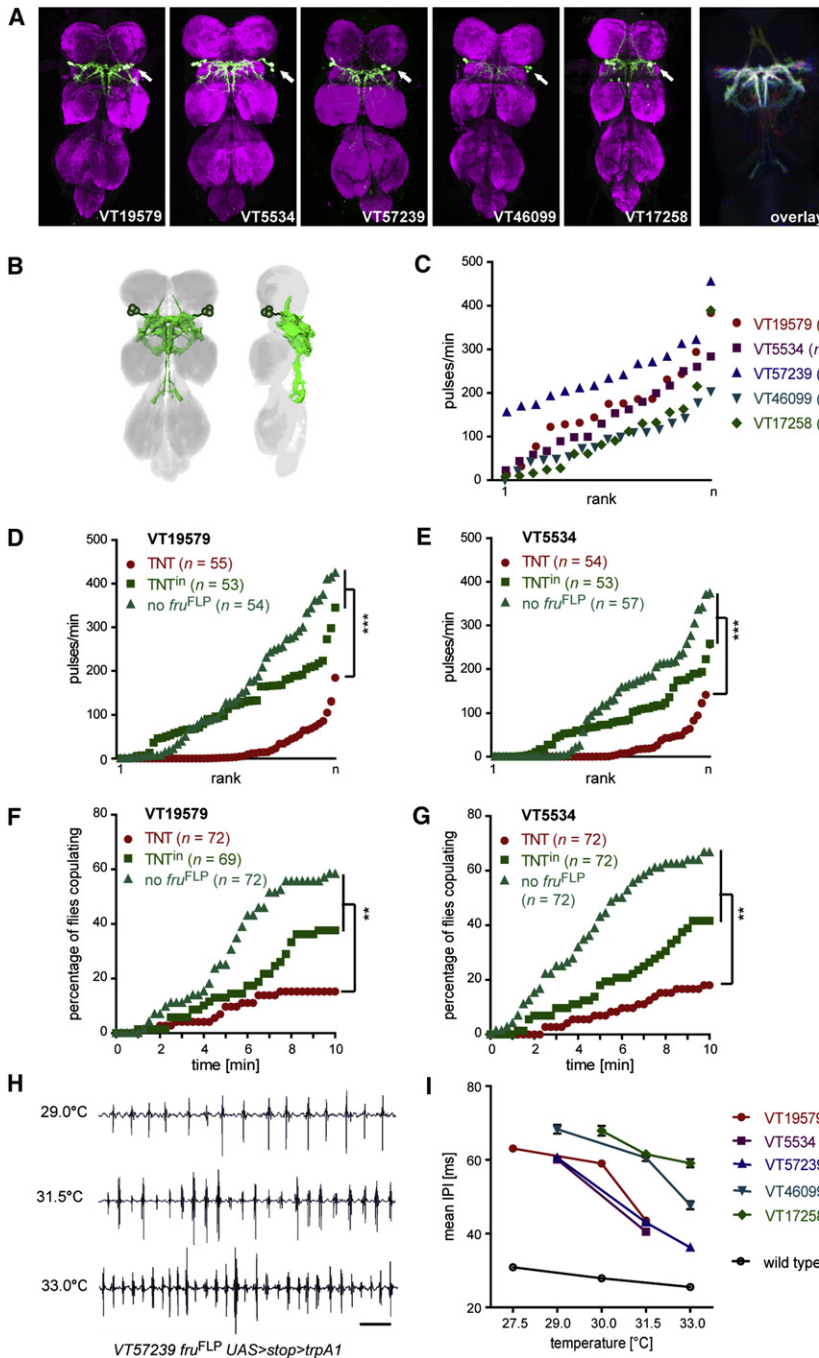


Figure 5. vPR6: A Thoracic Neuron that Influences the IPI

(A) VNCs of males carrying one of five vPR6 GAL4 lines, combined with *fru^{FLP} UAS>stop>mCD8-GFP*, stained with anti-GFP (green) and the synaptic marker mAb nc82 (magenta). The right panel shows an enlarged view of the overlaid registered and averaged GFP channels for VT17258 and VT5534 (red), VT19579 (green), and VT57239 and VT46099 (blue).

(B) Segmented arborization of the vPR6 class, showing ventral (left) and lateral (right) views of the VNC.

(C) Song production of isolated males carrying one of five vPR6 GAL4 lines, combined with *fru^{FLP} UAS>stop>trpA1*, at 31.5°C. Each data point represents a single fly, ranked by the amount of pulse song (see also Movie S8).

(D and E) Song production of VT19579 (D) and VT5534 (E) males, combined with either *fru^{FLP} UAS>stop>TNT* (TNT), *fru^{FLP} UAS>stop>TNTⁱⁿ* (TNTⁱⁿ), or *UAS>stop>TNT* (no *fru^{FLP}*), in pairings with wild-type virgin females. Each data point represents a single fly, ranked by the amount of pulse song. ****p* < 0.0001, Mann-Whitney test.

(F and G) Copulation success of males of the same genotypes as in (D) and (E), respectively. ***p* < 0.004, Fisher's exact test.

(H) Sample song traces of VT57239 *fru^{FLP} UAS>stop>trpA1* males at different temperatures. Scale bar: 100 ms.

(I) Mean IPI versus temperature for isolated males carrying one of the five vPR6 GAL4 lines in combination with *fru^{FLP} UAS>stop>trpA1*, as well as single wild-type males paired with virgin females (black circles).

classes, vMS11 and vMS12. All three cell types are located in the mesothoracic ganglia, with processes extending within the posterior wing neuropil.

We used the stochastic activation strategy with *UAS>stop>≥stop>trpA1^{myc}* to determine which of these three cell types is responsible for wing extension, selecting 34 flies that exclusively extended their left wing, 36 that extended only the right wing, and 55 that extended neither (Figure 6C; flies extending both wings were not observed in these stochastic activation experiments). The vMS11 neurons were significantly more often labeled in flies that

Staining CNSs of VT43702 *fru^{FLP} UAS>stop>mCD8-GFP* flies revealed expression in four classes of *fru* neuron in the brain and three in the VNC (Figures 6B and S5). Because wing extensions with *UAS>stop>trpA1* were also observed in beheaded flies, and none of the brain neurons have descending projections into the VNC, we attribute the songs of VT43702 flies to thermal activation of one or more of the *fru* neurons in the VNC. These are dMS2 neurons (Yu et al., 2010) and two previously undescribed

extended their wings (53/70) than in those that did not (9/55; *p* < 0.0001, Fisher's exact test). Moreover, of the 44 flies with unilateral labeling of vMS11 and wing extension, it was the ipsilateral wing that was extended in all but four cases (*p* < 0.0001, Fisher's exact test). In contrast, there was no correlation between wing extension and the expression of TrpA1^{myc} in either dMS2 or vMS12 (*p* > 0.4 in both cases; Figure 6C). There are approximately three vMS11 neurons in each hemisphere, with

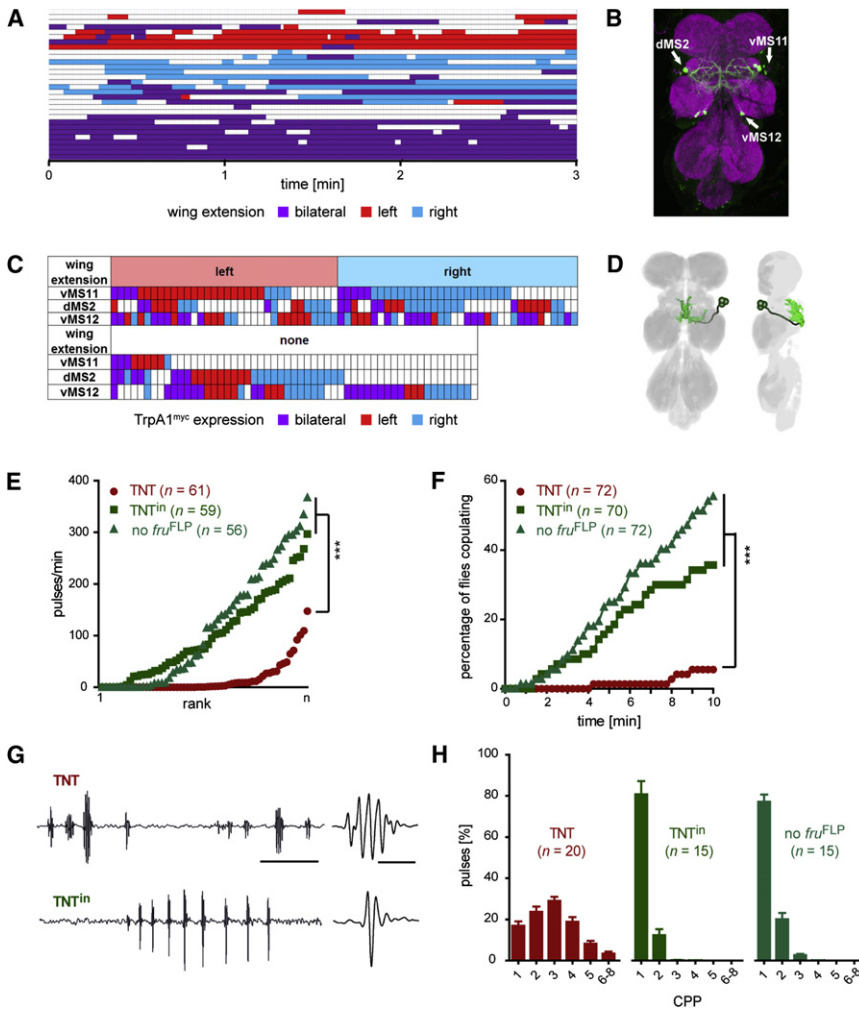


Figure 6. vMS11: A Mesothoracic Neuron that Controls Wing Extension and CPP

(A) Wing extension patterns of 30 *VT43702 fru^{FLP} UAS>stop>trpA1* male flies at 30.5°C. Each line represents a single fly.

(B) VNC of a *VT43702 fru^{FLP} UAS>stop>mCD8-GFP* male stained with anti-GFP (green) and the synaptic marker mAb nc82 (magenta).

(C) *TrpA1^{myc}* expression in each of the three *VT43702⁺ fru^{FLP+}* neuronal classes in the VNCs of *VT43702 hs-mFLP5 fru^{FLP} UAS>stop>≥stop≥trpA1^{myc}* males subjected to a brief heat shock during development, and sorted into those that persistently extended the left wing, the right wing, or neither. Each vertical column represents one fly; each row, one cell type. Color-coding indicates whether *TrpA1^{myc}* was in the left hemiganglion (red), the right (blue), or both (purple).

(D) Segmented arborization of the vMS11 class, showing ventral (left) and lateral (right) views of the VNC.

(E) Song production of *VT43702 fru^{FLP} UAS>stop>TNT* (TNT), *VT43702 fru^{FLP} UAS>stop>TNTⁱⁿ* (TNTⁱⁿ), and *VT43702 UAS>stop>TNT* (no *fru^{FLP}*) males paired with wild-type virgin females. Each data point represents a single fly, ranked by the amount of pulse song. ****p* < 0.0001, Mann-Whitney test.

(F) Copulation success of males of the same genotypes as in (E). ****p* < 0.0001, Fisher's exact test.

(G) Sample song traces of *VT43702 fru^{FLP} UAS>stop>TNT* (TNT) and *VT43702 fru^{FLP} UAS>stop>TNTⁱⁿ* (TNTⁱⁿ) males at 30.5°C (left panels), with enlarged views of a single pulse (right panels). Scale bars: 100 ms (left), 10 ms (right).

(H) CPP distribution in songs of males of the same genotypes as in (E) and (F). Data are mean ± SEM for *n* = 20 flies (1608 pulses), 15 flies (2281 pulses), and 15 flies (2616 pulses).

arborizations in the dorsomedial wing neuropil (2.9 ± 1.3 vMS11 cells, *n* = 12 hemispheres; Figure 6D).

Synaptic silencing experiments with *UAS>stop>TNT* males confirmed that activity of *VT43702⁺ fru^{FLP+}* neurons is also essential for normal song production and copulation success. Compared to control males, these test males extended their wings less often (*p* < 0.0001, Table S1), fewer than half of them produced any pulse song at all (*p* < 0.0001, Fisher's exact test; Figure 6E and Table 1), and most failed to copulate (*p* < 0.004; Figure 6F). The songs of these flies had significantly longer IPIs than normal (*p* ≤ 0.0002, Table S1) and, most strikingly, their pulses were frequently polycyclic ($59\% \pm 4\%$, *n* = 20, pulses have over two cycles compared with fewer than 3% in each control, *p* < 0.0001, Mann-Whitney test; Figures 6G and 6H and Table S1). Thus, activity of one or more of the *VT43702⁺ fru^{FLP+}* neurons is essential for song production, and for the restriction of wing vibrations to just one or two CPP. The vMS11 neurons are obvious candidates, but we cannot exclude the possibility that these song deficits are due to silencing of

dMS2, vMS12, or some of the *VT43702⁺ fru^{FLP+}* neurons in the brain.

A Neural Circuit for Courtship Song

To assess how the five distinct classes of *fru* neuron we have functionally characterized—P1, pIP10, dPR1, vPR6, and vMS11—might be integrated into a neural circuit, we examined their potential connectivity and polarity. Potential connectivity between each pairwise combination of neurons was assessed by labeling each class of neuron individually using the *UAS>stop>mCD8-GFP* marker, registering confocal images of these samples onto a common reference template, and digitally overlaying the two representations to compute the overlap between their arborizations (Yu et al., 2010). A high degree of overlap predicts (Braitenberg and Schuez, 1998), but does not establish, synaptic connectivity.

In the brain, the arborizations of P1 overlap extensively with both the ipsilateral and contralateral arborizations of pIP10 in the protocerebrum (Figures 7A and 7B). The arbors of pIP10 in

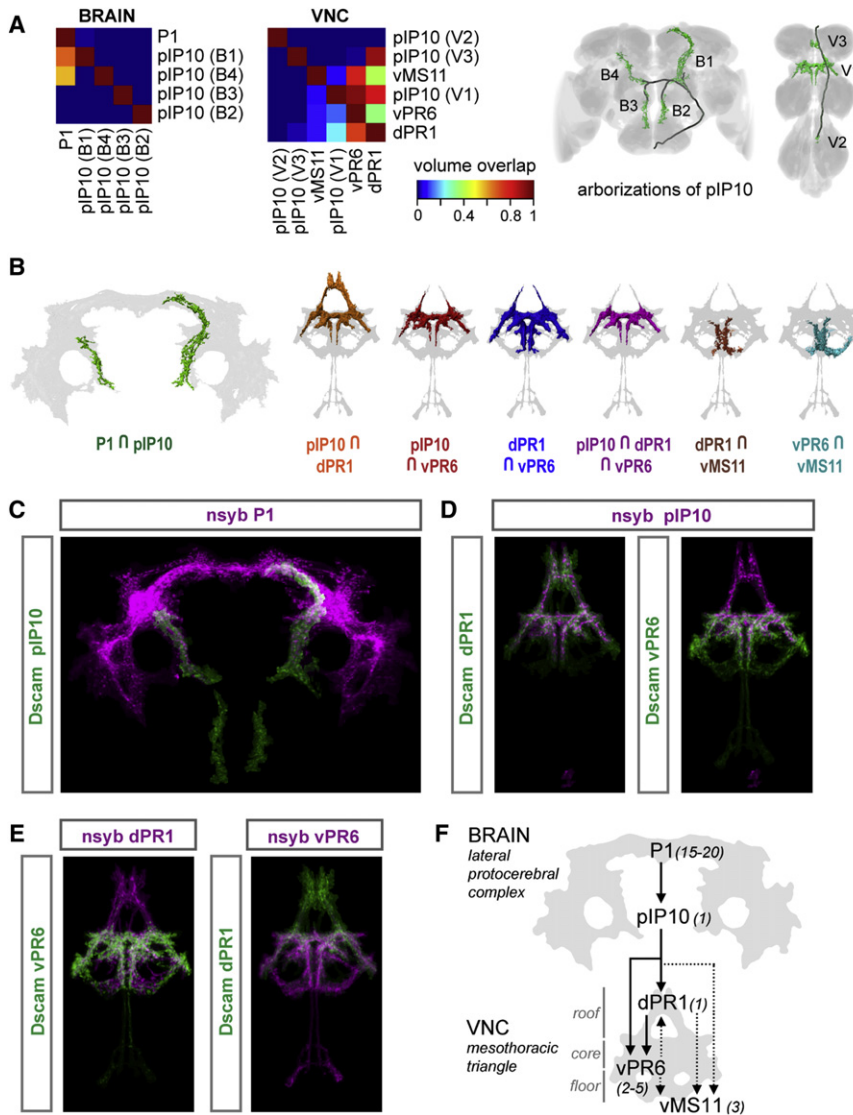


Figure 7. A Putative Neuronal Circuit for Pulse Song

(A) Calculated overlap between distinct arborization regions of P1 and pIP10 in the brain (left) and pairs of *fru* neurons in the VNC (middle), color-coded to show the fraction of the arbor indicated on the right that overlaps with the arbor indicated on the bottom. Individual arborizations of pIP10 are labeled as indicated in the segmented representation (right). Arborization volumes were segmented in both hemispheres for P1, dPR1, and vPR6, and in one hemisphere for pIP10 and vMS11.

(B) Segmented volume overlaps between the indicated sets of neurons. Gray backgrounds represent the full arborizations of P1 (for brain) or vPR6 (for VNC).

(C–E) Overlays of registered confocal images of brain (C) and VNC (D and E) samples stained to reveal either the presynaptic marker nsyb (magenta) or the dendritic marker Dscam17.1-GFP (green).

(F) A proposed neuronal circuit linking the *fru* song neurons P1, pIP10, dPR1, and vPR6. Average cell numbers per hemisphere are indicated in parentheses.

the presynaptic sites of P1 (Figure 7C), and its presynaptic termini in the VNC overlap in turn with the dendritic fields of both dPR1 and vPR6 (Figure 7D). The respective presynaptic termini and dendritic fields of dPR1 and vPR6 overlap with each other, but there is considerably more overlap between the presynaptic termini of dPR1 and the dendritic field of vPR6 than vice versa (Figure 7E).

In summary, these data suggest that the *fru* song neurons might be interconnected in a circuit in which P1 provides input to pIP10 in the brain, which in turn conveys a descending command type

signal to the thoracic neurons dPR1 and vPR6. Direct communication between dPR1 and vPR6 is likely, in particular from dPR1 to vPR6 (Figure 7F).

the VNC in turn overlap with those of dPR1 in the prothoracic ganglion, and in the anterior wing neuropil of the mesothoracic ganglion with both dPR1 and vPR6, and, to a lesser extent, with vMS11 (Figures 7A and 7B). dPR1, vPR6, and vMS11 arbors also overlap with each other in this region (Figures 7A and 7B). Neuronal polarity was assessed for P1, pIP10, dPR1, and vPR6 using the presynaptic marker nsyb-GFP (Deitcher et al., 1998) and the dendritic marker Dscam17.1-GFP (Wang et al., 2004), encoded in *UAS>stop>nsyb-GFP* and *UAS>stop>Dscam17.1-GFP* transgenes, respectively (Yu et al., 2010). We confirmed previous reports (Kimura et al., 2008; Yu et al., 2010) that P1 neurons have extensive presynaptic and dendritic arborizations within the ring and arch regions of the lateral protocerebral complex. The pIP10 neuron was strongly labeled with nsyb-GFP only in the VNC, and with Dscam17.1-GFP only in the brain, as expected for a descending interneuron (Figures 7C and 7D). The dendrites of pIP10 in the brain overlap with

signal to the thoracic neurons dPR1 and vPR6. Direct communication between dPR1 and vPR6 is likely, in particular from dPR1 to vPR6 (Figure 7F).

DISCUSSION

The courtship song of *Drosophila* serves as an ideal model system for investigating the neural mechanisms of decision-making, action selection, and motor pattern generation (Dickson, 2008). Here we have identified a set of song neurons in the *Drosophila* CNS and characterized their distinct roles in initiating or patterning the song. Artificial activation of these neurons triggers wing extension and/or vibration in isolated males deprived of the sensory inputs that would normally induce males to sing. Complementary silencing experiments suggest that these neurons also contribute to natural song production and mating success in the presence of a female.

Decision-Making and Action Selection: Song Circuits in the Brain

The male brain is presumed to contain neural circuits that integrate sensory information across multiple modalities, as well as internal information from prior experience, to create the percept of a receptive virgin female of the same species—a desirable courtship object (Dickson, 2008). These circuits would compute a decision to court the female. If acted upon, this decision would trigger courtship behavior, one prominent and critical manifestation of which is the courtship song. At any given moment, however, a male fly is likely to be confronted with multiple behavioral options, most of which are mutually exclusive. Courting a female may not be the most adaptive option, for example, in the presence of a predator or some other imminent danger. Decision-making circuits should thus be integrated with circuits that prioritize and select among alternative actions.

We propose that the P1 and pIP10 neurons are critical elements in these decision-making and action selection circuits in the fly brain. This notion rests on several lines of evidence. First, activation of either P1 or pIP10 elicits a faithful rendition of the natural song, suggesting that they trigger but do not pattern the song. Second, silencing small neuronal subsets that include either P1 or pIP10 dramatically reduces song output. Third, P1 neurons are intrinsic to the lateral protocerebral complex in the brain, where pathways from distinct sensory modalities converge (Yu et al., 2010). Fourth, pIP10 is a descending neuron that appears to collect some, but not all, of its inputs from the lateral protocerebral complex, most likely including P1.

We envision that P1 is critically involved in creating the percept of a suitable courtship object, and hence the decision to court, and that it communicates this decision to pIP10, a command-type neuron that selects and initiates the action of singing. Additional inputs to pIP10 would gate the P1 signal, so that pIP10 calls thoracic song circuits into action only if singing is judged to be the most appropriate behavioral choice at a given moment. These gating signals might also coordinate the timely execution of the courtship ritual itself, allowing the male to progress beyond singing once the female has indicated her willingness to mate. Further anatomical, physiological, and behavioral studies will test these ideas.

pIP10 is presumably not the only descending input to the thoracic song circuits. Other descending pathways might terminate the song, select between sine and pulse song (Clyne and Miesenböck, 2008), or dictate the choice of wing. Males typically sing using the wing facing toward the female, a choice governed primarily by visual (our unpublished observations) and possibly also gustatory (Koganezawa et al., 2010) cues. Unilateral activation of either P1 or pIP10 neurons does not lead to preferential extension of one or the other wing, and so if these neurons carry any laterality information at all, it must be encoded in a manner that cannot be mimicked by tonic thermal activation. Alternatively, and perhaps more likely, the choice of wing may be controlled by a separate descending pathway that collects its inputs, directly or indirectly, from the visual and gustatory centers of the brain.

Patterning the Song: Elements of a Thoracic CPG for Pulse Song

Photoactivation experiments (Clyne and Miesenböck, 2008) and gynandromorph studies (von Schilcher and Hall, 1979) have provided evidence that a CPG for song resides in the thoracic ganglia. We propose that the dPR1, vPR6, and vMS11 neurons are components of such a CPG for pulse song. In contrast to the P1 or pIP10 neurons in the brain, artificial activation of these thoracic neurons does not produce a faithful rendition of the natural song. Rather, these songs are perturbed in a characteristic fashion for each neuron, implying that each plays a distinct role in composing the pulse song.

The dPR1 and vPR6 neurons may be direct targets of the pIP10 command neuron. Songs induced by activating either of these neurons have extended IPIs. For vPR6, but not dPR1, IPI is inversely correlated with the presumed level of activation. The activity of vPR6 neurons may therefore be a critical determinant of the IPI. This prediction can now be tested by physiological investigation. If it holds up, these studies will also help to delineate the specific biophysical properties of vPR6 that determine the IPI. The corresponding genes would be candidates for the genetic changes that have diversified IPIs within the *Drosophila* genus.

The third thoracic song neuron, vMS11, appears to function in wing choice and extension. Unilateral activation of vMS11 results in the extension, but not vibration, of the ipsilateral wing. vMS11 may thus represent one of the output channels of the pulse song CPG. It may, for example, integrate song onset signals from the CPG with descending signals that convey the female's location, passing the result on to motor neurons that control the posture of the appropriate wing. A separate CPG output channel might carry precisely timed pulse signals that control wing vibration.

Synaptic silencing experiments hint that vMS11 may also control the CPP, although we cannot at present definitively assign this function to vMS11. If vMS11 is partially silenced, along with the thoracic neurons dMS2 and vMS12, fewer pulses are produced, as predicted, but most of them are also polycyclic. Feedback signals from wing sensory neurons are thought to dampen wing vibrations and limit each song pulse to one or two cycles (Ewing, 1979). Such proprioceptive signals might be blocked in these silencing experiments. If these feedback signals are conveyed by vMS11 activity, then tonic activation of this neuron might be predicted to freeze the wing in its extended position, just as we observed in the thermal activation experiments. Here too, physiological studies will further define the role of vMS11 in song production, and ultimately reveal how vMS11, vPR6, dPR1, and other song neurons function together to time and shape each pulse of the courtship song.

Sexual Differentiation of the Song Circuit

Although females do not sing naturally, photoactivation (Clyne and Miesenböck, 2008) and our thermal activation experiments imply the existence of a rudimentary song circuit in the female thoracic ganglia. This female circuit is presumably not so much a defective song circuit, but rather an overlapping circuit specialized for some other wing movements—such as those that accompany flight or aggressive displays—yet capable of

producing pulsed vibrations when inappropriately activated. That it does not normally operate in “song” mode in females suggests that this thoracic circuit might be controlled by distinct sets of descending signals in males and females. Because expression of *fru*^M in females endows them with the ability to sing to other females (Demir and Dickson, 2005), and also improves the song produced by photoactivated female thoraxes (Clyne and Miesenböck, 2008), we infer that *fru*^M masculinizes both the descending inputs from the brain and the thoracic song circuit itself. All five song neurons characterized in this study are candidates for such masculinizing influences of *fru*^M: P1, pIP10, and dPR1 are all male specific, and vPR6 and vMS11 appear to have sexually dimorphic arborizations within the wing neuropil.

The P1 neuron requires both *fru*^M and *dsx*^M for its male-specific differentiation (Kimura et al., 2008). Genetically mosaic females in which P1 neurons are mutant for the upstream regulator *transformer*, and hence express both *fru*^M and *dsx*^M, reportedly extended their wings, and presumably sing, to other females (Kimura et al., 2008). Not all such females courted in these experiments, and their overall courtship levels were low. Nonetheless, that some of these flies could sing at all implies that male P1 neurons can at least partially integrate into otherwise female circuits. The apparent ability of these male P1 neurons to correctly integrate inputs arriving through female sensory pathways may reflect the limited sexual dimorphism in the *fru* sensory pathways that converge upon the lateral protocerebral complex (Yu et al., 2010). That male P1 neurons could activate a female thoracic song circuit, however, is more difficult to reconcile with our notion that the male-specific pIP10 and dPR1 neurons form an essential conduit between these two centers. Although neither was specifically examined in that study (Kimura et al., 2008), both pIP10 and dPR1 were presumably lacking in most of these females. This may partly explain why these flies sang so rarely, but it does also suggest that alternative descending pathways exist, or can be recruited, to communicate between P1 neurons in the brain and the thoracic song circuits. This might include the additional descending pathways that we postulate control other aspects of song production, such as the choice of wing.

The extent to which the *fru*^{M+} neurons pIP10, dPR1, vPR6, and vMS11 actually require *fru*^M for their male-specific differentiation and function remains to be determined. The pIP10 and vMS11 neurons do not express *dsx*, and so *fru*^M is presumably the principle sex determinant for these neurons; dPR1 and vPR6 express and potentially require both *fru*^M and *dsx*^M. Whatever the precise genetic requirements, our functional characterization of dPR1 and vPR6 suggest that sex differences in these neurons may at least partly explain why the songs elicited by photoactivation or thermal activation of *fru* neurons in the female thorax have longer than normal IPIs. Similarly, sexual dimorphisms in vMS11 offer a potential explanation for the polycyclic pulses in these female songs.

Having delineated specific cellular components of the *Drosophila* song circuits, our work now paves the way for physiological studies to explore their operating principles in males, and how they differ in females. Genetic manipulation of individual neurons within these circuits, using strategies similar to those we

have used here, should also reveal how the *fru* and *dsx* genes act through their respective target genes to control the sex-specific differentiation of these circuits, and thereby endow males and females with their distinct behavioral repertoires.

EXPERIMENTAL PROCEDURES

Fly Stocks

fru^{FLP}, *UAS>stop>mCD8-GFP*, *UAS>stop>Dscam17.1-GFP*, and *UAS>stop>nsyb-GFP* are as described in Yu et al. (2010), and *UAS>stop>TNT* and *UAS>stop>TNTQ* (*TNT*ⁱⁿ) are as described in Stockinger et al. (2005). *UAS-trpA1*, *UAS>stop>trpA1*, *UAS>stop>trpA1^{myc}* and *UAS>stop>trpA1^{mCherry}* were generated by standard cloning procedures, with the *trpA1* reading frame amplified by PCR from genomic DNA of *UAS-trpA1* flies provided by P. Garrity (Hamada et al., 2008). The “>stop>” cassette is the same as that in the *UAS>stop>TNT* constructs of Stockinger et al. (2005). These transgenes were inserted by ϕ C31-mediated recombination into attP “landing sites” on the second chromosome (*UAS-trpA1* into VIE-260b and *UAS>stop>trpA1*, *UAS>stop>trpA1^{myc}* and *UAS>stop>trpA1^{mCherry}* into VIE-19a; K. Keleman and B.J.D., unpublished data). In *UAS>stop>≥stop≥trpA1^{myc}*, the “>stop>” cassette consists of a *his2A^{V5}* reporter followed by *α-tubulin84B* and *Act5C* transcriptional stop signals flanked by FRT sites, while the “≥stop≥” cassette contains a *lamin^{HA}* reporter followed by *Hsp70Aa* and *Hsp27* transcriptional stop signals flanked by mFRT71 sites. The *trpA1^{myc}* reading frame encodes a full-length TrpA1 protein tagged with two C-terminal c-myc epitopes. This transgene was inserted using ϕ C31 recombinase into the VIE-19a attP site. *hs-mFLP5* was inserted into the third chromosome attP site VIE-49a (Hadjieconomou et al., 2011).

Enhancer trap GAL4 lines obtained from the *Drosophila* Genetics Resource Centre, Japan, and the collection of U. Heberlein are described in Yu et al. (2010). The VT collection of molecularly defined enhancer GAL4 lines was generated using the strategy of Pfeiffer et al. (2008) (C.M., S.S.B., A. Stark, and B.J.D., unpublished data).

Thermal Activation Experiments

trpA1-expressing flies were reared at 22°C, and males collected shortly after eclosion were aged in groups of 10–20 for 10–15 days at 22°C. For the initial GAL4 screen, four to eight males per genotype were screened for wing extension by aspirating them into chambers placed on a heating plate that was gradually heated from 25°C to 32°C–33°C during a 10 min video recording. For recording and detailed analysis of courtship songs, single males were aspirated into a metal chamber surrounded by Peltier elements containing a temperature sensor and a feedback system to maintain a constant temperature. Songs were recorded for 3.5–4.0 min.

In the stochastic activation experiments with *hs-mFLP5 fru^{FLP} UAS>stop>≥stop≥trpA1^{myc}*, animals were heatshocked for 60–90 min at 37°C during the mid- to late-larval stage. Single males were assayed for song production and/or wing extension, then individually dissected to prepare their brains and/or VNCs for immunohistochemistry using anti-myc. For the analysis of wing extensions of *VT43702 fru^{FLP} UAS>stop>trpA1* males, all wing extensions of at least 3 s duration and an angle of 30° were manually recorded.

Neuronal Silencing Experiments

Flies were reared at 25°C and males were collected shortly after eclosion and aged individually for 6–7 days at 25°C. For pulse song evaluation, single males were paired with a 4- to 5-day-old wild-type (Canton S) virgin and the courtship song was recorded in a soundproof chamber for 3.5–4.0 min or until copulation occurred. Analysis of courtship behavior and copulation latencies was performed as described in Demir and Dickson (2005). Wing extension frequency was determined by examining single frames of a 10 min video, taken at 15 s intervals until copulation, and counting those in which the male extended a wing at an angle of at least 30°.

Song Analysis

Pulse song was analyzed with Signal 4.0 (Engineering Design) and LifeSong (Bernstein et al., 1992) software, following manual inspection and editing to

remove background noises. LifeSong settings were generally as follows: signal/noise ratio, 5; IPI, 15–100 ms; minimum train length, 2 (for pulses/min) or 3 (for IPI). For IPI analysis, pulse trains with subthreshold pulses were excluded. CPP analysis was performed manually, scoring up to the first 100–200 pulses. Low-amplitude pulses were excluded. CPP was determined as the minimum of positive and negative peaks, counting all peaks with at least half the amplitude of the largest peak. Flies producing fewer than 10 pulses during a 3.5 min recording were excluded from the analysis of song parameters.

Immunohistochemistry and Image Analysis

Flies were reared at 25°C and aged for 4–6 days prior to dissection and staining as described in Yu et al. (2010). Antibodies used were rabbit anti-GFP (1: 6000, Torrey Pines), chicken anti-GFP (1:3000, abcam), mouse mAb nc82 (1:20, Hybridoma Bank), rabbit anti-DsRed (to detect mCherry; 1:500 or 1:1000, Clontech), rabbit anti-myc (1:6000 or 1:12,000, abcam), rabbit anti-Fru^M (Stockinger et al., 2005), rat anti-Dsx^M (Hempel and Oliver, 2007) and secondary Alexa 488, 568, and 647 antibodies (1:500 or 1:1000, Invitrogen).

Confocal stacks of stained brains and VNCs were taken with a Zeiss LSM510 with a Multi Immersion Plan NeoFluor 25x/0.8 objective and analyzed with Amira software (Visage Imaging). Nonrigid registration, segmentation, analysis of overlap, and image preparation were performed as described previously (Yu et al., 2010).

SUPPLEMENTAL INFORMATION

Supplemental Information for this article includes five figures, two tables, and nine movies and can be found with this article online at doi:10.1016/j.neuron.2011.01.011.

ACKNOWLEDGMENTS

We thank P. Garrity for *UAS-trpA1* flies; B. Oliver for anti-dsx^M; U. Heberlein for GAL4 lines; A. Keene for help with the song recording unit; M. Kinberg, S. Wandl, and A. Gyorgy for technical assistance; P. Pasierbek and C. Machacek for technical advice; and K. Feng and M. Haesemeyer for valuable discussions and critical feedback on the manuscript. This work was supported in part by a research grant to B.J.D. from the Human Frontier Science Program and a postdoctoral fellowship to A.C.v.P. from the European Molecular Biology Organization. Basic research at the IMP is funded by Boehringer Ingelheim GmbH.

Accepted: January 18, 2011

Published: February 9, 2011

REFERENCES

Bennet-Clark, H.C., and Ewing, A.W. (1967). Stimuli provided by courtship of male *Drosophila melanogaster*. *Nature* 215, 669–671.

Bennet-Clark, H.C., and Ewing, A.W. (1969). Pulse interval as a critical parameter in the courtship song of *Drosophila melanogaster*. *Anim. Behav.* 17, 755–759.

Bernstein, A.S., Neumann, E.K., and Hall, J.C. (1992). Temporal analysis of tone pulses within the courtship songs of two sibling *Drosophila* species, their interspecific hybrid, and behavioral mutants of *D. melanogaster* (Diptera: Drosophilidae). *J. Insect Behav.* 5, 15–36.

Braitenberg, V., and Schuez, A. (1998). *Statistics and the Geometry of Neuronal Connectivity* (Berlin: Springer).

Cachero, S., Ostrovsky, A.D., Yu, J.Y., Dickson, B.J., and Jefferis, G.S.X.E. (2010). Sexual dimorphism in the fly brain. *Curr. Biol.* 20, 1589–1601.

Clyne, J.D., and Miesenböck, G. (2008). Sex-specific control and tuning of the pattern generator for courtship song in *Drosophila*. *Cell* 133, 354–363.

Deitcher, D.L., Ueda, A., Stewart, B.A., Burgess, R.W., Kidokoro, Y., and Schwarz, T.L. (1998). Distinct requirements for evoked and spontaneous

release of neurotransmitter are revealed by mutations in the *Drosophila* gene *neuronal-synaptobrevin*. *J. Neurosci.* 18, 2028–2039.

Demir, E., and Dickson, B.J. (2005). *fruitless* splicing specifies male courtship behavior in *Drosophila*. *Cell* 121, 785–794.

Dickson, B.J. (2008). Wired for sex: The neurobiology of *Drosophila* mating decisions. *Science* 322, 904–909.

Ewing, A.W. (1979). The role of feedback during singing and flight in *Drosophila melanogaster*. *Physiol. Entomol.* 4, 329–337.

Hadjieconomou, D., Rotkopf, S., Alexandre, C., Bell, D.M., Dickson, B.J., and Salecker, I. (2011). Flybow - genetic multicolor cell-labeling for neural circuit analysis in *Drosophila*. *Nat. Methods*. in press.

Hall, J.C. (1977). Portions of the central nervous system controlling reproductive behavior in *Drosophila melanogaster*. *Behav. Genet.* 7, 291–312.

Hamada, F.N., Rosenzweig, M., Kang, K., Pulver, S.R., Ghezzi, A., Jegla, T.J., and Garrity, P.A. (2008). An internal thermal sensor controlling temperature preference in *Drosophila*. *Nature* 454, 217–220.

Hedwig, B. (1994). A cephalothoracic command system controls stridulation in the acridid grasshopper *Omocestus viridulus L.* *J. Neurophysiol.* 72, 2015–2025.

Hedwig, B. (2000). Control of cricket stridulation by a command neuron: Efficacy depends on the behavioral state. *J. Neurophysiol.* 83, 712–722.

Hedwig, B. (2006). Pulses, patterns and paths: Neurobiology of acoustic behaviour in crickets. *J. Comp. Physiol. A Neuroethol. Sens. Neural Behav. Physiol.* 192, 677–689.

Hempel, L.U., and Oliver, B. (2007). Sex-specific Doublesex^M expression in subsets of *Drosophila* somatic gonad cells. *BMC Dev. Biol.* 7, 113.

Howse, P.E. (1975). Brain structure and behavior in insects. *Annu. Rev. Entomol.* 20, 359–379.

Kimura, K., Hachiya, T., Koganezawa, M., Tazawa, T., and Yamamoto, D. (2008). *Fruitless* and *doublesex* coordinate to generate male-specific neurons that can initiate courtship. *Neuron* 59, 759–769.

Koganezawa, M., Haba, D., Matsuo, T., and Yamamoto, D. (2010). The shaping of male courtship posture by lateralized gustatory inputs to male-specific interneurons. *Curr. Biol.* 20, 1–8.

Kyriacou, C.P., and Hall, J.C. (1982). The function of courtship song rhythms in *Drosophila*. *Anim. Behav.* 30, 794–801.

Lee, G., Foss, M., Goodwin, S.F., Carlo, T., Taylor, B.J., and Hall, J.C. (2000). Spatial, temporal, and sexually dimorphic expression patterns of the *fruitless* gene in the *Drosophila* central nervous system. *J. Neurobiol.* 43, 404–426.

Lima, S.Q., and Miesenböck, G. (2005). Remote control of behavior through genetically targeted photostimulation of neurons. *Cell* 121, 141–152.

Manoli, D.S., Foss, M., Vilella, A., Taylor, B.J., Hall, J.C., and Baker, B.S. (2005). Male-specific *fruitless* specifies the neural substrates of *Drosophila* courtship behaviour. *Nature* 436, 395–400.

Mellert, D.J., Knapp, J.-M., Manoli, D.S., Meissner, G.W., and Baker, B.S. (2010). Midline crossing by gustatory receptor neuron axons is regulated by *fruitless*, *doublesex* and the Roundabout receptors. *Development* 137, 323–332.

Pfeiffer, B.D., Jenett, A., Hammonds, A.S., Ngo, T.T., Misra, S., Murphy, C., Scully, A., Carlson, J.W., Wan, K.H., Lavery, T.R., et al. (2008). Tools for neuroanatomy and neurogenetics in *Drosophila*. *Proc. Natl. Acad. Sci. USA* 105, 9715–9720.

Pulver, S.R., Pashkovski, S.L., Hornstein, N.J., Garrity, P.A., and Griffith, L.C. (2009). Temporal dynamics of neuronal activation by Channelrhodopsin-2 and TRPA1 determine behavioral output in *Drosophila* larvae. *J. Neurophysiol.* 101, 3075–3088.

Rideout, E.J., Billeter, J.C., and Goodwin, S.F. (2007). The sex-determination genes *fruitless* and *doublesex* specify a neural substrate required for courtship song. *Curr. Biol.* 17, 1473–1478.

Rideout, E.J., Dornan, A.J., Neville, M.C., Eadie, S., and Goodwin, S.F. (2010). Control of sexual differentiation and behavior by the *doublesex* gene in *Drosophila melanogaster*. *Nat. Neurosci.* 13, 458–466.

- Ryner, L.C., Goodwin, S.F., Castrillon, D.H., Anand, A., Vilella, A., Baker, B.S., Hall, J.C., Taylor, B.J., and Wasserman, S.A. (1996). Control of male sexual behavior and sexual orientation in *Drosophila* by the *fruitless* gene. *Cell* *87*, 1079–1089.
- Shorey, H.H. (1962). Nature of the sound produced by *Drosophila melanogaster* during courtship. *Science* *137*, 677–678.
- Stockinger, P., Kvitsiani, D., Rotkopf, S., Tirián, L., and Dickson, B.J. (2005). Neural circuitry that governs *Drosophila* male courtship behavior. *Cell* *121*, 795–807.
- Sweeney, S.T., Brodie, K., Keane, J., Niemann, H., and O’Kane, C.J. (1995). Targeted expression of tetanus toxin light chain in *Drosophila* specifically eliminates synaptic transmission and causes behavioral defects. *Neuron* *14*, 341–351.
- Taylor, B.J., Vilella, A., Ryner, L.C., Baker, B.S., and Hall, J.C. (1994). Behavioral and neurobiological implications of sex-determining factors in *Drosophila*. *Dev. Genet.* *15*, 275–296.
- Vilella, A., and Hall, J.C. (1996). Courtship anomalies caused by *doublesex* mutations in *Drosophila melanogaster*. *Genetics* *143*, 331–344.
- Vilella, A., Gailey, D.A., Berwald, B., Ohshima, S., Barnes, P.T., and Hall, J.C. (1997). Extended reproductive roles of the *fruitless* gene in *Drosophila melanogaster* revealed by behavioral analysis of new *fru* mutants. *Genetics* *147*, 1107–1130.
- von Schilcher, F. (1976). The function of pulse song and sine song in the courtship of *Drosophila melanogaster*. *Anim. Behav.* *24*, 622–625.
- von Schilcher, F., and Hall, J.C. (1979). Neural topography of courtship song in sex mosaics of *Drosophila melanogaster*. *J. Comp. Physiol. A* *129*, 85–95.
- Voziyanov, Y., Konieczka, J.H., Stewart, A.F., and Jayaram, M. (2003). Stepwise manipulation of DNA specificity in Flp recombinase: Progressively adapting Flp to individual and combinatorial mutations in its target site. *J. Mol. Biol.* *326*, 65–76.
- Wang, J., Ma, X., Yang, J.S., Zheng, X., Zugates, C.T., Lee, C.-H.J., and Lee, T. (2004). Transmembrane/juxtamembrane domain-dependent Dscam distribution and function during mushroom body neuronal morphogenesis. *Neuron* *43*, 663–672.
- Yu, J.Y., Kanai, M.I., Demir, E., Jefferis, G.S.X.E., and Dickson, B.J. (2010). Cellular organization of the neural circuit that drives *Drosophila* courtship behavior. *Curr. Biol.* *20*, 1602–1614.

Curriculum vitae

Tianxiao Liu

email: tianxiao15@gmail.com

Date of birth: 31/12/1985

Place of birth: Beijing, China

Nationality: People's Republic of China

Education

- 2008-2012
Dr. rer. Nat.
The University of Vienna
Vienna, Austria
- 2004-2008
Bachelor of Science
Faculty of Science
Kyoto University
Kyoto, Japan

Research Experience

- 2008-2012
Anatomical and functional analysis of courtship circuit in *Drosophila melanogaster*
Dr. Barry J. Dickson
Research Institute of Molecular Pathology
Vienna, Austria
- 2004-2008
Investigation of molecular mechanism for synchronized oscillation of the clock gene
Hes7
Prof. Ryoichiro Kageyama
Institute for Virus Research
Kyoto University
Kyoto, Japan

Conferences:

- 2010 EMBL Symposium: Structure and Function of Neural Circuits
Heidelberg, Germany
- 2011 103rd ITC Genetic analysis of neural circuits
Titisee, Germany

Publications:

Von Philipsborn AC, Liu T, Yu JY, Masser C, Bidaye SS, Dickson BJ. (2011) "Neuronal control of *Drosophila* courtship song." *Neuron* 69(3):509-22.

Niwa Y, Masamizu, Y, Liu T, Nakayama R, Deng CX, Kageyama R. (2007) "The initiation and propagation of Hes7 oscillation are cooperatively regulated by Fgf and notch signaling in the somite segmentation clock." *Dev. Cell*, 13, 298–304

